

Review

Quiescent and active galactic nuclei as factories of merging compact objects in the era of gravitational-wave astronomy

Manuel Arca Sedda ^{1,2,3,*†}, Smadar Naoz ^{4,5†} and Bence Kocsis ^{6†}

¹ Dipartimento di Fisica e Astronomia “G. Galilei”, Università di Padova, Via F. Marzolo 8, 35131 Padova, Italy

² Gran Sasso Science Institute (GSSI), I-67100 L’Aquila, Italy

³ Astronomisches Rechen-Institut, Zentrum für Astronomie der Universität Heidelberg, Mönchhofstr. 12-14, D-69120 Heidelberg, Germany

⁴ Department of Physics and Astronomy, UCLA, Los Angeles, CA 90095, USA; snaoz@astro.ucla.edu

⁵ Department of Physics and Astronomy, Mani L. Bhaumik Institute for Theoretical Physics, UCLA, Los Angeles, CA 90095, USA

⁶ Rudolf Peierls Centre for Theoretical Physics, Clarendon Laboratory, Parks Road, Oxford OX1 3PU, UK; bence.kocsis@physics.ox.ac.uk

* Correspondence: m.arcasedda@gmail.com

† These authors contributed equally to this work.

Abstract: Galactic nuclei harbouring a central supermassive black hole (SMBH), possibly surrounded by a dense nuclear cluster (NC), represent extreme environments which house a complex interplay of many physical processes that uniquely affect stellar formation, evolution, and dynamics. The discovery of gravitational waves (GW) emitted by merging black holes (BHs) and neutron stars (NSs), funnelled a huge amount of work focused on understanding how compact object binaries (COBs) can pair-up and merge together. Here, we review from a theoretical standpoint how different mechanisms concur to the formation, evolution, and merger of COBs around quiescent SMBHs and active galactic nuclei (AGNs), summarizing the main predictions for current and future (GW) detections and outlining the possible features that can clearly mark a galactic nuclei origin.

Keywords: black hole physics, galactic nuclei, gravitational waves

Citation: Arca Sedda, M.; Naoz, S.; Kocsis, B. Merging compact objects in galactic nuclei. *Universe* **2022**, *1*, 0. <https://doi.org/>

Received:

Accepted:

Published:

Publisher’s Note: MDPI stays neutral with regard to jurisdictional claims in published maps and institutional affiliations.

Copyright: © 2023 by the authors. Submitted to *Universe* for possible open access publication under the terms and conditions of the Creative Commons Attribution (CC BY) license (<https://creativecommons.org/licenses/by/4.0/>).

1. Introduction

Most galactic nuclei (if not all) are expected to harbour in their centres either a dense Nuclear Cluster (NC), a massive stellar conglomerate typically comprised of 10^{4-9} stars [1–3], a supermassive black hole (SMBH), with typical masses $M_{\text{SMBH}} \simeq 10^{4-10} M_{\odot}$ [4,5], or both [6–10]. With densities up to several orders of magnitude larger than typical globular and young massive clusters but similar half-mass radii, NCs constitute the densest stellar systems in the Universe [1,3,10]. The unique feature of hosting a massive NC or an SMBH – or possibly both – makes galactic nuclei the ideal laboratories to study stellar dynamics at its extreme. A particularly interesting aspect of dynamics in such extreme environments is the formation of compact object binaries (COBs), comprised of stellar-mass black holes (BHs) or neutron stars (NSs).

From the theoretical standpoint, the formation of COBs in galactic nuclei is rather uncertain, as it depends on many features, among which the NC formation process, the SMBH influence, especially if it is in its active phase, the stellar evolution and the secular dynamics. The high densities of galactic nuclei and NCs can favor stellar interactions, potentially boosting COBs formation, but the large velocity dispersion associated with a central SMBH or a cuspy matter distribution hampers them, making hard to assess the actual formation, and merger,

arXiv:2302.14071v1 [astro-ph.GA] 27 Feb 2023

rate of COBs in galactic nuclei. After formation, a COB can undergo further interactions with passing by stars, which can lead to the binary shrinkage, to the replacement of one component, or to its disruption [11–13]. The SMBH gravitational field can alter the COB evolution, causing periodic oscillations of the binary eccentricity, the so-called Eccentric-Lidov-Kozai (EKL) mechanism [14–21], which can ultimately lead to its coalescence. The gaseous disc surrounding SMBHs in active galactic nucleus (AGN) can strongly affects compact objects (COs) dynamics, damping their orbits and boosting binary-single and single-single scatterings, possibly favoring binary formation [e.g. 22–35].

From the observational point of view, the Milky Way centre, with an SMBH weighing $M_{\text{SMBH}} \simeq 4.1 \times 10^6 M_{\odot}$ [36–39] and a NC with a mass $M_{\text{NC}} = 2.5 \times 10^7 M_{\odot}$ [12,40–42], constitutes an excellent, and our closest, observation site. Over a time-span of more than 30 yr, we have been capable of literally observing stars moving within a few thousand AU from the Galactic SMBH, SgrA*, with a precision sufficiently high to probe general relativity [36,43,44]. These observations permitted to reconstruct the mass distribution in the inner 0.2 pc, suggesting that such a region would contain $\sim 10,000 M_{\odot}$ in BHs, and it is an unlikely nursery for an intermediate-mass black hole (IMBH) heavier than $10^3 M_{\odot}$ [39,45], supporting previous theoretical arguments [e.g., 46–52]. Further evidence of BHs at the Galactic Centre comes from recent observations of X-ray emission from a dozen X-ray binaries in the inner pc that suggest the presence of over 20,000 stellar BH and NS lurking there [53]. Despite this observational finding is still under debate [54], it finds support in several theoretical works [55–57], and seems a reasonable and natural outcome of stellar evolution for the Galactic NC [58,59].

Placing stringent constraints on the theoretical models of COBs formation in galactic nuclei can enable us to create diagnostic scheme to interpret their observations, especially with regards to stellar BHs in the era of gravitational wave (GW) astronomy.

In fact, despite the observations of BHs in binary systems became recently possible by observing the stellar companion’s motion [60–62], and electromagnetic emission (EM) from accreted material [63,64], even in the Galactic Centre [53], GW detections represent so far the only known technique to provide uncontroversial proof of the existence of black hole binaries (BBHs). Since the groundbreaking discovery of GWs emitted by a merging BBH [65], the LIGO-Virgo-Kagra collaboration (LVC) performed three observing runs and assembled a catalogue of almost 100 GW sources [65–78], making clear that the interpretation of these observations requires a profound rethinking of our understandings of COBs formation and evolution. So far, the so-called GWTC-3 catalogue of GW sources includes mergers from ~ 60 BBHs, 2 double NSs, and 2 NS-BH binaries, the first merger with total mass in the IMBH mass range above $100 M_{\odot}$, and the first merger involving one object with mass $2.6 M_{\odot}$, either the lightest BH or the heaviest NS ever detected in a merging binary. With a number of detections that doubles the number of detections performed via EM emission and proper motion, the LVC BHs are becoming sufficiently numerous to enable placing constraints on the overall properties of the underlying population of BHs in merging binaries [77]. Interpreting the inferred properties of observed BBH mergers requires to understand the physics that regulates the formation and evolution of single and binary COs and their stellar progenitors, and the impact of different formation channels on their global properties.

Significant improvements in stellar evolution theories undoubtedly helped us to better understand the processes that govern the evolution of single and binary massive stars and how they can merge in galactic fields, despite the still many uncertainties about the CO mass spectrum, natal spins, and kicks [for an extensive review on the topic, see 79]. In particular, there are two aspects of stellar evolution particularly relevant to the formation and merger of COBs, namely the so-called *upper* and *lower* mass-gaps.

Generally, stars with zero-age main sequence (ZAMS) masses in the $22 - 26M_{\odot}$ range are expected to end their life in a supernova (SN) event. If the SN explosion happens on a timescale ~ 250 ms [rapid SN model, 80] the remnant will have a mass falling in the $3 - 5M_{\odot}$ range, whilst if the explosion timescale is order of seconds the star undergoes a failed SN and directly collapse to a BH with a mass above the $3 - 5M_{\odot}$ range [delayed SN model, 80]. This opens a gap in the CO mass spectrum, called the lower mass-gap, whose existence is highly uncertain observationally [e.g. 81,82] and intrinsically relies on the uncertain physics of stellar evolution [79]. Heavier stars that develop a He core with a mass $\sim 64 - 135M_{\odot}$, instead, are expected to undergo an explosive process, the pair-instability supernova (PISN), which rips the star apart and leaves no remnant [83,84]. Stars with a lighter core ($32 - 64M_{\odot}$) develop rapid pulses that enhances mass-loss before the SN explosion – so-called pulsational pair instability (PPISN) [84,85]. These two processes, PISN and PPISN, cause a dearth of BHs with masses in the $40 - 150M_{\odot}$ range [85–90]. The extent of this "upper" mass-gap is rather uncertain, as it depends on stellar rotation, nuclear reaction rates, and accretion physics [91–95].

Broadly speaking, the formation channels of merging COBs are grouped into two main channels: isolated, i.e. a stellar binary paired at birth which turns into a COB that eventually merges without the intervention of other objects, and dynamical, i.e. a COB assembled dynamically which eventually merges with the aid of multiple gravitational scatterings in star clusters. Unfortunately, the localization accuracy of current GW detectors is too low to pinpoint the location of the merger event, thus generally the impact of different formation channels onto the overall merger population is assessed on a statistical basis. Several recent works tried to untangle signatures of different formation scenarios in BBH merger populations by looking at different parameters that can be retrieved from GW detections – like component mass, chirp mass, effective spin parameter – but hugely depends on many uncertainties: the cosmic star formation history or metallicity distribution, BH natal spins and mass spectrum, the physics of single and binary stellar evolution, the properties of star clusters at birth, and the physics of galactic nuclei [96–102].

The mass of the merging objects represents one of the possible quantities that can be used to discern between an isolated and dynamical origin. BBHs formed in isolation is expected to have components with a mass below $40 - 60M_{\odot}$, owing to PISN and PPISN mechanisms [e.g. 86,103], thus making hard to explain the existence of upper mass-gap objects – like the one observed in GW190521 source [76] – via isolated stellar evolution only. Upper mass-gap objects are easier to form in dynamically active environments, like star clusters and galactic nuclei, where they can form either via stellar mergers [104–110], BH-star accretion events [105–107], or repeated – so called *hierarchical* – mergers [98,99,105,111–116]. These processes are affected by uncertainties though: stellar evolution of post-merger stars is poorly known and requires detailed hydrodynamical simulations [e.g. 109,110,117], the fraction of stellar matter actually accreted onto a BH in a star-BH collision is rather unknown [118–122], and repeated mergers are hampered by post-merger GW recoil kicks [123–125] that can eject the remnant BH from the host cluster and avoid further mergers [98,98,126–129]. Similarly, the development of mergers with one component in the lower mass-gap, like GW190814 [74], seem to be unlikely in isolated binary models [100], whilst they can more easily form dynamically [130–136].

The level of spin alignment represents another quantity useful to discern isolated and dynamical mergers. In fact, isolated mergers are expected to feature (approximately) aligned spins [137–139], whilst in dynamical mergers the chaotic process forming the binary is expected to distribute the spin-orbit angle isotropically [99,102,138,140].

Hierarchical mergers, which are a natural byproduct of dynamics in high-density environments, might have unique mass-spin features, thus a combined statistical analysis of such quantities could help determining whether an observed GW source originated from remnants of previous merger episodes. For example, assuming that the cosmic population of merging

BHs is characterised by a spin distribution peaked at relatively low values, as indicated by GW observations [141], implies that a population of second generation mergers will be inevitably characterised by larger masses and higher spins, thus being clearly discernible from the population of first generation mergers and possibly from isolated mergers too [99,142].

Aside from masses and spins, there is a further binary parameter that could represent a smoking gun of a dynamical origin, the binary orbital eccentricity. Placing constraints on the eccentricity of observed mergers became possible only in recently [e.g. 143–146], and led to place constraints on the eccentricity of up to 4 LVC sources, for which possibly $e > 0.1$ [147–150]. Interestingly, for eccentric sources the accuracy on the parameter measurement can significantly increase, e.g., the chirp mass (localization) accuracy of an eccentric $30 - 30M_{\odot}$ BBH can be $\sim 10^1(10^2)$ times higher than for the circular case [151]. Generally, LVC detectors at design sensitivity could distinguish between circular and eccentric models provided that $e_{10\text{Hz}} > 0.04$, being the measurement error on the eccentricity around $\delta e \sim (10^{-4} - 10^{-3})(D/100\text{Mpc})$ [151,152].

In isolated COBs several processes (e.g., tidal interactions or dynamical friction during a common envelope phase) tend to circularise the orbit of the binary progenitor [e.g. 153–157], although some of the physical processes still partly unknown – like common envelope – could produce mildly eccentric binaries [158]. Conversely, the eccentricity distribution of dynamically assembled BBHs generally follows a thermal distribution, $P(e)de \sim 2e$, which implies a probability of 50% to form a binary with eccentricity $e > 0.7$. Theoretical models predict that around 1 – 10% of mergers forming in globular clusters can have an eccentricity $e > 0.1$ in the frequency band typical of LVC and ground-based GW detectors (i.e. 10 Hz) [138,159–161], and up to 30% could be eccentric in the LISA band ($\sim 10^{-3}$ Hz) [162–164].

What about galactic nuclei? In such complex environments, the formation of COBs is regulated by a variety of dynamical processes – some acting in concert, others acting in contrast – which intrinsically affect the overall properties of those that eventually merge, and may leave imprints that could differ from the general expectations of the dynamical channels.

This review aims at providing a broad overview of the processes that can aid or hamper COB formation and mergers in galactic nuclei harbouring a central SMBH, either in its quiescent or active phase, possibly surrounded by a NC, and to discuss the main properties and detection prospects of GW sources formed in galactic nuclei. We organise the review according to the main phases characterising the evolution of a galactic nucleus, following a zoom-in scheme, from the possible formation of the central NC to the coalescence of COBs:

- We start by briefly reviewing the current knowledge on the observational evidence of single and binary COs in galactic nuclei (Section 2);
- We describe how the environment, stellar evolution, and dynamics can affect CO populations (Section 3 and 4);
- Moving closer to the SMBH, we describe the main dynamical processes at play to form COBs in galactic nuclei (Section 5) and discuss the impact of secular processes in quiescent galactic nuclei (Section 6) and gaseous effects in AGNs (Section 7) on the formation of merging COB;
- Finally, we discuss the main properties of merging COBs in galactic nuclei, focusing on the prospects for current and future GW detections (Section 8).

Figure 1 sketches the main phases of COB formation in galactic nuclei, and provides a schematic and ordered illustration of the themes touched on in this review.

2. Observational evidence of binaries in galactic nuclei: the Milky Way test case

Most if not all of high mass stars *in the field* reside in a binary or higher multiple configurations [166–169]. Although challenging, observations of the inner pc of the Milky Way revealed the presence of a handful spectroscopic and eclipsing binaries comprised of massive OB and

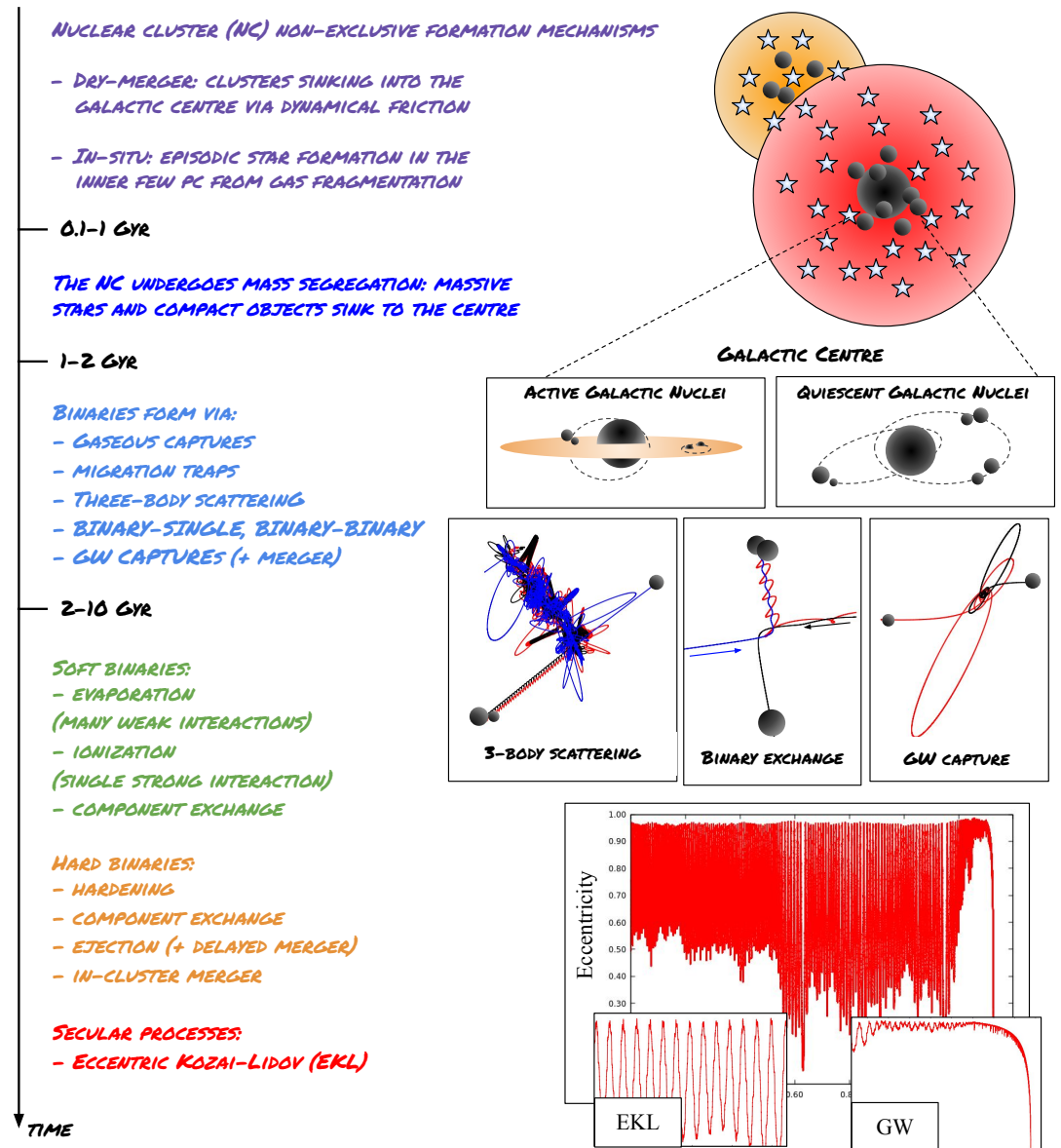


Figure 1. Schematic illustration of the galactic nuclei zoo: a nuclear cluster (NC) forms via in-situ star formation and mass transport from infalling star clusters; in its inner parts a variety of dynamical interactions can trigger the formation of compact object binaries (COBs); in other cases, COBs promptly merge releasing gravitational waves (GWs); in some other cases, the COBs evolution is determined by the central supermassive black hole (SMBH) gravitational field, which can impinge periodic oscillations on the binary eccentricity and ultimately lead to their coalescence. The depicted interactions are actual N -body simulations carried out with the ARGd code described in Arca-Sedda and Capuzzo-Dolcetta [165].

Wolf-Rayet (WR) stars [170–174]. These observations suggest that the fraction of spectroscopic binaries attain values $f_b \simeq 0.34$, whilst this quantity drops to $f_b \sim 0.03 - 0.04$ for eclipsing binaries, similar to the binary fraction inferred in young clusters. More in general, the aforementioned observations suggest that the total fraction of massive binaries in the Galactic NC is comparable to the field [e.g. 170,172]. The observation of X-ray sources [53,175], and diffuse X- [e.g. 176–178] and γ -ray [179–186] emission at the Galactic Centre support the presence of COBs in galactic nuclei, although it is unclear whether they are related to X-ray binaries, millisecond pulsars, or cataclysmic variables [e.g. 53,56,59,175–178,187,188].

Complementary theoretical and modelling studies of these observations also suggested that the binary fraction in the inner 1 pc at the centre of the Galaxy is high. For example, star formation models suggest that *in situ* formation of stars and thus binaries is expected at the centre of galaxies [e.g. 189,190]. Hyper velocity stars [e.g. 191–195] may imply the existence of binaries that arrive on a nearly radial trajectory to the tidal breakup radius of the SMBH, known as the Hills mechanism [196]. This mechanism may eject one star at a high velocity while the other one may be captured on an eccentric orbit close to the SMBH, which was proposed to explain the existence of the S-cluster [e.g. 58,197–202].

Other theoretical and observational analyses suggest that binaries can remain stable for long-time even when interacting with neighboring stars [e.g. 173,203]. Thus, over the age of the young stars of the nuclear star cluster, estimated as a few Mys [204], about 70% of the binaries may retain their binary configuration [205]. Lastly, it was suggested that some of the peculiar features of the stellar disc in the Galactic Centre [206,207], can be explained by the possible observed high fraction of binaries [208].

3. Environmental effects on binary formation in galactic nuclei

How can COBs form in galactic nuclei? This is one of the key questions that we try to address in this review. This section is devoted to discuss how the presence of pristine stellar binaries and the formation process of the galactic nucleus can impact the formation of COB and COBs.

3.1. Binaries in galactic nuclei: primordial, dynamical, or hybrid?

Generally, it is possible to distinguish two main formation channels for stellar and CO binaries: either the binary components were already paired at birth, in which case the binaries are called *primordial*, or they found each other via multiple interactions with other stars and COs forming *dynamical* binaries. In dense stellar environments, such as massive clusters and NCs, a further possibility suggests that primordial binaries underwent interactions with other members of the galactic nucleus and either suffered orbital modifications or exchanged one of their components, thus they constitute a *hybrid* class, half-way between purely primordial and dynamical binaries.

Either way, after their formation, the evolution of these binaries will inevitably be affected by dynamical encounters, which in galactic nuclei are typically more frequent and violent than in galactic fields. During each subsequent interaction, binaries and single objects suffer a change of their energy and angular momentum, up to a point where the system will have lost memory of its initial conditions. This process, called relaxation, occurs on a time-scale roughly given by [209,210]:

$$t_{\text{relx}} = 4.2 \text{ Gyr} \left(\frac{15}{\log \Lambda} \right) \left(\frac{R_h}{4} \right)^{3/2} \sqrt{\frac{M_c}{10^7 M_\odot}}, \quad (1)$$

where $\log \Lambda$ is the Coulomb logarithm, R_h is the cluster half-mass radius, and M_c its total mass.

There is a plethora of dynamical processes that can concur with the formation and evolution of binaries in a dense galactic nucleus. Some of them involve single or multiple dynamical interactions with other stellar objects (see Section 5), like GW bremsstrahlung in single-single encounters (cap), three-body encounters (3bb), binary-single (bs) and binary-binary (bb) encounters, triple evolution (3ev). Others, involve secular effects impinged by the galactic nucleus morphology, the gravitational field of the central SMBH, or the collective effect of all stars orbiting around the SMBH (see Section 6), including the eccentric-Kozai-Lidov (EKL) oscillations, general relativistic effects arising from the motion around the SMBH (1pN), and scalar (rr,s) and vector resonant relaxation (rr,v) processes, which torque the orbit of the i -th star owing to the overall perturbation from all the $N - i$ stars in the nucleus.

The concurring action of one process or another is regulated by their typical timescales, which can vary over many orders of magnitude depending on the galactic nucleus' properties. Figure 2 briefly summarizes how the timescales connected to these different mechanism vary at varying COB separation and assuming a COB with mass $M_{\text{COB}} = 20M_{\odot}$ and an SMBH with mass $M_{\text{SMBH}} = 10^6 M_{\odot}$. To make the plot more readable we do not include the AGN typical lifetime, which is expected to be a constant value in the range 1 – 100 Myr and the three-body scattering time, which, for this specific example, is several orders of magnitude larger than all other timescales. From the plot, we see that dynamical friction and some of the secular effects, like EKL, clearly operates over timescales shorter than the typical timescale of stellar evolution for CO progenitors (i.e. $\sim 1 - 10$ Myr), suggesting that dynamics may play a role even before massive stars turn into COs.

This dynamical process has crucial implications for the evolution of primordial binaries in massive galactic nuclei like the one in the Milky Way. For example, it has been shown that a population of stellar binaries, in a Milky Way-like NC, would be strongly affected by both dynamical and secular mechanisms, undergoing several possible pathways that take place prior to CO formation, like [see e.g. 59,205]: a) dissociation (75% of the population), b) merger induced by eccentric-Kozai-Lidov oscillations (10%), c) shrinkage and circularization of the orbit due to tidal synchronization (13%), or d) radial mergers and nearly head-on collisions (2%).

Among binaries that shrunk via stellar evolution – i.e. the case c) above – only a fraction of 0.5% decouple from the SMBH dynamics and evolve into a COB that possibly merge within a Hubble time [59]. Note that assuming that the Galactic NC contains $\sim 2.5 \times 10^7$ stars and a primordial binary fraction $f_b = 0.3$ implies a number of *primordial* merging COBs of around $N_{\text{COB}} \sim 2,500$, although such an estimate certainly depends on the details of binary stellar evolution. The population of merging COBs formed from binary stellar evolution is expected to be comprised of BBH ($\sim 75\%$) and NS-BH binaries ($\sim 25\%$), whilst double NS are unlikely to form [59]. These binaries may further interact with neighbouring single objects, possibly leading to the formation of new binaries via component exchange or the binary abundance may be reduced following ionization by strong encounters.

3.2. Nuclear cluster formation processes: *in-situ* versus *dry-merger*

In Section 3.1, we briefly described how primordial binary formation and dynamical and secular processes can affect the formation of stellar and CO binaries. The dominance of one process over another intrinsically depends on the environment. For example, the density and velocity dispersion in the nucleus strongly affect the interaction rate of few-body interactions, whilst matter density distribution determines how likely is for a star to orbit within a given distance from the central SMBH, thus affecting the development of secular effects like EKL indirectly.

In these regards, the presence of a NC in the galactic centre, which is clearly much denser than the stellar distribution of the galactic field, can substantially affect the formation and

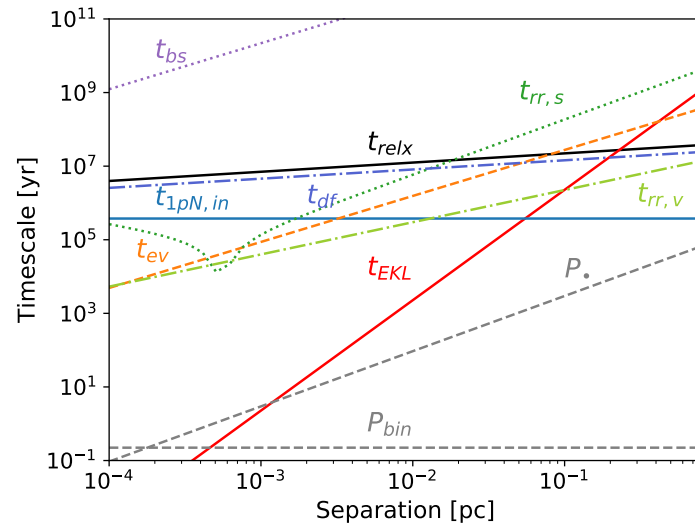


Figure 2. Timescales of several mechanisms affecting the formation of single and binary compact objects in a galactic nucleus similar to the Milky Way. Here we assume a binary mass $M_{\text{COB}} = 20M_{\odot}$ and a supermassive black hole mass $M_{\text{SMBH}} = 10^6M_{\odot}$. Different lines identify different processes: 2-body relaxation (t_{relx}), scalar ($t_{\text{rr,s}}$) and vector ($t_{\text{rr,v}}$) resonant relaxation, evaporation (t_{ev}), dynamical friction (t_{df}), binary-single scattering (t_{bs}), eccentric-Kozai-Lidov (t_{EKL}), general relativistic precession ($t_{1\text{pN,in}}$), binary period (P_{bin}), orbital period of the binary about the supermassive black hole (P_*). For the sake of visibility, the plot does not include the AGN lifetime (nearly constant line 1 – 100 Myr), and the three-body and gravitational-wave capture (single-single) scattering time, which are much larger than all other timescales for the adopted example.

evolution of both single and binary COs. As we will see in this and following sections, high densities and large masses make NCs potential factories of COs and COBs and might provide a significant contribute to the overall population of GW sources, but assessing the actual properties of “nuclear” COB mergers demands to understand how the macro-physics that regulates NC formation affects the micro-physics that governs COs and COBs in galactic nuclei.

NCs are pretty peculiar objects that exhibit a clear flattened morphology and rotation [3,8,211–215], a complex star formation history and multiple stellar populations [216,217], and, in some cases, harbor a central SMBH [6–8,218].

Although the actual fraction of NCs containing an SMBH is rather uncertain [3], this sub-class of NCs represents, as we will discuss in the next section, the ideal place where to study a huge variety of dynamical processes acting simultaneously. Further insights on NCs harbouring an SMBH come from a special class of objects called ultracompact dwarf galaxies (UCDs) [219]. Generally, a UCD is a compact stellar system characterised by a complex star formation history, a central SMBH, and an associated stellar stream [220]. These objects are thought to be the relics of galactic nuclei stripped in a galaxy merger event [221,222], and their properties apparently overlap with those of massive globular clusters and NCs [223]. If UCDs are what remain of NCs stripped away from their parent galaxies, the fraction of NCs harbouring an SMBH could be as large as 75 – 90% [224]. Generally, the mass of NCs and SMBHs seems to linearly scale with the host galaxy stellar mass [1,225,226]. Moreover, the SMBH-to-NCs mass ratio increases with the galaxy mass [3], and NCs become too faint to be identified in galaxies with masses $M_g \gtrsim 10^{10}M_\odot$, i.e. when the SMBH-to-NCs mass ratio becomes larger than 1 [7].

These interesting peculiarities may be intrinsically related to the processes that regulate NC formation, which are still partly unknown.

There are currently two most debated formation scenarios for NCs: in-situ and dry-merger. In the in-situ scenario, gas funnelled toward the galactic centre, e.g.owing to the effect of the galactic bar or inhomogeneities associated with a galaxy merger, cools and fragments, forming stars in a dense NC [227–236]. The in-situ scenario may explain some of the features observed in NCs, like rotation and flattening, the development of multiple episodes of star formations, and the absence of NCs in galaxies heavier than $10^{11}M_\odot$, where the radiative feedback of the central SMBH becomes sufficiently strong to quench star formation and hamper the NC growth [e.g. 233].

The basic idea behind the dry-merger formation scenario, instead, is that massive bodies traveling through a sea of lighter particles, like a star cluster moving in the galaxy field, experience a drag, called dynamical friction, that slowly forces it to spiral inward and ultimately collide to form a NC [223,235,237–244]. The typical timescale of this process can be relatively short ($\sim 0.1 - 1$ Gyr) [242,243,245]. As the clusters move inward, the increasing tidal force exerted from the galactic field and possibly from the central SMBH strips their outer regions while their core keeps spiralling in. The competing action between tidal forces and dynamical friction ultimately determine whether spiralling clusters can efficiently build-up an NC. Both observations [7,37], simulations [246], and semi-analytic models [235,242,245] seem to support this picture, suggesting a typical host galaxy virial mass, $M_g \gtrsim 10^{11}M_\odot$, above(below) which nuclei are dominated by a central SMBH(NC). Therefore, both the in-situ and dry-merger scenario may be able to explain (some) observational features of NCs, making it difficult to identify a single dominant process. In fact, the most recent works indicate that the in-situ and the dry-merger scenario work in concert, with the former possibly leading NC formation in galaxies heavier than $10^9 - 10^{10}M_\odot$ and the latter being the dominant channel in smaller galaxies [215,235,246–249].

Interestingly, it seems that the average age of NC stars increases at decreasing the host galaxy mass [215,248,249], indicating that NCs in galaxies like the Milky Way likely formed

through either a recent star formation burst (in-situ) or the collisions of young massive clusters born close to the galactic nucleus (dry-merger), whilst NCs in dwarf galaxies might be the relics of ancient cluster collisions or star formation occurred during an early stage of the galaxy life.

Do NCs form first and SMBHs grow later or viceversa? This basic “chicken or egg” question is still unanswered. From the observational point of view, while SMBHs candidates have been observed up to redshift $z \gtrsim 7$ [250], it is practically impossible to distinguish a NC at those cosmological distances, thus making impossible to date the oldest and farthest NCs. From the theoretical point of view, some works propose that *primordial* NCs in high-redshift galaxies can sustain the formation of SMBH seeds via BH merger and accretion events [e.g. 251–253], whose subsequent growth could evaporate the NC. Whilst this possibility may explain the dearth of NCs in the most massive galaxies, it is at odds with their observation in low-redshift ($z < 1$) galaxies with masses $M_g < 10^{11} M_\odot$, thus suggesting that there may be different NCs formation processes. Other theoretical works, instead, propose that the SMBH forms first and a NC forms later either via fragmentation of gaseous clouds [233] or star cluster infall [238]. For simplicity, in the following we assume that SMBHs are already fully grown at NCs formation.

3.2.1. The impact of nuclear cluster formation scenarios on the population of compact objects in galactic nuclei

How can the NC formation scenario affect the formation of single and binary COs?

In the case of the in-situ scenario, stellar and CO binaries form either *primordially* during the star formation process, or *dynamically* via multiple encounters. The total number of CO progenitors is set by the NC mass and the adopted initial mass function (IMF) of stars, and could be possibly enriched by multiple star formation episodes over cosmic history. In this sense, both COs and their progenitors form in the same environment. Let us consider a NC formed purely through the in-situ mechanism, with a total mass of $M_{\text{NC}} = 10^7 M_\odot$ and an average stellar mass of $m_* = 1 M_\odot$. Assuming a typical initial mass function [254], and considering the fact that COs forms from the death of stars heavier than $\gtrsim 18 M_\odot$, we expect that COs constitute a fraction $f_{\text{BH}} \sim 10^{-3}$ of the whole population. Therefore, the total number of BHs harbored in our in-situ NC should be simply given by

$$N_{\text{BH},in} = f_{\text{BH}} M_{\text{NC}} / \langle m_* \rangle = 10,000. \quad (2)$$

The population of NSs, instead, are significantly affected by two processes. The first is related to the fact that NSs at birth receive a natal kick that in 60 – 90% of the cases exceeds 100 km s⁻¹ [see e.g. 255], thus NSs would be promptly ejected even if they formed in a dense NC. Note that the problem of NS natal kicks is still actively debate. Observations of Galactic pulsars suggest that the distribution of NS kicks is either Maxwellian, with a dispersion of $\sigma = 265$ km s⁻¹ [256], or bimodal [257–259]. From the theoretical standpoint, recent models focused on SN explosion predicts that the kick amplitude depends on the mechanism that trigger the explosion [e.g. 260,261], with the so-called electron-capture SN (ECSNe) possibly being the main source of NS retention in star clusters [262]. Moreover, once BHs settle in the galactic centre owing to mass-segregation, they will prevent the segregation of lighter stellar species, pushing them onto wider orbits [e.g. 133,263]. Since the fraction of stars turning into a NS is expected to be roughly $f_{\text{NS}} = 10^{-3}$, we would expect only $N_{\text{NC},in} = f_{\text{ret}} f_{\text{NS}} M_{\text{NC}} / \langle m_* \rangle = 6,000 - 9,000$, with $f_{\text{ret}} = 0.6 - 0.9$ the NS retention fraction for an escape velocity of 100 km s⁻¹. Despite being much lighter than BHs, also NSs may follow a cuspy surface density profile with $r^{-1.5}$, as shown in [264–266].

Let us consider now the dry-merger scenario.

In the case in which the galactic nucleus is entirely made up by spiralled star clusters, the total amount of mass in BHs brought there will represent a fraction f_{BH} of the cluster mass. If the BHs were mass-segregated in the parent cluster, it is reasonable to assume that

$M_{\text{BH}} \sim f_{\text{BH}} M_c$. However, owing to the galactic field, only a fraction f_i of the clusters mass will reach the centre and build-up the NC, $M_{\text{NC}} = \sum_i f_i M_c$.

Let us assume that a population of $N_c = 20$ clusters with mass $M_c = 10^6 M_\odot$ fall in a galactic nucleus and lose a fraction $f_i = 0.5$ of their initial mass [see e.g. 48]. The NC mass will thus be $M_{\text{NC}} = f_i N_c M_c$. In the process, the clusters will bring into the growing nucleus a fraction $f_{\text{BH}} \sim 10^{-3}$ of their total number of stars in the form of BHs, because BHs are likely segregated in the cluster core and they will not be affected by the cluster mass-loss process. Thus, the number of BHs lurking in the final nucleus will be equal to

$$N_{\text{BH,dry}} = f_{\text{BH}} N_{\text{cl}} M_{\text{cl}} / \langle m_* \rangle = 20,000, \quad (3)$$

around twice compared to the mass inferred for an in-situ NC, although the difference in the numbers of BHs can be substantially affected by a number of unknown quantities, like the star cluster mass function and galactocentric distribution, the SMBH mass, or the amount of cluster mass actually brought into the galactic centre. In the case of the dry-merger scenario, the timescale over which clusters collide to form an NC can crucially determine whether dynamics and stellar evolution processes have already affected the population of COs in the infalling clusters. This aspect is particularly important for the population of NSs that can be transported into a galactic nucleus through this process. For clusters with escape velocity $\sim 40 \text{ km s}^{-1}$, it has been shown that only 5–10% of NSs receives a kick sufficiently small to be retained [255,262]. If the infall process proceeds slower than stellar evolution, NSs will form in their parent cluster and most of them will likely be ejected well before reaching the galactic nucleus. If we assume that only a fraction $f_{\text{ret}} \sim 0.05 - 0.1$, the number of NSs that can be accumulated in a Milky Way-like nucleus is $N_{\text{NS,dry}} \sim f_{\text{ret}} f_{\text{NS}} N_{\text{cl}} M_{\text{cl}} / \langle m_* \rangle \sim 1,000 - 2,000$, thus a factor 4-5 smaller than in the case of the in-situ NC formation scenario. Suppose the infall process, instead, is faster than the stellar evolution process. In that case, stars will evolve into NSs after settling into the galactic center, and their retention fraction will likely be similar to the one inferred for the in-situ process, in which case $N_{\text{NS,dry}} \sim 12,000 - 18,000$.

Future observations capable of providing insights onto the population of BHs and NSs at the Galactic Centre could thus provide crucial information about the NC formation history [267], as different formation channels are expected to produce a substantially different population of COs. Clearly, the arguments above serve as an order of magnitude estimate, and a more detailed approach is needed to fully characterise the properties of COs in galactic nuclei and the processes operating there.

Given a star cluster with mass M_c , orbital radius r_c and eccentricity e_c , dynamical friction will drag it into the galactic centre over a timescale [243,268]

$$t_{\text{df}} = 0.3 \text{ Myr} \left(\frac{R_g}{1 \text{ kpc}} \right)^{3/2} \left(\frac{M_g}{10^{11} M_\odot} \right)^{-1/2} \left(\frac{M_g}{M_c} \right)^{0.67} \left(\frac{r_c}{R_g} \right)^{1.76} f(e_c, \gamma), \quad (4)$$

where M_g , R_g , and γ represent the galaxy total mass, length scale, and slope of the density profile. The term $f(e_c, \gamma)$ is a function of the infaller orbital eccentricity and the density slope [243]:

$$f(e_c, \gamma) = (2 - \gamma) \left[a_1 \left(\frac{1}{(2 - \gamma)^{a_2}} + a_3 \right) (1 - e_c) + e_c \right], \quad (5)$$

where $a_1 = 2.63 \pm 0.17$, $a_2 = 2.26 \pm 0.08$, and $a_3 = 0.9 \pm 0.1$. It is worth noting that this simple expression for the dynamical friction timescale represents a relatively good approximation also for COs orbiting inside a massive star cluster [263].

As the cluster orbit around the galactic centre, and slowly sink, its internal dynamics will be regulated by several internal processes, the earliest of which will be mass-segregation [209,269], a mechanism driven by dynamical friction [270] by which the most massive stars

rapidly segregate toward the cluster centre [269]. The mass-segregation time-scale can be expressed as [210]:

$$t_{\text{seg}} = 0.42 \text{ Gyr} \left(\frac{10m_*}{m_{\text{CO}}} \right) \frac{t_{\text{relx}}}{4.2 \text{ Gyr}} \left(\frac{r_{\text{CO}}}{R_h} \right)^{3/2}, \quad (6)$$

where $m_{*,\text{CO}}$ is the average mass of stars(COs), and t_{relx} is the half-mass relaxation time. 378

Mass-segregation gathers the most massive objects into the inner cluster regions, favouring 379
the development of strong interactions and ejection of the most massive components. This 380
mechanism is particularly effective once BHs have formed and settled in the centre of the 381
cluster. In fact, owing to their cross section, larger than for “normal star”, the most massive 382
BHs tend to undergo the strongest interactions in cluster nuclei, pairing together and ejecting 383
each other from the parent cluster in what is called the *BH burning process* [e.g. 271,272]. 384

As a consequence, internal dynamics will have time to affect the CO population in star 385
clusters with sufficiently short segregation times, i.e. $t_{\text{seg}} < t_{\text{df}}$, before they reach the galactic 386
centre and collide to build-up the NC. If the segregation time is even shorter than the timescale 387
of stellar evolution for massive stars, though, interactions among the most massive stars 388
can trigger runaway stellar collisions and possibly the formation of a very massive star that 389
ultimately can collapse in an IMBH [e.g. 273–275]. 390

Figure 3 compares the dynamical friction and mass-segregation timescales for a population 391
of COs with mass $m_{\text{CO}} = 5 - 50M_{\odot}$ inhabiting star clusters with a mass in the range $M_c =$ 392
 $10^4 - 7M_{\odot}$ and half-mass radius $R_h \sim 1\text{pc}(M_c/M_{\odot})^{0.13}$ [276], orbiting at a distance of $r_c =$ 393
 $50 - 100 \text{ pc}$ in a galaxy with total mass $M_g = 10^{11}M_{\odot}$, scale radius $R_g = 1 \text{ kpc}$, and slope of 394
the density profile $\gamma = 0.5$. 395

The plot suggests that the population of massive stellar objects has already been “dynamically 396
processed” in clusters with a mass $M_c < 10^5M_{\odot}$ when they reach the galactic centre, 397
whilst the population in the heavier cluster should be more representative of the cluster’s 398
initial population. Let us consider a population of N_{dec} clusters each composed on average 399
of $N_* = 10^6$ members, a fraction f_{BH} of which being in COs, and a fraction η of their COs in 400
binaries. If a fraction δ of all COBs survives the cluster infall, the total number of delivered 401
COBs via dry-merger mechanism will be [48] 402

$$N_{\text{dec}} = 2,000\delta \left(\frac{N_{\text{dec}}}{20} \right) \left(\frac{f_{\text{BH}}}{10^{-3}} \right) \left(\frac{N_*}{10^6} \right) \left(\frac{\eta}{0.1} \right). \quad (7)$$

Note that if the infalling clusters are “dynamically young”, meaning that the cluster relaxation 403
time is much shorter than the infall time, their CO population will still be unaffected by 404
dynamical processes and a fraction $\delta = 0.7 - 0.88$ of their BH population can be brought to the 405
galactic centre [48]. 406

Once COs are formed, or are brought, in the galactic centre, their subsequent evolution will 407
mostly driven by dynamics, making it hard to distinguish objects formed in-situ or delivered 408
by infalling clusters. Possible differences may arise in the number and orbital properties of 409
COBs and the mass spectrum of COs. For example, dynamical processes will have had time 410
to substantially affect the population of BHs and NSs in clusters falling into the NC over 411
timescales longer than clusters’ dynamical times, likely reducing the number of COs and 412
the average BH mass – owing to the BH-burning process. Exploring how different can CO
populations in in-situ or dry-merger NCs is difficult, owing to the underlying uncertainties,
and in fact generally in the literature the initial properties of single and binary COs relies upon
agnostic guesses. Devising and developing self-consistent NCs models that implement both
the NC formation process and the detailed stellar dynamics and evolution is key to shed light
on the fingerprints of NC formation history on the population of single and binary COs in
galactic nuclei.

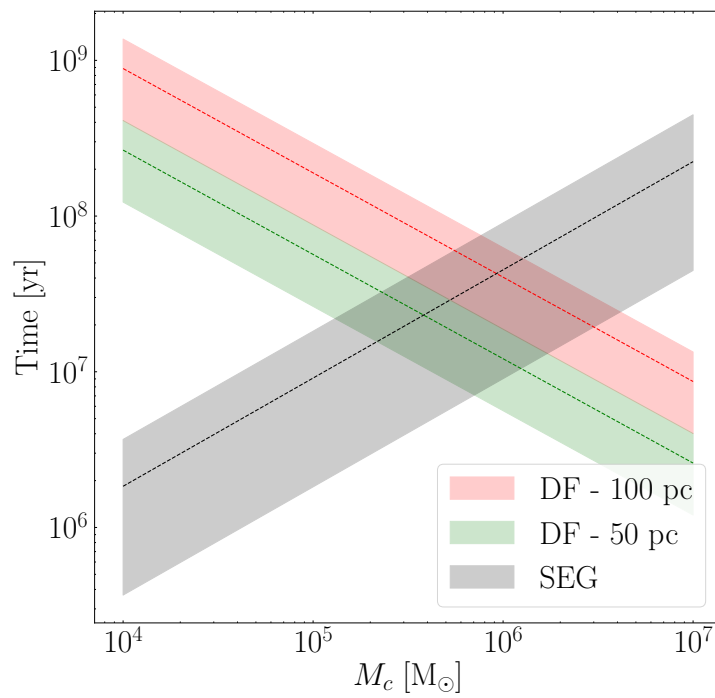


Figure 3. Dynamical friction timescale as a function of the cluster mass assuming that the cluster orbits at 50 pc (green) or 100 pc (red) in a galaxy with total mass $M_g = 10^{11}M_\odot$, scale radius $R_g = 1$ kpc, and slope of the density profile $\gamma = 0.5$. For comparison, we show also the cluster mass-segregation time (grey). The shaded areas embrace the boundaries assuming COs with masses $m_{\text{CO}} = 5 - 50M_\odot$.

4. Early black hole dynamics in nuclear clusters and galactic nuclei

After the NC assembly its stars and COs will inevitably undergo mass-segregation, which can be described in terms of the "individual" dynamical friction time of each CO or massive star from Equation 4:

$$t_{\text{df}} = 1680 \text{yr} \left(\frac{R_{\text{NC}}}{2 \text{pc}} \right)^{3/2} \left(\frac{M_{\text{NC}}}{2.5 \times 10^7 M_{\odot}} \right)^{-1/2} \left(\frac{M_{\text{NC}}}{m_{\text{BH}}} \right)^{0.67} \left(\frac{r}{R_{\text{NC}}} \right)^{1.76} f(e, \gamma), \quad (8)$$

where now M_{NC} , R_{NC} , and γ represent the NC mass, length scale, and density slope, respectively, whilst m_{BH} represents the CO mass and r its orbit. Note that the scaling values adopted above correspond to the Galactic NC. Note that t_{df} is valid also for galaxies without a central NC – in which case one should consider the properties of the bulge in Equation 8 – and can return a more accurate estimate of the mass-segregation time in the case of galactic nuclei, which are often characterised by cuspy density profiles [2].

An important element that needs to be taken into account to estimate how many COs inhabit a galactic nucleus is related to the stellar evolution of COs progenitors, especially for what concern stellar BHs. On the one hand, stellar progenitors are somewhat heavier than their remnants, thus dynamical friction is more effective on them. On the other hand, COs at formation can undergo a recoil, owing to supernova (SN) kick, which can delay their orbital segregation.

The motion of a CO, or its progenitor, subjected to dynamical friction can be expressed as [277]

$$r_{\text{CO}}(t) = r_{\text{CO},0} \left(1 - \beta \frac{t}{t_{\text{df}}} \right)^{1/\beta}, \quad (9)$$

with $\beta = 1.76$.

From Equation 8, a star sufficiently massive ($\gtrsim 18 - 20 M_{\odot}$) starting from 0.1 – 1 pc from the SMBH in a MW-like nucleus will reach the centre in $t_{\text{df}} \sim 1 - 80$ Myr, thus it will likely reach its last evolutionary stage while travelling through the galactic nucleus. If the newborn CO receives a natal kick, as expected for both BHs and NSs [see e.g. 80,257,258,278], the imparted momentum will suddenly displace the object from its orbit, or even eject it from the galactic nucleus. If the kick amplitude is smaller than the host escape velocity, the CO will eventually return toward the centre over a dynamical friction timescale.

In order to provide the reader with a simple view on how the interplay of single star stellar evolution and dynamics can shape the evolution of COs in galactic nuclei we exploit the B-POP population synthesis code [99], which combines stellar evolution models for single and binary BHs obtained with the MOBSE tool [279] and semi-analytic recipes to describe the motion and pairing of BHs via dynamics. Using B-POP, we consider a NC with mass $M_{\text{NC}} = 2.5 \times 10^7 M_{\odot}$ and assume that a fraction $\sim 10^{-3}$ of such mass consists of BH progenitors, assuming that the underlying mass distribution follows a standard initial mass function [254]. For each BH progenitor in the NC, we retrieve the final BH mass, the life-time, and the SN kick. We divide the time in logarithmic bins and calculate the BH progenitor position via Equation 9. As soon as the time exceeds the i -th progenitor life-time, we turn it into a BH (assuming a metallicity $Z = 0.0002$) and assign a natal kick amplitude v_{kick} , which is based on the stellar evolution recipes implemented in the MOBSE population synthesis tool. Given the kick, we assume that the newborn BH will reach a maximum distance r_{max} in a travel time $t_{\text{tr}} = r_{\text{max}}/v_{\text{kick}}$, and then it comes back over a dynamical friction time. In order to simplify the visualization of such complex system, we present in the sketch in the left panel of Figure 4 a cartoon showing the evolution of BH progenitor stars. More quantitatively, we show in the right panel of the same figure the time evolution of the radii containing the 10%, 25%, 50%, 75% – referred to as *lagrangian* radii – of BH mass in this simple toy model. The SN-kick effect is rather

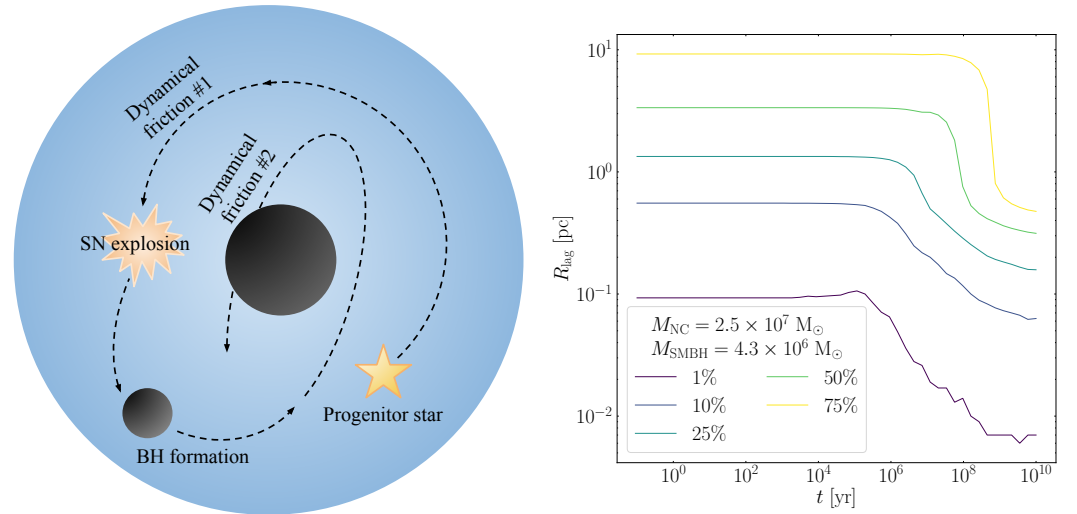


Figure 4. Left panel: schematic view of the orbit of a BH progenitor in a galactic nucleus. The occurrence of a SN event can impart a kick on the newborn BH and delay the segregation. Right panel: lagrangian radii enclosing 10%, 25%, 50%, and 75% of BH (or BH progenitor) mass as a function of time assuming a nucleus with mass $M_c = 2.5 \times 10^7 M_{\odot}$ and an SMBH with mass $M_{\text{SMBH}} = 4.3 \times 10^6 M_{\odot}$.

small, owing to the relatively small kick amplitude compared to the NC velocity dispersion, suggesting that in a MW-like nucleus mass segregation is practically accomplished over a time span of $\sim 10^{7-8}$ yr. 452
453
454

The population of BHs accumulated in the galactic centre will be characterised by a steeper density profile compared to normal stars and possibly by larger densities [268,280,281], a feature that can crucially affect COB formation. Once BHs settled in, they can efficiently evacuate lighter objects [e.g. 263], removing normal stars but also other COs like white dwarfs and NSs, and hampering the possible formation of double NS or NS-BH binaries. 455
456
457
458
459

This *shielding* operated by BH dynamics can be alleviated by the BH burning process, opening the possibility to NS-BH binary formation over a few relaxation times [130,136]. 460
461

In the next section we will describe how COs and especially BHs interact once they have gathered into the innermost regions of the host galaxy centre. 462
463

5. Dynamical formation of black hole and compact object binaries in galactic nuclei 464

5.1. Galactic threats: what binaries can survive around a supermassive black hole? 465

Regardless the formation scenario, in a dense environment around an SMBH, a binary system frequently encounters other stars [e.g., 30,203,210,282–288]. This process results in a variation of the angular momentum and energy of interacting stars or COs with passing neighbours, displacing them from their position and forcing them to wander around the SMBH [e.g., 203]. When a passing star or a compact object approaches the binary with impact parameter on the order of the binary’s separation, it interacts more strongly with the closer binary member. The outcome of this interaction depends on the ratio of the binary’s gravitational binding energy to the kinetic energy of the neighboring stars. We will discuss in detail the possible outcomes of these “binary-single” interactions in Section 5.3.3. 466
467
468
469
470
471
472
473
474

Generally, the “resistance” of a binary against a strong interaction with another object can be quantified via the *softness* parameter [e.g., 282,289]

$$s = \frac{E_{\text{bind}}}{\langle m_* \rangle \sigma^2} \begin{cases} < 1 & \text{Soft} \\ > 1 & \text{Hard} \end{cases} \quad (10)$$

where $E_{\text{bind}} = Gm_1m_2/(2a_{\text{bin}})$ is the binary binding energy, $\langle m_* \rangle$ is the average mass of the objects (either stars or compact objects) in its vicinity and σ is the velocity dispersion of the environment. If the softness is larger(smaller) than unity, the binary is labelled as hard(soft), and a strong interaction will harden(soften) the binary further, a mechanism known as *the Heggie's law* [282,286].

In the case of hard – or immortal [237] – binaries, interactions become rarer and more violent as they get harder and harder, until either the binary is kicked out from the environment or, in the case of COBs, GW emission kicks in and drives them toward coalescence [127]. If the hardening process involves massive stellar binaries and occurs over a timescale shorter than the typical timescale of massive star evolution, i.e. before the formation of COs, it can determine the onset of stellar collisions, which in turn can result in the formation of final BHs with masses larger than expected, possibly falling in the so-called pair-instability mass gap [e.g. 51,99,111,128,290].

Soft binaries, instead, are likely subjected to disruption, either via a single strong interaction, if the perturber passes at a distance comparable to the binary semimajor axis, or via a series of distant flybys [see 210]. In soft-binary flyby interactions, the passing object increases the energy of the binary system and widens the binary, eventually leading to its *evaporation* over a timescale given by the ratio between the energy gained/lost by the binary and the rate of change of the kinetic energy, or diffusion energy coefficient, which can be expressed as [205,210,277,291]:

$$t_{\text{ev}} = \frac{\sqrt{3}\sigma}{32\sqrt{\pi}G\rho_* \ln \Lambda a_{\text{bin}}} \frac{m_{\text{bin}}}{\langle m_* \rangle} = \quad (11)$$

$$= 1 \text{ Gyr} \left(\frac{M_{\text{SMBH}}}{4.3 \times 10^6 M_\odot} \right)^{1/2} \left(\frac{r}{0.5 \text{ pc}} \right)^{-1/2} \left(\frac{\log \Lambda}{\log(15)} \right)^{-1} \times$$

$$\times \left(\frac{\rho}{2.8 \times 10^6 M_\odot \text{ pc}^{-3}} \right) \left(\frac{a_{\text{bin}}}{1 \text{ AU}} \right)^{-1} \left(\frac{m_{\text{bin}}}{30 M_\odot} \right) \left(\frac{\langle m_* \rangle}{1 M_\odot} \right)^{-1}$$

and depends on the binary semi-major axis (a_{bin}), eccentricity (e_{bin}), as well as on several environmental properties, like the stellar density, ρ_* , the velocity dispersion, $\sigma = (GM_{\text{SMBH}}/r)^{1/2}$, and the average stellar mass, m_* .

From the softness parameter defined above, we can determine a critical binary semimajor axis, a_{hard} , that separates hard and soft binaries:

$$a_{\text{hard}} = \frac{2Gm_{\text{bin}}}{\sigma^2} = \frac{2m_{\text{bin}}}{M_{\text{SMBH}}} r, \quad (12)$$

where the latter equality represents a valid approximation at a distance r to an SMBH, where $\sigma^2 \sim M_{\text{SMBH}}/r$.

Assuming a semi-major axis distribution flat in logarithmic values between 0.01 – 10³ AU [13,127,292] implies that $\sim 30\%$ (70%) of binaries are hard(soft) at the Galactic Centre ($r < 0.1$ pc). Within $r < 0.1$ pc from SgrA*, the Galactic SMBH, binaries with a semimajor axis $a_{\text{bin}} > 0.29$ AU are soft, thus their existence will be endangered by the effect of the closeby SMBH.

However, a typical equal-mass circular binary with mass $m_{\text{bin}} = 30M_\odot$ and semi-major axis $a_{\text{bin}} = 0.1$ AU orbiting at a distance $r = 0.1$ pc from SgrA*, evaporates in $t_{\text{ev}} = 24$ Gyr, thus, even though in a soft state, the binary could still survive in the dense environment of the Galactic Centre, despite a single, strong encounter can disrupt it.

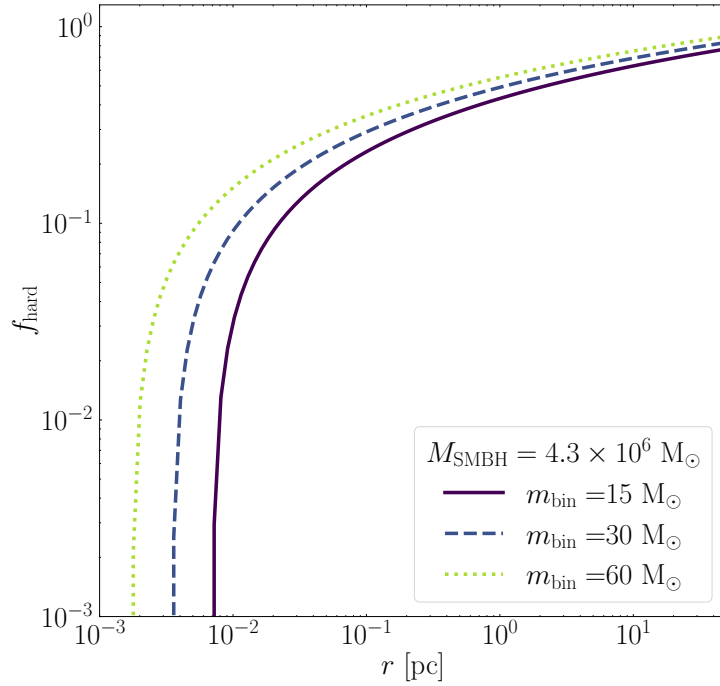


Figure 5. Fraction of hard binaries, normalised to the total population of binaries, as a function of the distance from an SMBH with mass $M_{\text{SMBH}} = 4.3 \times 10^6 M_{\odot}$, assuming a primordial semimajor axis distribution flat in logarithmic values and limited between $10^{-2} - 10^3$ AU.

Having typical binary masses in the range $m_{\text{bin}} = 3 - 5 M_{\odot}$, double NSs can, instead, evaporate over a timescale shorter than a Hubble time, taking only $t_{\text{ev}} = 2 - 4$ Gyr in the aforementioned example.

Note that the fraction of binaries with a semi-major axis smaller than a_{hard} in the case of a logarithmically flat distribution is given by

$$f(< a_{\text{hard}}) = \frac{\log(a_{\text{hard}}/a_{\text{min}})}{\log(a_{\text{max}}/a_{\text{min}})} = \frac{1}{\log(a_{\text{max}}/a_{\text{min}})} \log\left(\frac{r}{a_{\text{min}}} \frac{m_{\text{bin}}}{M_{\text{SMBH}}}\right), \quad (13)$$

which implies that the fraction of hard binaries diminishes closer to the SMBH. Assuming an SMBH of mass $M_{\text{SMBH}} = (1 - 4.3 - 10) \times 10^6 M_{\odot}$ and $a_{\text{min,max}} = 0.01 - 10^3$ AU, the percentage of hard binaries drops below 10% at a distance $r_0 = (0.015 - 0.067 - 0.15)$ pc. The depletion of hard binaries toward the galaxy centre has been also demonstrated via self-consistent N -body models of the Milky Way nucleus [281].

Figure 5 shows how the hard binary fraction varies as a function of the distance to the SMBH for the Milky Way centre, highlighting how only a tiny fraction of the most massive binaries can still be hard within 1 – 10 mpc from the SMBH. At those distances, though, the hard binary separation is $a_h \sim 1 R_{\odot} (M_{\text{SMBH}}/4.3 \times 10^6 M_{\odot}) (r/1 \text{ mpc})^{-1}$, thus it is highly likely that a stellar binary would quickly merge.

Additionally, the evaporation process depends on the binary's eccentricity around the SMBH [e.g. 203]. In the case of soft binaries, each new interaction causes an increase of the semi-major axis with time, due to the single-fly by interactions. Additionally, in the case of soft stellar binary mass loss can further widen the orbit. Thus, the evaporation time of soft binaries

changes with time. If we assume that the binary softens over time, we can find an upper limit on the evaporation time:

$$t_{\text{ev,max}} = t_{\text{ev}} S_h \quad (14)$$

where

$$S_h = \frac{s_h}{s_0} \quad (15)$$

represents the possible binary history, namely its semi-major axis evolution [289]. In particular, s_0 is the softness parameter calculated when the binary is observed and s_h represents the hardest possible initial configuration. In other words,

$$s_h = \min[1, s(a_{\text{bin}} = R_1 + R_2)] , \quad (16)$$

where $R_{1,2}$ are the initial ZAMS stellar radii, assuming that the two stars were originally paired. The hardest limit taken in Equation (16), is when the binary begins as a contact binary [289].

The equations above for the evaporation timescale are derived under the assumption that the binary moves on a circular orbit about the SMBH. However, many of the stars in the Galactic Centre are in fact on an eccentric orbit [e.g. 37–39,44,206,207,293–295]. A binary on an eccentric orbit may pass through a denser, inner regions of the Galactic Centre unlike a binary on a circular orbit. Therefore, extra term should be introduced (see for full derivation Ref. [203]), namely:

$$t_{\text{ev,Ecc}} = t_{\text{ev}} f(e_{\text{SMBH}}) \quad (17)$$

$$\begin{aligned} f(e_{\text{SMBH}}) &= \frac{(1 - e_{\text{SMBH}})^{\alpha + \frac{1}{2}}}{2} {}_2F_1\left(\frac{1}{2}, -\frac{1}{2} - \alpha; 1; \frac{2e_{\text{SMBH}}}{e_{\text{SMBH}} - 1}\right) \\ &+ \frac{(1 + e_{\text{SMBH}})^{\alpha + \frac{1}{2}}}{2} {}_2F_1\left(\frac{1}{2}, -\frac{1}{2} - \alpha; 1; \frac{2e_{\text{SMBH}}}{e_{\text{SMBH}} + 1}\right), \end{aligned} \quad (18)$$

where ${}_2F_1$ is the hypergeometric function.

Binary hardening and softening processes are highly sensitive to the underlining density profile of the surrounding galaxy or NC [e.g. 48,203], with cusp-like density profiles leading to more expedite hardening and softening processes.

In the next section, we will discuss in detail what dynamical processes intervene in the formation of binaries in galactic nuclei.

5.2. Moving through a swarm: orbital evolution of compact binaries in galactic nuclei

As we have discussed in the previous section, binaries are more likely to orbit in an outer layer of the galactic nucleus, where the effect of the central SMBH is less disruptive.

This has two crucial implications on the binary dynamics. On the one hand, the binary will drift toward the galactic centre owing to dynamical friction. On the other hand, while migrating the binary will sweep through regions at increasing density and velocity dispersion. This will affect the boundary between hard-soft binaries, and can either boost the binary shrinkage or cause its evaporation (or ionization).

The binary infall rate can be described via the dynamical friction timescale as:

$$\frac{dr}{dt} = -\frac{r}{t_{\text{df}}}, \quad (19)$$

while the binary hardening rate due to binary-single interactions is given by [127,296]

$$\frac{da_{\text{BBH}}}{dt} = -H \frac{G\rho(r)}{\sigma(r)} a_{\text{BBH}}^2. \quad (20)$$

If the nucleus density is $\rho \sim r^{-\gamma}$ we can express the hardening timescale as

$$t_{\text{hard}} \simeq \left(\frac{1}{a_{\text{BBH}}^2} \frac{da_{\text{BBH}}}{dt} \right)^{-1} \propto r^{\gamma-1/2} M_{\text{SMBH}}^{1/2}, \quad (21)$$

thus the heavier the SMBH the smaller the hardening, and the steeper the density profile, for $\gamma > 1/2$, the larger the hardening as the binary migrate inward. Note that values of $\gamma < 1/2$ produce an unphysical distribution of energies for a matter distribution around an SMBH [297], and would imply that the hardening drops closer to the SMBH.

The fact that the hardening process proceeds at an increasing pace might have crucial consequences on the late evolution of the binary. For example, also the hard-binary separation changes getting closer to the SMBH, thus despite the increasing hardening a binary could still become soft in some regions of the nucleus. Figure 6 shows the evolution of the semimajor axis normalised to the hard binary separation ($a_{\text{BBH}}/a_{\text{hard}}$) and distance to the SMBH (r/r_0) for a BBH with mass $M_{\text{BBH}} = 30M_{\odot}$ and different values of a_{BBH} .

It is quite evident that, depending on the binary properties and its initial position within the nucleus, as the binary gets closer to the SMBH it can become softer and softer, and from that point the evaporation time will represent a rough estimate of the binary lifetime. Note that the $a_{\text{BBH}}/a_{\text{hard}}$ increase is only due to the environment, which becomes denser and hotter.

Moreover, as the binary gets closer to the SMBH, the increasing tidal field can exert important effects on the binary evolution, which we review in the next section.

5.3. Multiple encounters make bound pairs: how dynamical processes aid binary formation in galactic nuclei

The accumulation of BHs toward the cluster centre will maximise the level of contraction of the cluster central regions, a process known as core-collapse that ideally drives the central density to grow up to infinity. The density increase onset the formation of binaries and multiple systems that, strongly interacting with each other and with single object. Binaries thus act as “heating sources” for the cluster nucleus, efficiently transferring energy to lighter single and multiple stars and ejecting them from the inner cluster regions. As a consequence, the cluster centre expands, causing a reduction of density and velocity dispersion that leads to a significant reduction of the interaction rate, reversing the core-collapse process. The combination of mass-segregation and core-collapse results in a different density distribution for COs, steep and more concentrated, and stars, much shallower and sparse [see e.g. 268,281,298].

The energy exchange promoted by mass-segregation translates into a redistribution of energy among the objects with different masses that can trigger the formation of bound binaries via few-body interactions.

The earliest studies about the formation of binaries in dense stellar environments date back to early 1960s, when the first Fokker-Planck, Monte Carlo, and N -body models were developed [e.g. 11,282,299–308].

These pioneering experiments were developed to understand the complex evolution of star clusters, and shed light on the fundamental dynamics regulating the formation and disruption of binaries in star clusters and the feedback that binaries have on the whole cluster evolution.

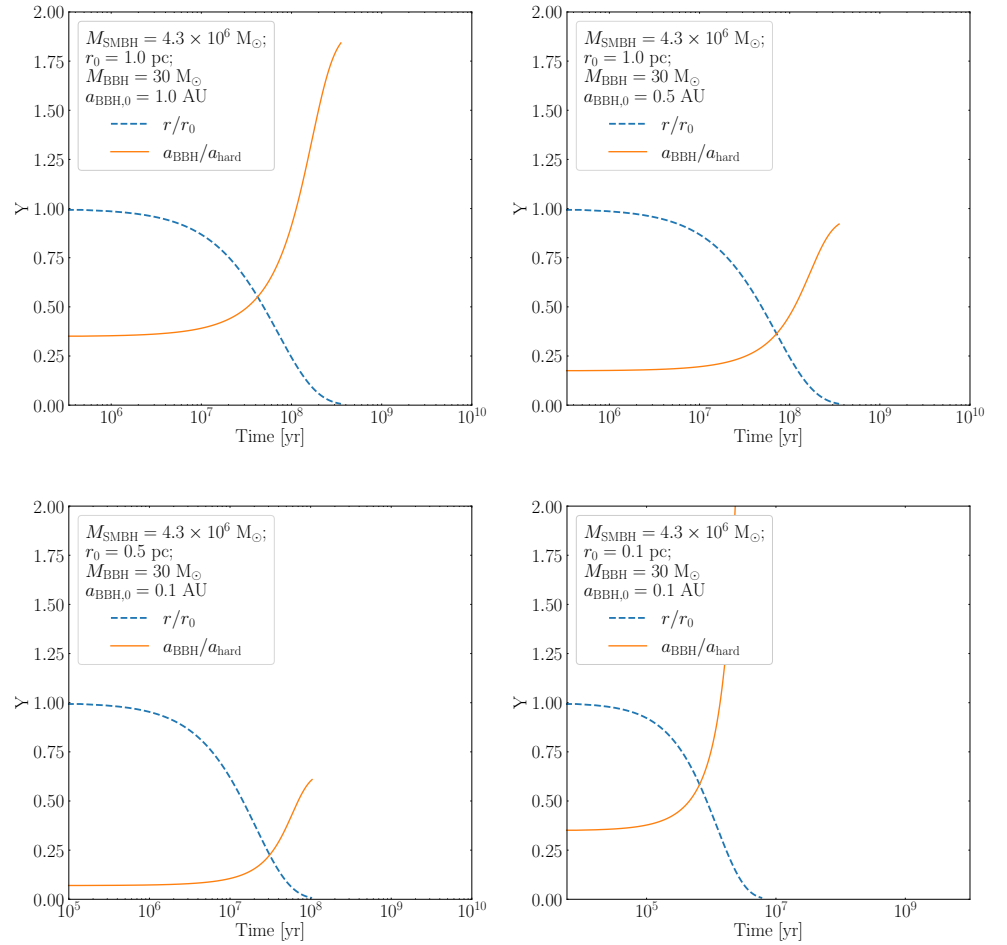


Figure 6. Time evolution of the BBH semimajor axis normalised to the *local* hard-binary separation (orange straight line) and the BBH position within the cluster normalised to the initial position (blue dashed line). We assume an SMBH with mass $M_{\text{SMBH}} = 4.3 \times 10^6 M_{\odot}$ and a BBH with mass $M_{\text{BBH}} = 30 M_{\odot}$.

As we will see in the next sections, such fundamental dynamics can be generally dissected into several processes, namely single-single GW captures and three-body, binary-single, and binary-binary scatterings.

5.3.1. GW-capture binary formation

Aside three-body interactions, a binary can form also via GW bremsstrahlung during a single-single interaction, provided that the two objects come sufficiently close. The maximum impact parameter below which two BHs pair can be calculated by equalling the potential energy between the interacting objects and the energy lost to GWs during the closest passage, and can be expressed roughly as [265,309]

$$b_{\text{bnd}} = 2.4R_{\odot} \left(\frac{\sigma}{100 \text{ km s}^{-1}} \right)^{-9/7} \left(\frac{m_1 + m_2}{10M_{\odot}} \right) \left(\frac{\eta}{0.25} \right), \quad (22)$$

where $\eta = m_1 m_2 / (m_1 + m_2)^2$ is the asymmetric mass-ratio. For a MW-like nucleus, assuming a typical BH number density of 10^6 pc^{-3} and velocity dispersion $\sigma \sim 100 \text{ km s}^{-1}$, this condition implies around 0.01 – 0.1 binary captures per Gyr [e.g. 265,310]. The timescale for these interactions can be written as a function of the SMBH

$$t_{\text{cap}} = (n\sigma\pi b_{\text{bnd}}^2)^{-1} = 353 \times 10^{12} \text{ yr} \left(\frac{n}{10^6 \text{ pc}^{-3}} \right)^{-1} \left(\frac{M_{\text{SMBH}}}{4.3 \times 10^6 M_{\odot}} \right)^{11/14} \left(\frac{r_0}{0.22 \text{ pc}} \right)^{-11/14} \left(\frac{r}{r_0} \right)^{-11/14 + \gamma}, \quad (23)$$

where we assumed $\sigma = (M_{\text{SMBH}}/r)^{1/2}$ and $n = n_0(r/r_0)^{\gamma}$. Figure 7 shows the GW capture timescale for different values of the number density of BHs in the nucleus and the SMBH mass. It appears evident how this process can operate quickly close to the most dense nuclei and the most massive SMBHs. At formation, the pericentre of a GW-capture binary is typically $r_p \lesssim 7.4 \times 10^{-3} R_{\odot} (\sigma/100 \text{ km s}^{-1})^{-4/7}$, thus these binaries are characterised by extremely short merging times, order of minutes to hours, and their merger rate will directly follow the binary formation rate, which is expected to be in the range 0.2 – 150 Gyr^{-1} [265].

As we will discuss further in Section 8, among all the channels for BBH formation in galactic nuclei, the GW-capture enables the production of highly eccentric sources ($e > 0.1$) in the typical frequency band where the sensitivity of ground-based interferometers like LVC peaks, i.e. $f > 1 - 10 \text{ Hz}$.

5.3.2. Three-body binary formation

By definition, a *three-body* interaction involves 3 unbound objects scattering onto each other. Statistically speaking, this type of interactions leads to the ejection of the least massive object and the formation of a bound pair. The formation rate for three-body binaries can be obtained by equalling the rate at which new binaries form and soft binaries are ionised via multiple or single interaction, and can be expressed as [11,311]

$$\frac{dn_{3\text{bb}}}{dt} = \alpha (Gm)^5 n^3 \sigma^{-9}, \quad (24)$$

where α is a normalization constant, m is the average mass of the interacting bodies, n is the environment number density, and σ its velocity dispersion. The timescale associated to this process, $t_{3\text{bb}} \sim m^{-5} n^{-2} \sigma^9$, immediately highlights how crucial is the environment, and its evolution, in determining binary formation via three-body interactions.

The binary formation rate above is derived under the assumption that only hard binaries are "immortal" [282]. However, in environments with a particularly large velocity dispersion,

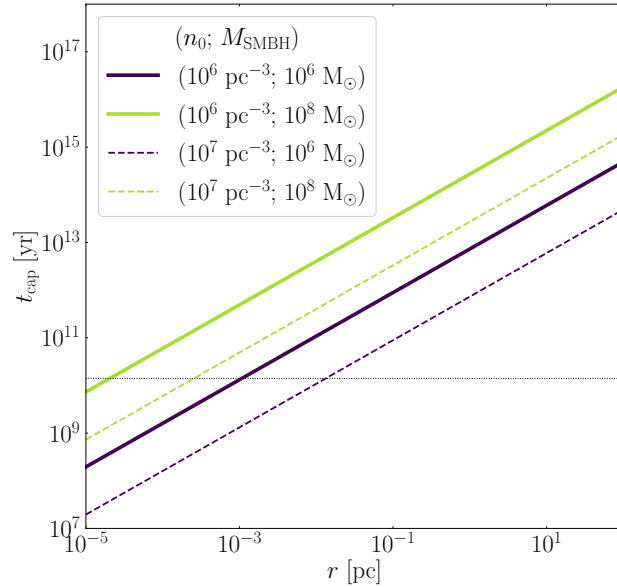


Figure 7. Timescale for gravitational-wave capture assuming a black hole mass $m_{\text{BH}} = 15M_{\odot}$ as a function of the distance from the SMBH and for different values of the SMBH mass and BH number density.

thus a small hard-binary separation limit, soft binaries can harden via GW emission and cross the soft-hard boundary, provided that the hardening time is shorter than the evaporation time. This mechanism to harden soft binaries works for particularly dense nuclei where encounters with a relative velocity close to the speed of light ($v_{\text{rel}} \gtrsim 0.3c$) become possible [312].

At a distance r from an SMBH, the velocity dispersion is Keplerian, $\sigma^2 \propto M_{\text{SMBH}}/r$, whilst the matter density is expected to follow a power-law [298,313–318], $n \propto r^{\gamma}$, with $\gamma = -3/2 - m/4m_{\text{max}}$, and $m(m_{\text{max}})$ the average(maximum) stellar mass [317,319]. For a monochromatic mass spectrum, the matter density around an SMBH follows the so called Bahcall-Wolf cusp, with slope $-7/4$ [313]. In a multimass system, stellar BHs, which are the heaviest objects in a stellar ensemble, are expected to distribute according to a Bahcall-Wolf cusp or even a steeper one [265,266,298,318,319], whilst lighter stars follow a shallower density distribution [264,280,281,320].

The energy transfer from the heaviest to the lightest object progressively leads to a decrease of the heavy object velocity dispersion owing to the equipartition principle. Mass segregated BHs are characterised by a velocity dispersion $\sigma_{\text{BH}}/\sigma_* \sim 1/\zeta(m_{\text{BH}}/m_*)^{-\eta}$, with $\zeta \leq 1$. In the ideal case of “perfect equipartition”, $\eta = 0.5$ [209], however simulations have shown that equipartition is hard to reach in dense clusters, even in presence of a central massive object, as shown for globular cluster models hosting a central IMBH, which suggest $\eta = 0.08 - 0.15$ [321].

Given the dependencies above, the three-body timescale can be re-written as

$$\begin{aligned}
 t_{3bb} &= (Gm_{\text{BH}})^{-5} n_{\text{BH}}^{-2} \sigma_{\text{BH}}^9 = & (25) \\
 &= (Gm_{\text{BH}})^{-5} \left(\frac{\rho_0}{m_*}\right)^{-2} \left(\frac{GM_{\text{SMBH}}}{r_0}\right)^{9/2} \left(\frac{m_*}{m_{\text{BH}}}\right)^{9/2} \left(\frac{r}{r_0}\right)^{2\gamma-9/2} \\
 &= 12.5 \text{ Gyr} \left(\frac{m_{\text{BH}}}{30M_{\odot}}\right)^{-19/2} \left(\frac{\rho_0}{2.8 \times 10^6 M_{\odot} \text{ pc}^{-3}}\right)^{-2} \left(\frac{M_{\text{SMBH}}}{4.3 \times 10^6 M_{\odot}}\right)^{9/2} \times \\
 &\quad \times \left(\frac{r_0}{0.22 \text{ pc}}\right)^{-9/2} \left(\frac{m_*}{0.5M_{\odot}}\right)^{13/2} \left(\frac{r}{r_0}\right)^{2\gamma-9/2},
 \end{aligned}$$

where we used the fact that $n = \rho_0/m_*(r/r_0)^\gamma$ and $\sigma_{\text{BH}}^2 = (m_*/m_{\text{BH}})GM_{\text{SMBH}}/r$. Note that the Galactic NC is characterised by $\rho_0 \sim (2.8 \pm 1.3) \times 10^6 M_{\odot} \text{ pc}^{-3} (r/r_0)^{-\gamma}$, with $\gamma = 1.2(1.75)$ inside(outside) the inner $r_0 = 0.22 \text{ pc}$ [39,322].

Note that for NSs the three-body interaction time becomes incredibly long, owing to the steep dependence on the CO mass. The t_{3bb} time becomes shorter than a Hubble time only if we consider nuclei with considerably lighter SMBH, $\sim 10^5 M_{\odot}$, and in the outermost ($r > 5 \text{ pc}$) regions of the NC.

Under the rather simplistic assumption that the NC properties do not vary significantly over time, Equation 24 can be integrated over time to obtain how the following, time-dependent, expression of the binary fraction [for a full derivation, see 277]:

$$f_{\text{BBH}} = \frac{1}{2} \left(1 - \frac{1}{\sqrt{1 + t/t_{3bb}}} \right). \quad (26)$$

Figure 8 shows the BH binary fraction (over the total population of BHs) as a function of the distance to the Galactic Centre after a time $t = 0.1 - 10 \text{ Gyr}$, assuming an average BH mass $m_{\text{BH}} = 15M_{\odot}$. The figure makes clear that a pure three-body formation process is highly inefficient in the innermost Galactic regions, owing to the large velocity dispersion that hampers three-body interactions. Nonetheless, it also highlights that, at distances $1 - 10 \text{ pc}$ the BBH fraction attains values $f_{\text{BBH}} \sim 10^{-3} - 10^{-2}$, which could imply the formation of a few tens BBHs over a 10 Gyr time-span, but how many? Let us assume that the inner pc in the Milky Way contains around $N_{\text{BH}}(< 1\text{pc}) = 20,000 \text{ BHs}$ [53] and that the BH density distribution at the Galactic Centre is represented by a simple broken power-law [323], with a total number of BHs $N_{\text{BH}} = 10^{-3} N_{\text{NC}}$, a scale radius of $a = 0.1 \text{ pc}$ and density slope $\gamma = 2^1$, it is possible to show that at a distance $1 - 10 \text{ pc}$ from the Galactic Centre we expect $O(10^3)$ BHs, thus the number of binaries formed in the Galactic NC in 10 Gyr solely via three-body scattering would be $N_{\text{BBH}} \sim 2 - 20$. A way to increase the number of BBHs is via exchange in binary-single scatterings involving a binary star and a single BH [e.g. 127,277].

For the NC in the Milky Way and CO average mass of $m_{\text{BH}} = 30M_{\odot}$, the three-body timescale is shorter than the dynamical friction timescale at distances $r > 3.8 \text{ pc}$, thus suggesting that binaries containing at least one BH could form in the outer NC regions.

From the equation above, for a Bahcall-Wolf cusp $-\gamma = -7/4$ – the 3-body interaction time increases toward the SMBH as $t_{3bb} \propto 1/r$.

Equation 25 implies that three-body scatterings are highly suppressed for objects lighter than $30M_{\odot}$, thus the formation of stellar binaries in such extreme environments must resort to

¹ This choice of parameters returns a number of BHs inside 1 pc similar to the value inferred from observations of the Galactic Centre

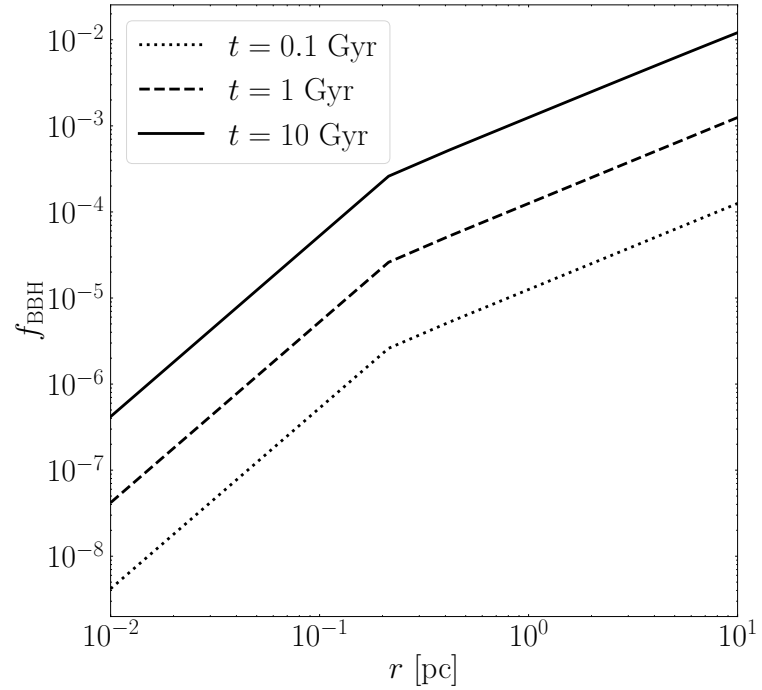


Figure 8. Fraction of binary black holes as a function of the distance to the Galactic Centre after an evolutionary time of 0.1 Gyr (dotted line), 1 Gyr (dashed line), and 10 Gyr (straight line).

other mechanism to sustain their binary population, or need to harbor a substantial fraction of “primordial” hard binaries. 639
640

It must be also noted that the steep dependence on the density and velocity dispersion makes the three-body time estimates extremely susceptible to the choice of initial conditions, as suggested by Figure 9, which shows how t_{3bb} varies at varying the SMBH and NC masses and the distance to the galactic centre. This owes to the fact that $t_{3bb} \propto M_{NC}^{-2} M_{SMBH}^{9/2}$, thus reducing the SMBH mass by 5 times causes a reduction of the three-body time by a factor ~ 1400 . For the sake of comparison, note that for BHs with mass $\sim 10M_{\odot}$ in a typical globular cluster, with density $n \sim 10^4 \text{ pc}^{-3}$ and velocity dispersion $\sigma = 5 - 10 \text{ km s}^{-1}$, the three-body timescale reduces to $t_{3bb} \sim 0.004 - 2 \text{ Gyr}$. 641
642
643
644
645
646
647
648

5.3.3. Binary-single scatterings 649

The presence of even a few binaries in the nucleus, either primordial or formed dynamically, will lead to a series of binary-single interactions with other members. 650
651

The cross-section of a strong encounter between a binary with mass m_{bin} and semimajor axis a and a perturber m_p from the binary can be expressed as

$$\Sigma = \pi a^2 (1 - e)^2 \left[1 + \frac{2G(m_{bin} + m_p)}{3\sigma^2 a (1 - e)} \right]. \quad (27)$$

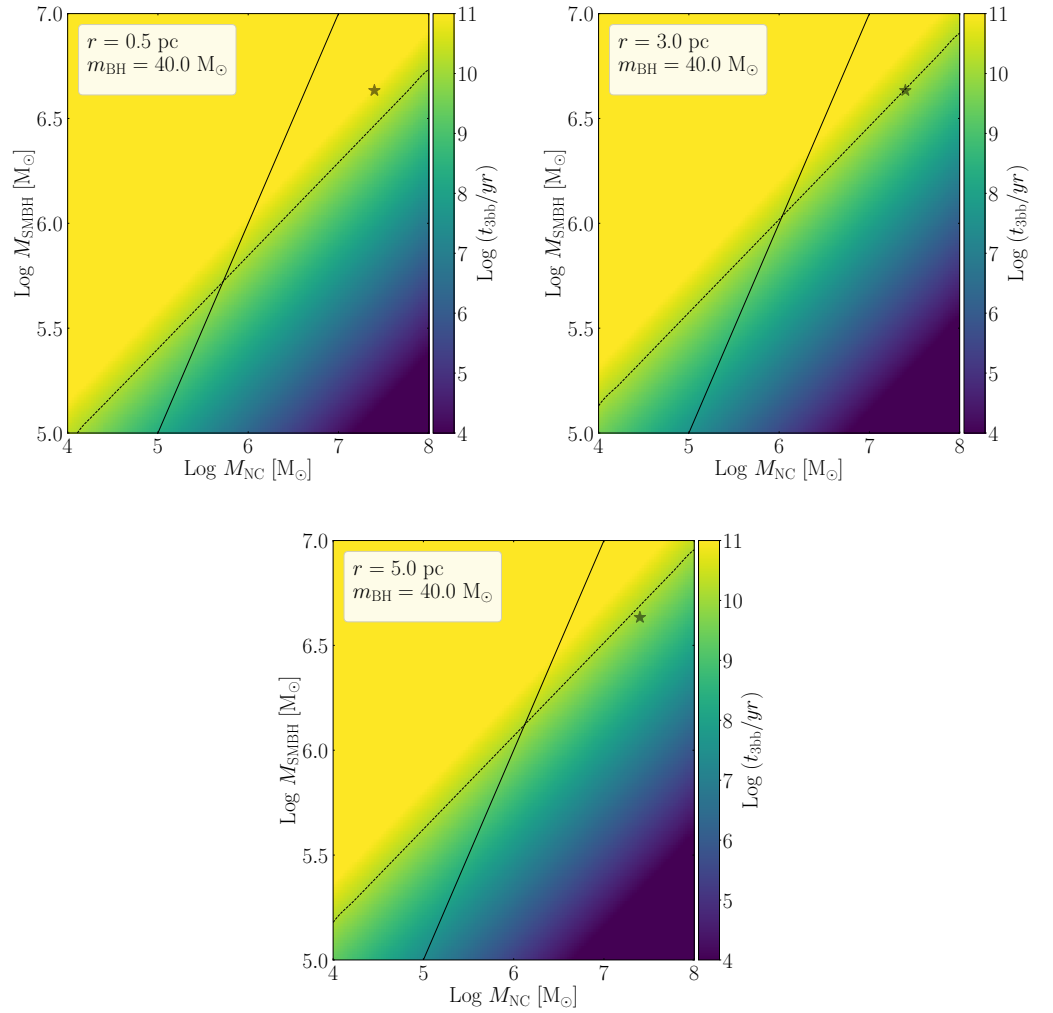


Figure 9. Three-body timescale as a function of the NC (x-axis) and SMBH (y-axis) mass. We assume three equal mass BHs ($m_{\text{BH}} = 40M_{\odot}$) orbiting at $r = 0.5 - 0.3 - 5$ pc from the SMBH (from left to right, respectively). The star marks typical values in the Milky Way. The straight line marks the case $M_{\text{NC}} = M_{\text{SMBH}}$, whilst the dotted line separates the region with a t_{3bb} smaller (below the line) or larger (above the line) than the Hubble time.

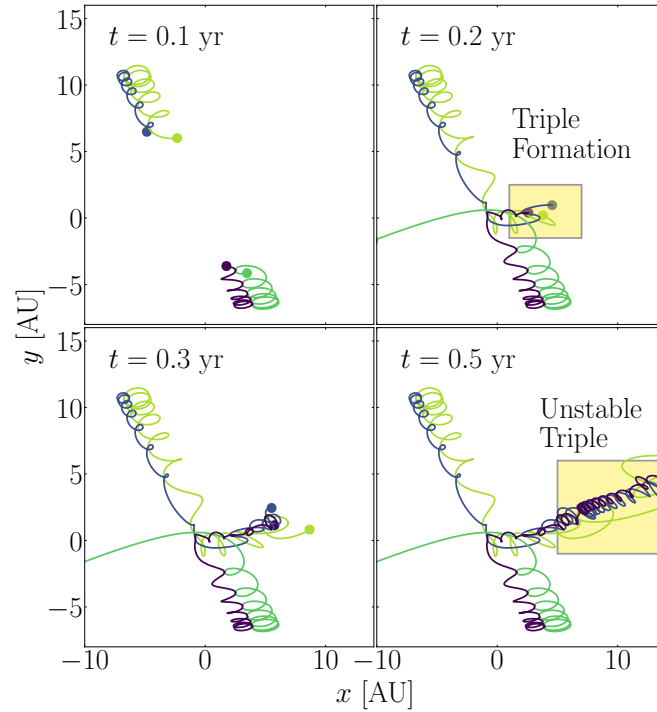


Figure 10. Binary–binary interaction involving four BHs in a dense star cluster. After the close encounter, one BH is ejected and the remaining three BHs form an unstable triple. Taken from Figure 2 in Arca Sedda et al, *A&A*, 2021, 650, A189, reproduced with permission ©ESO [163].

The number of interactions per time unit that the binary will undergo while moving with velocity σ in an environment with stellar density n is $dn \simeq n\Sigma\sigma dt$. The associated time-scale of this process, $t_{\text{bs}} = (n\Sigma\sigma)^{-1}$, can be conveniently written as [13,127]:

$$t_{\text{bs}} = 3.2 \times 10^9 \text{ yr} \left(\frac{n}{10^6 \text{ pc}^{-3}} \right)^{-1} \left(\frac{f_{\text{bin}}}{0.01} \right)^{-1} \times \left(\frac{r}{2 \text{ pc}} \right)^{-1/2} \left(\frac{M_{\text{SMBH}}}{4.3 \times 10^6 M_{\odot}} \right)^{1/2} \left(\frac{m_{\text{bin}} + m_p}{30 M_{\odot}} \right)^{-1} \left(\frac{a}{1 \text{ AU}} \right)^{-1}, \quad (28)$$

where f_{bin} represents the binary fraction.

If the perturber is a BH whilst the binary contains stars, the interaction will take place proportionally to the fraction of binaries present in the cluster. In such a case, the binary will likely acquire the BH if it is more massive than at least one component. In this case, Equation 28 remains valid even in the case of binary–binary interactions, provided that the perturber mass is replaced with the typical binary mass. Binary–binary interactions represent a viable way to produce CO triples. On the one hand, triples can undergo secular evolution, with the least bound object – or outermost – possibly impinging EKL oscillations onto the most bound pair, eventually driving it to coalescence [159,163,324]. On the other hand, triples formed out of binary–binary interactions can undergo a chaotic unstable evolution that, in some cases, can trigger the formation of highly eccentric merging binaries [159,163]. Figure 10 shows one example of BBH–BBH strong scattering from numerical simulations described in [163]. The plot highlights how, after the encounter between the two binaries, one of the BHs – the lightest – is ejected away and an unstable triple forms. The triple eventually breaks-up and lead to the formation of a tight binary that merges after 10^2 yr [see Figure 6 in 163]. The presence

652
653
654
655
656
657
658
659
660
661
662
663
664
665
666

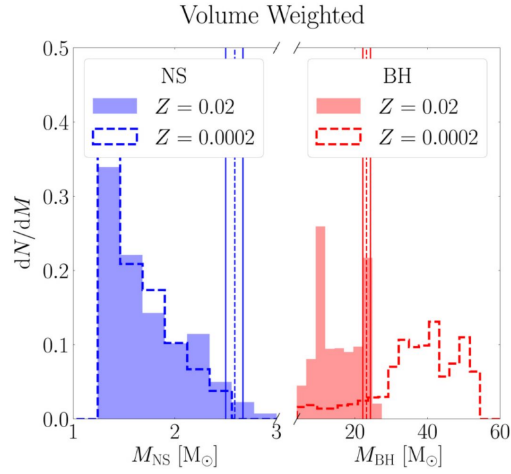


Figure 11. Merging NS-BH binaries formed via binary-single encounters in dense clusters and corrected for ground-based GW detectors. Vertical lines correspond to the median value (dashed line) and 95% confidence level boundaries (stright lines) of the mass of GW190814 source components. Taken from Figure 4 in Arca Sedda, ApJL, 2021, 908, L38 ©AAS [136]. Reproduced with permission.

of a SMBH in the galactic centre can significantly influence triple evolution, tidally limiting them and enabling only the formation of triples whose maximum size remains within the triple Roche lobe [325], and possibly boosting the COB merger rate owing to a more efficient development of EKL mechanism [326].

If, instead, the BH is already in a binary, it can interact with all the stars in the nucleus and the actual binary-single scattering time becomes $t_{bs,BBH} \sim f_{bin} t_{bs}$, thus BHs in binaries can undergo binary-single interactions at a rate up to 100 times larger than single BHs.

If NSs or BHs are paired in a binary already, either because of previous dynamical processes or owing to primordial stellar evolution, it has been shown that binary-single interactions are particularly efficient at producing merging NS-BH binaries [130,132,133,136], especially in dense galactic nuclei [130]. The typical properties of dynamical NS-BH mergers formed this way, or at least of a sub-population of them, differ significantly from the observed properties of NS-BH binaries formed in isolation, permitting to clearly identify their origin in GW observation [130,136, but see also Section 8]. Figure 11 shows the mass spectrum of merging NS-BH binaries formed via binary-single interactions in dense clusters with velocity dispersion in the 10 – 100 km/s range, for two different values of the stellar metallicity. The distribution takes into account observational biases, in particular the fact that LIGO-Virgo detectors can access a larger volume for nearly equal mass binaries with large masses in comparison to low-mass or highly asymmetric binaries [136,327].

The typical outcome of a binary-single encounter depends on the ratio between the energy transferred during the encounter, which is roughly given by $\Delta E_{bs} \sim (r_{p,e}/a)^{3/2}$ [282,328], where $r_{p,e}$ represents the minimum binary-perturber separation, and the kinetic energy calculated in the centre of mass of the triple, i.e. [328]

$$\Delta E_c = v_\infty^2 \frac{m_p m_{bin}}{2(m_p + m_{bin})}, \quad (29)$$

with v_∞ the velocity at infinity of the perturber in the binary reference frame. If the energy transferred is small, i.e. $\Delta E_{bs} < \Delta E_c$, the binary has two possible fates, depending on its binding energy E_{bin} :

- i if $\Delta E_{bs} < E_{bin}$, the binary will harden or soften depending on the environment;

- ii if $\Delta E_{bs} > E_{bin}$, the binary will exchange one component, most likely the least massive, if the perturber is heavier than the binary or its components, i.e. $m_p > (m_1 + m_2)$ or at least $m_p > m_{1,2}$.

If the binary preserves its components, the perturber will recede to infinity with velocity $v_p < v_\infty$, otherwise the former binary component with mass m_{exc} will escape with velocity $v_p < \sqrt{(m_p/m_{exc})}v_\infty$.

In the case of a high-energy transfer, $\Delta E_{bs} > \Delta E_c$, the outcome of the scattering is a bit more complex, but can be determined statistically by comparing the interaction velocity v_∞ and the critical velocity value above which the perturber can promptly ionize the binary, defined as [329]

$$v_c^2 = \frac{Gm_1m_2(m_p + m_{bin})}{am_pm_{bin}}. \quad (30)$$

In such a way, the possible final states can be categorized as follows:

- i if $v_\infty < v_c$ the perturber cannot recede to infinity and the three bodies undergo a resonant interaction that can culminate in the exchange of one binary component if:
- $\Delta E_{bs} > E_{bin}$,
 - $\Delta E_{bs} < E_{bin}$ and $m_p > m_{bin}$.
- Either ways, the perturber or the exchanged component recedes to infinity and possibly leaves the host system;
- ii if $v_\infty < v_c$ and $\Delta E_{bs} < E_{bin}$ and $m_p < m_{bin}$ the system undergoes a resonant interaction that generally leads to the ejection of the lighter component;
- iii if $v_\infty > v_c$ the binary undergoes:
- component exchange if $\Delta E_{bs} < E_{bin}$,
 - ionization if $\Delta E_{bs} > E_{bin}$.

For a BH population with equal mass m_{BH} and a binary population with semimajor axis $a_{BBH} = 1$ AU, the critical velocity is $v_c \sim 50 \text{ km s}^{-1}$. The speed of the encounters around an SMBH, instead, is $\sigma_{SMBH} = 65 \text{ km s}^{-1} (M_{SMBH}/10^6 M_\odot)^{1/2} (r/1 \text{ pc})^{-1/2}$.

This implies that the binary-single interactions inside the SMBH influence radius will be characterised mostly by $v_\infty \sim \sigma_{SMBH} > v_c$.

Depending on the masses involved and the semimajor axis of the binary, it can be shown that the energy transferred in a binary-single encounter rapidly drops when $\sigma/v_c > k$, where $k \sim 0.1 - 1$, whilst the critical energy transfer ΔE_c increases with $(\sigma/v_c)^2$. Thus it seems reasonable to expect that in the closest vicinity of an SMBH binary-single encounters tend to favour small energy transfer. Since the binary in these encounters is likely hard, thus $E_{bin} \propto \sigma^2$, binary-single interactions close to an SMBH might result statistically in the binary hardening, i.e. case $\Delta E_{bs} < \Delta E_c$ and $\Delta E_{bs} < E_{bin}$. In other words, component exchange and binary ionization might be significantly suppressed in galactic nuclei unless the binary semimajor axis is close to the hard-soft separation value [see e.g. 277]. This simple line of thought find support in recent scattering simulations tailored on binary-single scattering around a MW-like SMBH [see e.g. 325]. After the interaction, the binary will recoil at a velocity $v_{rec} = k\sigma$ [127], with $k \simeq 0.3$ for a monochromatic BH mass spectrum.

6. Secular dynamical effects on binary evolution around a supermassive black hole

6.1. Secular perturbations on black hole binaries in galactic nuclei: the impact of a supermassive black hole

While the effects of binary interactions have been shown to play a crucial role in the global dynamical evolution of dense systems such as globular clusters, only recently the effect of binaries in NCs have been investigated. Within the vicinity of an SMBH, the members of a

stable binary have a tighter orbital configuration than the orbit of their mutual centre of mass around the SMBH. In such a system, gravitational perturbations from the SMBH can induce large eccentricities on the binary orbit, which can cause the binary members to merge. Below we outline the relevant physical processes that characterise the COB-SMBH co-evolution.

6.1.1. Three-body Newtonian Limit

In the three-body approximation, dynamical stability requires that the system has either circular, concentric, coplanar orbits or a hierarchical configuration, in which the inner binary, with semimajor axis a_1 , is orbiting a third body (in this case the SMBH) on a much wider orbit, the outer binary, with semimajor axis a_2 . In such hierarchical configurations it is possible to apply the so-called secular approximation. In essence, this means that orbital period can be averaged on, thus the interactions between two non-resonant orbits are equivalent to treating the orbits as massive “wires” where the line-density is inversely proportional to orbital velocity. Under this approximation, the gravitational potential is expanded in the ratio of orbital separations – which, in this approximation, remains constant, since $(a_1/a_2) \ll 1$ [e.g. 14–16,21,330].

The Hamiltonian of such a system can be written as:

$$\mathcal{H} = -\frac{Gm_1m_2}{2a_1} - \frac{GM_{\text{SMBH}}(m_1 + m_2)}{2a_2} - \mathcal{R}_{\text{pert}}, \quad (31)$$

where the first two parts represent the Keplerian energies of the two orbits, and $\mathcal{R}_{\text{pert}}$ is the perturbation function [331]. The perturbation function can be written as a function of the orbital (Delaunay’s) elements, the arguments of periastron, ω_1 and ω_2 , the longitudes of ascending nodes, Ω_1 and Ω_2 , and the mean anomalies μ_1 , and μ_2 for the inner and outer orbits, respectively. In particular:

$$\mathcal{R}_{\text{pert}} = \frac{G}{a_2} \sum_{n=2}^{\infty} \left(\frac{a_1}{a_2}\right)^n \mu_n \left(\frac{r_1}{a_1}\right)^n \left(\frac{r_2}{a_2}\right)^{n+1} P_n(\cos \psi), \quad (32)$$

where r_1 (r_2) is the position radius of the inner (outer) orbit, P_n are the Legendre polynomials, and ψ is the 3D angle between the position vectors of the inner and outer orbits.

The nominal procedure in such a system is perform a canonical transformation to a set of coordinates that eliminates the short-period angles of the inner and outer orbits. This transformation is known as the Von Zeipel transformation, see for details appendix B in Ref. [331].

The resulting (often called double-averaged) Hamiltonian is thus a multiple expansion of a_1/a_2 . The lowest order of approximation, (proportional to $(a_1/a_2)^2$) is called the quadrupole level, and corresponds to $n = 2$ in Eq. (32).

In early studies of high-inclination, hierarchical, secular perturbations [14,15], the outer orbit (in this case, about the SMBH) was assumed to be circular, with one of the inner binary members being a test (massless) particle. In this scenario, the component of the inner orbit’s angular momentum along the z-axis (set to be the total angular momentum) is conserved – known as the Kozai’s integral of motion– and the lowest order of the approximation, the quadrupole approximation, is valid.

In this regime, the conservation of the vertical angular momentum and energy implies that the eccentricity and mutual inclination vary along the orbit. An illustrative case is represented

by an initially circular binary inclined by an angle i_0 with respect to the binary-SMBH orbital plane, in which case the maximum eccentricity is given by [e.g. 19,188,332]

$$e_{\max} = \sqrt{1 - \frac{5}{3} \cos^2 i_0}. \quad (33)$$

The eccentricity excitation is triggered above a minimum value of the initial inclination, given by $\cos i_{\min} = \pm\sqrt{3/5}$, thus implying that only orbits having $39.2^\circ < i_{\min} < 140.77^\circ$ can undergo eccentricity variations. The timescale for KL oscillations to develop is [e.g. 333]

$$t_{\text{KL}} = \frac{16}{30\pi} \frac{m_1 + m_2 + m_3}{m_3} \frac{P_2^2}{P_1} (1 - e_2^2)^{3/2}, \quad (34)$$

$$= 40 \text{ Myr} \left[\left(\frac{m_1 + m_2}{30M_\odot} \right) \left(\frac{m_3}{10^6 M_\odot} \right)^{-1} + 1 \right] \left(\frac{a_2}{0.1 \text{ pc}} \right)^3 \left(\frac{a_1}{0.1 \text{ AU}} \right)^{-3/2} (1 - e_2^2)^{3/2},$$

with $P_i = \sqrt{a_i^3 / (Gm_{\text{bin},i})}$ is the inner ($i = 1$) or outer ($i = 2$) binary orbital period. 761

About a decade ago, it has been shown that relaxing either one of these assumptions leads to qualitatively different dynamical behaviors (already at the quadrupole level). Considering systems beyond the test particle approximation, or a circular orbit, requires higher terms in the Hamiltonian, called the octupole-level of approximation, proportional to $(a_1/a_2)^3$, i.e., $n = 3$ in Eq. (32), [e.g. 16–18,330]. In the past years, the octupole-level approximation was proven to have an important role in the evolution of many triple configurations, for different astrophysical settings [e.g. 19,20,188,205,291,331,332,334–344]. 762–768

In the octupole level of approximation, the inner orbit eccentricity can reach extremely high values [17,331,338,345]. This process was coined as the eccentric Kozai-Lidov (EKL) mechanism [21]. The hallmark of the EKL mechanism results in large eccentricity peaks, chaotic behaviour, and also flips the inclinations of both the inner and outer orbits from prograde to retrograde [19,332,334,345–348]. 769–773

The quadrupole-level of approximation relates to the low-level resonance that causes precession of the orbits and thus results in excitation of the orbital inclination and eccentricity [e.g. 331,346–349]. The higher level approximation, results in resonances that often are overlapping. These resonances result in extreme eccentricity values as well as flips and chaos [e.g. 19,331,332,334,345,346,348]. These extreme eccentricities are valuable for the mergers of compact objects. In Figure 12, left side, we show a representative example of the effect of octupole on merging binary. In general, octupole effects shorten the timescale and thus have significant effect on the merger rate [291], and see Figure 12 left panel for example. 774–781

6.2. Other physical processes 782

Aside two-body relaxation, which we discussed in the previous section, and the secular effect of the SMBH field onto binary members, different physical and astrophysical processes can contribute to the overall evolution of the system. These include short range forces between the binaries as well as dynamical interaction with the neighboring objects in NCs. Below, we briefly review these processes and their affects. 783–787

Tidal Dissipation: Considering the full evolution of binaries (i.e., starting from main-sequence stars), requires the inclusion of tidal dissipation. As the system evolves, the inner orbit can become highly eccentricity which could, on one hand drive the inner binary to merge, while on the other hand, could allow tidal forces to shrink and circularize the orbit. The latter happens if during the evolution the tidal precession timescale (or the general relativistic, GR, timescale) is similar to that of the lowest EKL timescale, which corresponds to the quadrupole. Thus further eccentricity excitations are suppressed [e.g. 349–351] and tides shrink the binary separation 788–794

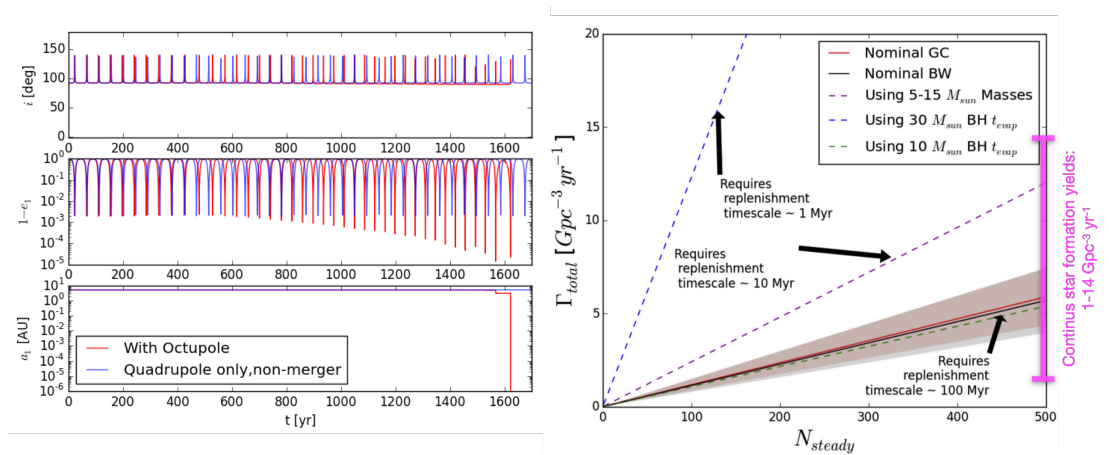


Figure 12. Left panel: A representative Example from Ref. [291], that depicts the evolution of BBH while solving the deafeningly equations up to the octupole level of approximation (red) and only up to the quadrupole level of approximation (blue). As shown the octupole-level evolution results in a merger after 1623 years, while the quadrupole-level approximation never merge. Right panel: volumetric BH merger rate as a function of the number of BBHs. This rate represents Monte Carlo results from Hoang et al, ApJ, 2018, 856(2), 140 ©AAS [291]. Reproduced with permission.

forming a tight binary that is decoupled from the SMBH. Conversely, if the eccentricity is excited on a shorter timescale than the typical tidal (or GR) precession timescale the orbit becomes almost radial, and the stars can cross the Roche-limit. In that case, the tidal precession does not have enough time to affect the evolution. 795

Most studies in this field use the equilibrium tides models [352,353]. The strength of the equilibrium tide model is that it is self-consistent with the secular approach used throughout this study. Further, assuming that the stars are polytropic, this model has only one dissipation parameter for each member of the binary. Using this tidal description we are able to follow the precession of the spin of each star in the binary due to the stars' oblateness and tidal torques [e.g. 350]. The disadvantage of using equilibrium is that for sufficiently large eccentricity, they tend to underestimate the efficiency of the tides compared to chaotic dynamical tides [e.g. 354,355]. 796
797
798
799
800
801
802
803
804
805
806

While the equilibrium tidal model seems to roughly consistent with the qualitative behavior of polytropes with convective envelopes, tides for radiative stars are estimated to be much weaker than for convective stars. Thus, within this framework a different tidal model for (radiative) main-sequence and (convective) red-giant stars is invoked [e.g. 356,357]. Within the context of EKL evolution only a few studies began including the less efficient radiative tides [e.g. 59,342,344,358,359]. 807
808
809
810
811
812

Overall tides between the binary members largely influence the EKL evolution of the stars. It tends to shrink and circularize the orbit [e.g. 205,350], thus hardening the binary to flyby interactions [e.g. 203,360]. During the binary stellar evolution, if the eccentricity spikes take place faster than the tides can suppress the high eccentricity values, the binary star may merge, (typically of few $\times 10 M_{\odot}$), and is speculated to form a G2-like object [e.g. 59,205,361,362]. Surviving stars undergo a combination of EKL, tides, GR, and stellar evolution (see below). 813
814
815
816
817
818

Stellar evolution Stellar evolution plays an important role for the evolution of binaries and especially massive binaries. Specifically, it was shown that mass loss can have a significant effect on the dynamical evolution of binaries and triples [e.g. 188,205,337,363–366]. For near equal-mass binaries the mass loss associated with the AGB phase can re-trigger the EKL 819
820
821
822

mechanism, either by changing the mass ratio, or by expanding the semi major axis of the inner orbit faster than that of the outer one [337,367].

Often, in the literature, the post-main sequence evolution model is adopted from a combination of stellar evolution codes, such as BSE/SSE [154] and MESA [368], which are publicly available. Furthermore, once the binaries cross each other Roche-limit the binary stellar evolution is often followed using COSMIC binary stellar evolutionary code [369].

The effects of supernova explosion and asymmetric and/or instantaneous mass loss (i.e., pulse-like, instantaneous, relative to the secular timescale) can affect the orbital parameters of massive binaries [e.g. 370–373] and triples [e.g. 374,375]. Sudden mass loss can cause a rapid change of the mass ratio, but more importantly, it can change the eccentricity of the inner and outer orbit due to a supernova kick.

In particular, there is a variety of dynamical outcomes resulting from SN kicks, in binaries at the centre of galaxies. For example, it can result in hypervelocity star [e.g. 376] and binary candidates [e.g. 374,377], as well as x-ray binaries [377]. Finally, GW events triggered by SN kicks can result in binary merger events, and EMRIs [e.g. 374,376,377].

General Relativity precession, 1st pN In the 1st post Newtonian (pN) approximation the inner (and outer) binary exhibit an additional precession of the nodes. The typical timescale for this mechanism can be written as [18,378]

$$t_{1\text{pN}} = \frac{a_1^{5/2} c^2 (1 - e_1^2)}{3G^{3/2} m_{\text{bin}}^{3/2}} \quad (35)$$

$$= 103 \text{ yr} \left(\frac{m_{\text{bin}}}{30M_{\odot}} \right)^{-3/2} \left(\frac{a_1}{0.1 \text{ AU}} \right)^{5/2} (1 - e_1^2).$$

If the precession timescale of the inner binary is shorter than the quadrupole timescale, eccentricity excitations can be suppressed [e.g. 17,20,351,379]. If the GR timescale is comparable to the octupole time scale, the system can be excited to larger eccentricities than the ones reached without the GR effects [e.g. 20,380]. Similar result takes place for the hexadecapole level of approximation $n = 4$, in Eq. (32) [e.g. 381].

Spin effects, 1.5pN: The compact objects' spins can cause a variety of precessions that may affect the overall dynamics. For example, de-Sitter precession [e.g. 382] can cause the precession of the compact object spin vector about the angular momentum of the binary. On the other hand Lense–Thirring Precession can cause the precession of the angular momentum about the spin of the compact object [e.g. 382], if the two vectors are initially misaligned. This effect translates to eccentricity excitation as the angular momentum changes.

We will see in Section 8 that these effects may leave an imprint detectable by future GW detectors, like LISA.

During the EKL mechanism, the binary's spin axes undergo chaotic evolution, similarly to non-compact object case [e.g. 334,336,350,383,384]. This process leads to a wide range of the final spin–orbit misalignment ($0^\circ - 180^\circ$), thus favouring the formation of merging binaries with misaligned spins.

Unlike strong scatterings, which dominate mergers in massive clusters and produce an isotropic distribution of spin orientations, the compact object spins in this EKL+1.5pN case are strongly correlated with one another [e.g. 385].

GW, 2.5pN: The higher pN terms affect the Gravitational Wave (GW) emission of compact object binaries [e.g. 386]. The large eccentricity, potentially produced via the octupole level of approximation, can produce pulse-like GW emissions which shrinks the binary semi-major axis, and later circularizes the orbit [e.g. 387,388].

Resonant relaxation processes: Binaries embedded inside a dense stellar cluster are subjected to a continuous influence from the gravitational field generated by all the other cluster members,

which can impinge secular effects on its orbital evolution [e.g. 203,389–392]. These effects include different relaxation processes and precession of the orbit due to the extended and possibly anisotropic gravitational potential.

Within the sphere of influence of the SMBH the motion of stars and compact objects is nearly Keplerian, therefore the encounters between stars are correlated. These correlated gravitational encounters result in torques that can change both the direction and magnitude of the angular momentum of the orbit of the binary about the SMBH, known as resonant relaxation processes [e.g. 389,391,393–398].

Resonant relaxation causes the variation of magnitude and direction of the outer angular momentum (thus eccentricity) over a timescale [e.g. 389,391,399]

$$t_{rr,s} = 0.9 \text{Gyr} \left(\frac{M_{\text{SMBH}}}{4.3 \times 10^6 M_{\odot}} \right)^{1/2} \left(\frac{a_2}{0.1 \text{ pc}} \right)^{3/2} \left(\frac{m}{1 M_{\odot}} \right)^{-1} \quad (36)$$

Vector resonant relaxation, instead, tends to alter the orientation of the angular momentum, thus changing the binary's mutual inclination between the inner and the outer orbit over a timescale [e.g. 389,391,400]

$$t_{rr,v} = N^{-1/2} t_{rr,s}, \quad (37)$$

where N is the number of stars within the outer orbit a_2 . While the vector resonant relaxation rate depends on the underlying density distribution profile, it may be comparable to the EKL timescale at distances of ≤ 0.5 pc, depending on the binary's separation [400]. Overall vector resonant relaxation may work to enhance the merger rate by changing mutual inclination to a more EKL-favorite regime of the parameter space [400]. Given the uncertainties, this regime yields a BH merger rate similar to the one expected from the inner ≤ 0.1 pc region.

For even further distances from the SMBH, at the edge of the sphere of influence, deviation from spherical potential of the nuclear star cluster can result in a long-term effect, similar to the EKL [392]. This processes also yields a similar BH merger rate as the one expected from the inner ≤ 0.1 pc merger rate. Below we discuss the overall expected merger rate and the relevant uncertainties.

6.3. Initial Conditions and Unknowns

The description of the interplay among COs, COBs, and a central SMBH relies upon several unknowns, which may significantly affect the possible development of both COB and SMBH-CO mergers.

The number of binaries, their period and eccentricity distribution, the CO mass distribution, are poorly constrained by observations and largely influence the final outcomes of dynamics. The density distribution of COs around the SMBH is another crucial, but poorly constrained, quantity that affects all dynamical processes, from relaxation to binary hardening [e.g. 48], dynamical friction [e.g. 268], collision rate [e.g. 51,310]

Since binary's inner and outer period distribution are degenerate, the EKL efficiency is less sensitive to the aforementioned uncertainties. While at first glance this may be counter intuitive, it can be understood when considering the stability requirement. Long term stability yields a hierarchical configuration and avoiding the breakup of the binary due to the SMBH tidal forces (i.e., the Hills mechanism, [283]). Therefore, binaries closer to the SMBH may have shorter inner period than those further away from the SMBH [e.g. 205].

Regarding the formation of COB mergers, surely one important parameter is represented by the number of binaries that can actually form [see 291], which in turn depends on the star formation rate in the galaxy centre and the rate at which infalling clusters can supply new COs and COBs to the nucleus [277].

The Milky Way centre represents our benchmark, and in principle can be used to estimate the star formation rate inside a NC. Within the SMBH sphere of influence, the Milky Way contains about $\sim 10^7 M_{\odot}$ of stars and stellar remnants [e.g. 401,402], assuming a continuous star formation rate, and the age of the galaxy of about 10 Gyr, this gives an approximate rate of $10^3 M_{\odot} \text{ Myr}^{-1}$. Despite this rough estimate is consistent with recent observations and theoretical advancements [e.g. 204,206,403], it remains highly uncertain and should be taken with a grain of salt.

7. Dynamics of black hole binaries in active galactic nuclei

The presence of an accretion disc feeding a central SMBH is a natural requirement to explain the luminosity, variability, and spectra of observed AGN, although both the pathways that can lead to the accretion disc formation and the physics regulating its evolution are still not fully understood. In the classical framework depicted by Shakura and Sunyaev [404], and extended by Novikov and Thorne [405] to include general relativistic effects, the disc settles into a stationary configuration owing to inwards angular momentum transport due to an effective viscosity in the disc.

Above a critical value of the disc surface density, the angular momentum and energy transfer that a star experiences while passing through the disc becomes significant, causing dissipation that can *capture* the star, forcing its orbit to settle into the disc plane and undergo inward migration, causing a steepening of the radial density profile [406–409]. Two-body relaxation with objects outside the disc competes with this dissipative process, leading to an almost stationary state where two-body relaxation scatters stellar objects off the disc whilst dissipation captures them [410]. When the timescales of these competing process are comparable, solar-mass objects are more easily accreted onto the central SMBH, possibly enhancing the rate of tidal disruption events [27,411] and naturally leading to the formation of a nuclear stellar disc [29]. Once stars and stellar compact objects are captured into the disc, the relative velocity among disc-objects decreases, leading to a significant increase of the collision rate, $\sigma_c \propto v_{\text{rel}}^{-2}$, especially in the outer regions of the disc, possibly favouring the formation of an IMBH seed [e.g. 26].

Depending on the disc properties, the swift growth of an IMBH-seed via gas accretion can be so efficient to deplete gas from the AGN disc, a feature that is inconsistent with the properties of observed AGNs. However, winds and jets launched by the accreting IMBH could create a hole around the IMBH. This feedback mechanism could quench the IMBH growth in MW-sized galaxies, and almost eradicate the disc in AGNs with an SMBH lighter than $10^5 M_{\odot}$, thus explaining the dearth of high-Eddington ratio AGNs in that SMBH mass range [412].

The stellar object motion is driven by different forces owed to accretion, dynamical friction exerted by the gaseous medium, and stellar scatterings [33,413].

Whilst moving in the disc, the BH motion is subject to migration induced by the resonant gravitational interaction with the gas disc [414]. If the gravitational torque of the moving body is smaller than the gas viscous torque, the body undergoes the so-called Type I migration, triggered by Lindblad and corotation resonances [25,414–416]. The typical timescale of Type I migration depends on the mass of the object and the central BH, the AGN surface density and thickness, and the location of the captured object.

Sufficiently large gravitational torques, instead, enable the moving object to open a gap in the disc. In such a case, the object migrates due to the torque exerted by the gas on the gap boundary, leading to the Type II migration [415,417–419]. The timescale of Type II migration is generally larger than that of Type I migration, depending on the SMBH mass, the moving object, and the viscosity of the gas. Non-axisymmetric streamers flowing across the gap may significantly alter the migration rate [419,420].

Depending on the gas structure and properties, gas torques can also push the object away from the disc centre, thus causing an outward migration [421,422]. Inward and outward torques can cancel out in particular regions of the disc and form a so-called *migration trap* that halts the migration. Migration traps are natural predictions of protoplanetary disc models [423] and could be a possible mechanism to form the core of giant gaseous planets [424]. The location of the trap inside the disc may be independent of the SMBH mass and the SMBH-to-BH mass ratio, as these quantities only affect the amplitude of the torque [86]. However, details of migration trap formation are still unclear and are mostly connected with the study of protoplanetary disc formation: inefficient viscous mixing can cause torque saturation, damping migration for sufficiently small objects [425] and leading to a mass dependency on the location of the traps [426–428], the establishment of a dynamic torque can halt(boost) inward(outward) migration [429,430], whilst a heating torque derived from accretion processes onto the moving body can counteract inward migration [431–433]. Whilst some elements of protoplanetary disc dynamics can be borrowed to explain compact object dynamics in AGNs, any parallelism must be cautionary, taking into account that the latter are generally comprised of hotter, high-viscosity, turbulent gas, where torque saturation is less likely [434,435].

Depending on the disc model adopted, these migration traps set at tens and a few hundred times the SMBH gravitational radius, i.e. $\sim (0.4 - 3)$ mpc for an SMBH mass $M_{\text{SMBH}} = 10^8 M_{\odot}$ [86].

More generally, even if such migration traps do not exist in AGN discs [434,435], a similar accumulation of objects may take place at radii where the inward migration rate becomes slower than the rate at which objects get captured in the disc. This may happen in regions where the physical properties of the disc change (e.g., source of opacity, self-gravity, etc.) or where gaps are opened by the gravitational torques of objects in the disc [33]. Binary formation and mergers may be especially abundant in these regions.

Once BHs and COs have settled in the disc, the formation of binaries can be triggered by three- and few-body interactions as in galaxies harboring a quiescent SMBH, and by single-single triggered by gas dissipation [33]. Three-body scattering process can efficiently aid binary formation in AGN discs, owing to the fact that gas damps stellar velocities via gaseous dynamical friction and torques [33], thus providing low velocities and high densities. Further, the presence of a gaseous medium offers a further mechanism: gas capture binary formation. In such mechanism, two objects passing through their mutual Hill spheres can bind together if the Hill sphere crossing time is longer than the timescale over which gas dynamical friction damps the relative velocities of the two objects [436]. As discussed in Ref. [33], the gas assisted binary formation rate steeply increases toward the disc inner regions, and clearly overtakes the formation rate associated with three-body scattering. Thus, gas capture binary formation is expected to be the dominant process for binary formation in AGN discs. This also favours the mass growth of IMBH-sized objects via gas accretion and repeated mergers with stars and compact objects in the disc [26,33,34,434,437].

All these processes are nicely sketched in Figure 13, a schematic view on binary formation activities in AGNs described in [33].

Once binaries start forming in the disc, their long-term evolution is regulated by both dynamical and gaseous processes. Having a relatively large cross section compared to single objects, newborn hard binaries will further harden via binary-single scattering [11,210,282,328]. Binary-single interactions with stars or compact objects in the spherical star cluster typically kicks the binary from the gaseous disc to inclined orbits, while gas-dynamical friction drives the binaries to settle back to the disc. Furthermore, binary-single interactions increase the binary eccentricity in a disc configuration more than in isotropic scatterings, which accelerates the subsequent GW-driven merger [35,438], and are expected to work even more efficiently close to migration traps, where the binary-single interaction rate increases significantly [434,439]. Aside

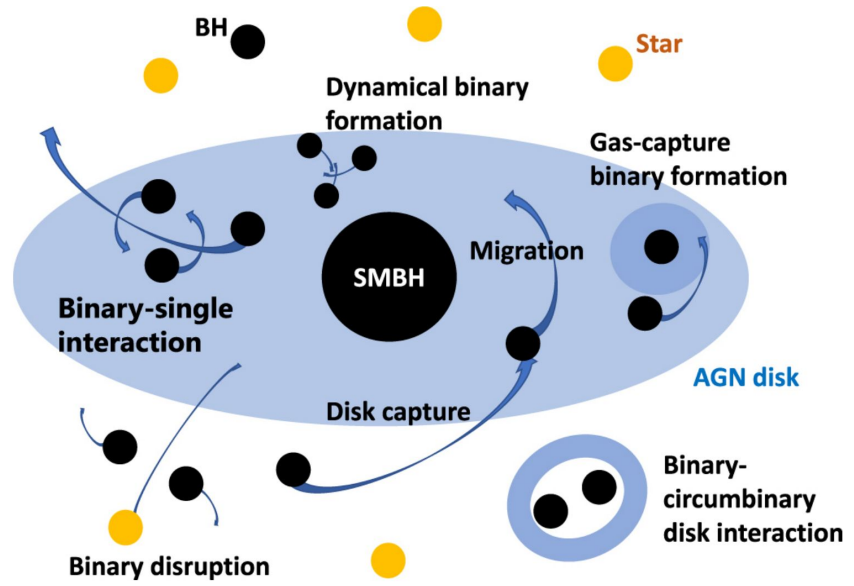


Figure 13. Schematic illustration of the different processes that contribute to black hole binary formation in the disc of an active galactic nucleus. Taken from Tagawa et al, *ApJ*, 2020, 898(1), 25 ©AAS. [33]. Reproduced with permission.

binary-single interactions, which represent the dominant process in binary hardening [30,33], the gaseous medium in which the binary is embedded can trigger further binary hardening owing to dynamical friction [28] and type I/II torques exerted from a circumbinary disc formed around the moving binary [25,418,439–441].

Despite the many processes likely at play in an AGN, one seems clearly dominating in determining BBH formation, namely the gas-capture process, which accounts for 64 – 85% of all BBH mergers occurring around a MW-like SMBH [33]. Once formed, binaries merge very efficiently in AGN due to binary-single interactions, even if gas driven migration effects and accretion effects are completely neglected [33].

8. Black hole and neutron star mergers around supermassive black holes: implications for current and future gravitational-wave detections

The various physical processes described in the previous sections leave an imprint on the population of merging COs. In the following, we discuss in more detail what properties characterise the population of merging BBHs and NS-BH binaries formed in galactic nuclei, differentiating between quiescent SMBHs and AGNs, and the consequences for current and future GW detectors.

In these regards, it is worth recalling here that eccentric COBs emit broadband GWs with a characteristic peak frequency that can be expressed as [163,442]

$$f_{\text{peak}} = 4.6 \text{ Hz} \left(\frac{k}{30} \right)^{-3/2} \left(\frac{m_{\text{bin}}}{30M_{\odot}} \right)^{-1} \zeta(e_{\text{bin}}), \quad (38)$$

where $k = a_{\text{bin}}/R_{\text{Schw}} = c^2 a_{\text{bin}}/(2Gm_{\text{bin}})$ represents the ratio between the binary semimajor axis and the COB total Schwarzschild radius, in such a way that $k = 3$ corresponds to the

innermost stable circular orbit (ISCO) for non-spinning BH. There are different expression for the function $\zeta(e_{\text{bin}})$ [265,442]

$$\zeta(e_{\text{bin}}) = \begin{cases} (1 + e_{\text{bin}})^{1.1954} / (1 - e_{\text{bin}}^2)^{3/2} & \text{Wen [442]} \\ (1 + e_{\text{bin}})^{1/2} / (1 - e_{\text{bin}})^{3/2} & \text{O'Leary et al. [265]} \end{cases} \quad (39)$$

From the Equation above we see that a typical hard BBH with mass $m_{\text{bin}} = 30M_{\odot}$ and $a_{\text{hard}} = 0.1 \text{ AU}$, i.e. $k = 9 \times 10^6$, will emit GWs with frequency peaked at $f \sim 0.35 \text{ mHz}$.

Thus, merging BBHs represents potentially multiband GW sources [e.g. 443] that could be visible to both low-frequency GW detectors like LISA [444–446], TianQin [447], Taiji [448,449], mid-range frequencies like ALIA [450], DECIGO [451,452], and other decihertz observatories [453–455], and high-frequency detectors like LIGO-Virgo-Kagra [456,457], and future detectors like Einstein Telescope [458,459] or Cosmic Explorer [460,461].

Next section will focus on the properties of COB mergers in galactic nuclei, attempting at highlighting how they could be used to identify the COB origin in different GW detectors.

8.1. Population properties: masses, mass-ratio, spins, and eccentricity

There are several parameters that could help unravelling BBH mergers with a dynamical origin, although the uncertainties in the theoretical models for both stellar evolution and dynamics make it harder to find a truly unique spot where dynamical mergers stand apart from the isolated ones.

A merging COB can be characterised primarily through intrinsic quantities, like the j -th component mass m_j and adimensional spin $\chi_j = \frac{cS_j}{Gm_j^2}$ (with S_j the spin), and the binary eccentricity e and semimajor axis a . Nonetheless, there are further quantities that are particularly important from the perspective of GW detection. Among other, the so-called chirp mass, a parameter that, at the lowest order, can be linked to the frequency (f) and its variation (\dot{f}) of the emitted GW via the relation

$$\mathcal{M} = (m_1 m_2)^{3/5} / (m_1 + m_2)^{1/5} = \frac{c^3}{G} \left(\frac{5}{96} \pi^{-8/3} f^{-11/3} \dot{f} \right)^{3/5}, \quad (40)$$

and thus can be directly measured by GW detectors [462–464].

Similarly, also spins affect the evolution in phase and amplitude of the emitted GW, but it is hard to fully untangle the two spin vectors [465,466], even in space-borne detectors like LISA [e.g., see 463,464]. Nonetheless, it is still possible to retrieve information encoded in the dominant spin effect by using a one-dimensional parametrization that, in the simplest form, can be written as a simple mass-weighted linear projection of the spins onto the binary orbital momentum vector \vec{L} [467–471]

$$\chi_{\text{eff}} = \frac{(m_1 \vec{\chi}_1 + m_2 \vec{\chi}_2) \cdot \vec{\tilde{L}}_{\text{bin}}}{m_1 + m_2} = \frac{m_1 \chi_1 L \cos(\theta_1) + m_2 \chi_2 L \cos(\theta_2)}{m_{\text{bin}}}, \quad (41)$$

with θ_j the angle between the binary angular momentum and the spin of the j -th binary component. As suggested by the BBH mergers detected during the three LVC observation runs [141], this parameter seems to cluster around low value [e.g. 472–476].

Spins' information is encoded also in another measurable quantity, unfortunately poorly constrained in current detectors[68]: the precession spin parameter χ_p [477], which measures

the degree of in-plane spin and parametrizes the rate of relativistic precession of the binary orbital plane [141,478]

$$\chi_p = \max \left[\chi_1 \sin \theta_1, \left(\frac{3 + 4q}{4 + 3q} \right) q \chi_2 \sin \theta_2 \right]. \quad (42)$$

Aside from masses and spins, another parameter that could be measured from GW detectors is the binary eccentricity. This became possible only relatively recently [e.g. 143,144, 479], because binary parameter estimation from the detected signal exploits Bayesian inference, which can be extremely computationally demanding. This led to the development of, on the one hand, numerical relativity simulations aimed at obtaining waveform templates [480], and, on the other hand, approximate methods, or *approximants*, that greatly reduced the computational cost of data analysis but generally they are generally constructed on the leading order of GW signal expansion [479, e.g.]. A recently developed technique, however, enabled the possibility to retrieve information on the binary eccentricity at a small computational cost [481,482], and permitted to place constraints on the eccentricity of LVC sources, suggesting that up to 4 of them might be eccentric sources [146,148]. In the frequency range of LVC detectors, i.e. $f \sim 10$ Hz, it has been shown that at design sensitivity it would be possible to discern an eccentric source provided that $e_{10\text{Hz}} > 0.04$, being the error on the eccentricity measurement around $\delta e \approx (10^{-4} - 10^{-3})(D/100\text{Mpc})$ [151,152].

Merging COBs developing in different environments may exhibit peculiar values of the aforementioned quantities, thus their measurement is crucial to assess the origin of GW sources. For example, mergers with one or both components in the upper mass-gap, like GW190521 [483], could represent the best candidates to identify signatures of a dynamical origin.

Generally, the formation of mass-gap BH mergers in the isolated binary scenario is rather unlikely, whilst in dynamical environments hierarchical mergers represent a viable possibility to explain them, especially in the case of galactic nuclei. Close to an SMBH, the escape velocity is roughly given by

$$v_{\text{esc}} = 2076 \text{ km s}^{-1} \left(\frac{M_{\text{SMBH}}}{10^6 M_{\odot}} \right)^{1/2} \left(\frac{r}{1 \text{ mpc}} \right)^{-1/2}, \quad (43)$$

thus close to a MW-sized SMBH the escape velocity can favour the retention of first-generation merger products (1g), or second-generation BHs (2g), which are subjected to GW recoil kicks as large as 10^3 km s^{-1} . Once recoiled, the BH will eventually come back into the galactic centre over a mass-segregation time, form a new binary via binary capture [13] or three-body scattering [309], harden and merge. Depending on the nucleus properties, the whole process can take much longer than a Hubble time, owing to the steep dependence of the dynamical timescales (Eqs. 4, 25, 28) on the nucleus velocity dispersion and density. Nonetheless, the development of mergers involving 2g or 1g BHs, is more likely in galactic nuclei – O(10%) – than in globular or young massive clusters [98,99,111,116,127,484,485].

To discuss other potential characteristic traits of COBs mergers in galactic nuclei, let us divide the processes that can trigger a merger into three main categories: i) gravitational scatterings, ii) EKL-driven, iii) AGN-driven.

8.1.1. Gravitational scatterings

Gravitational scatterings are likely the main engine triggering COB mergers around SMBHs in the $M_{\text{SMBH}} = (10^6 - 10^8) M_{\odot}$ mass range, being responsible of up to 20 – 70% of mergers in galactic nuclei [30,277,438,486]. BBH merger products formed via binary-single scatterings affect the overall BH mass spectrum, populating the upper mass-gap and extending beyond $M_{\text{BH}} \gtrsim 100 M_{\odot}$ [114,116,277,446,484]. Binary-single scatterings in galactic nuclei can

also favour the formation of NS-BH binary mergers, being the individual merger rate – i.e. the number of mergers per cluster – around 10(100) times larger compared to globular(young) clusters [e.g. 130,136,310]. A substantial fraction of NS-BH mergers forming in galactic nuclei, and in dense star clusters in general, is expected to clearly differ from those formed in isolation, having larger chirp masses and primary components with a mass $m_1 > 20M_\odot$ [130,132]. Binary-single scatterings and GW captures are efficient mechanisms to form eccentric binaries: 50 – 90% BBH mergers formed this way have an eccentricity $e_{10\text{Hz}} > 0.9$ when sweeping through the typical LIGO band [151,152,265,487].

The geometry of the scattering can be rather important in determining the merger characteristics: if the scattering occurs in a plane, as it can happen in AGN discs, for example, the merger rate is boosted by a factor 10-100 owing to the fact that the merger efficiency in three-body scattering increases at decreasing the binary-single object mutual inclination [35,438]. The enhancement in the merger rate is also accompanied by an enhancement in the probability to form merging binaries with a high eccentricity in the LVC band [35]. Mergers induced by a "single" binary-single scattering, i.e. in which the merger occurs before the next interaction takes place, are more likely to emit GWs in the 1-10 mHz frequency range, where LISA and space-borne detectors are sensitive [35], whilst those formed chaotically during a 3-body resonant interaction, or scramble, and via GW captures typically quickly merge in the 1-10 Hz band, where LIGO and ground-based detectors are sensitive [35,265]. Given the chaotic nature of the gravitational scattering process, mergers formed this way are expected to feature an isotropic distribution of their spin orientation, which implies generally small χ_{eff} values. For comparison, fully (anti)aligned spins implies (negative)positive values of χ_{eff} .

8.1.2. Eccentric Kozai Lidov mechanism

When the effect of the SMBH tidal field cannot be neglected, the EKL mechanism can aid the COB coalescence through eccentricity excitation. The merger efficiency for the EKL-driven channel weakly increases with the SMBH mass in the $M_{\text{SMBHs}} = (10^6 - 10^8)M_\odot$ mass range and decreases for heavier SMBH mass values [101,277,291,399,486].

Around 40% of EKL-assisted mergers have primary masses in the upper mass-gap, $m_1 = (50 - 90)M_\odot$, and around 30% have also a companion with mass $m_2 < 20M_\odot$, thus mass ratios $q \simeq (0.1 - 0.6)$ [88,277]. Only a fraction $\sim 1 - 20\%$ of EKL-driven mergers is expected to preserve an eccentricity $e > 0.1$ at $> 10\text{Hz}$ [378,399], owing to the fact that the eccentricity increase driven by the EKL mechanism can drive to merger binaries that are initially relatively loose. Nonetheless, around 40% of these binaries may appear eccentric in the LISA band and up to 5% of them could preserve an $e > 0.1$ while sweeping through the deci-Hz band, thus representing potentially bright multiband sources [98]. Although LISA is unlikely to observe more than a few tens of BBH mergers [e.g. 358,488], it could be possible to observe eccentricity variation for BBHs in the Galactic Centre [489].

The development of EKL resonances and the consequent increase of the binary eccentricity up to a maximum value e_{max} reduces the merging timescale, possibly affecting the overall delay time of EKL-driven mergers. In such case, the merger time can be expressed as [378,490,491]:

$$t_{\text{GW}} = t_{\text{GW},0}(1 - e_{\text{max}}^2)^\alpha, \quad (44)$$

with $\alpha = 1.5 - 2 - 2.5 - 3$ in the eccentricity ranges $e_{\text{max}} = (0 - 0.6), (0.6 - 0.8), (0.8 - 0.95)$, and $(0.95 - 1)$, respectively [378,490,491]. This implies that the larger the maximum eccentricity, the shorter the merging time. Let us consider an initially circular, equal-mass binary with $m_{\text{bin}} = 30M_\odot$ and semimajor axis $a = 0.1$ AU, its merging time is $t_{\text{GW},c} = 4.8$ Gyr [386]. Eccentricity increases owing to EKL up to $e_{\text{max}} = 0.5(0.9)$, thus the binary merges after $t_{\text{GW}} = 1.7(0.02)$ Gyr, a notable difference that highlights how crucial is the orbital distribution of compact objects around an SMBH.

If the SMBH is spinning, as indicated by several observations [e.g. 492,493], the coupling among the SMBH spin and the BBH-SMBH and BBH angular momenta can cause an efficient *apsidal precession resonance*, meaning that the outer and inner binaries have the same pericentre precession rate owing to both Newtonian and General relativistic effects [494]. This results in an angular momentum exchange between the BBH-SMBH and the BBH, which leads to a significant growth of the BBH eccentricity up to a maximum value that increases at increasing the BBH-SMBH initial eccentricity [494–497]. This mechanism can lead to an increase of the BBH even in cases in which the EKL resonance don't develop, e.g., nearly coplanar systems, and could leave an imprint in the merging BBH waveform that might be detectable with LISA and help constraining the SMBH spin amplitude and its mass [495,498,499].

A binary undergoing EKL around a Kerr SMBH can undergo de Sitter and Lense-Thirring precession mechanisms, which cause the chaotic re-orientation of the spins [e.g. 385], leading to merging binaries with misaligned spins and nearly zero χ_{eff} [e.g., 96,98,99,385,490,491,500,501].

8.1.3. Active galactic nuclei

Merging BBHs in AGN discs are expected to exhibit several peculiarities, compared to those developing in quiescent nuclei via EKL oscillations or gravitational scatterings.

Given the large escape velocities in AGNs, repeated mergers can be quite common in such environments, thus providing a further channel to produce mass-gap objects. If migration traps do exist, repeated merger might constitute up to 20 – 50% of all COB mergers [32,502], with more than 40% of all mergers involving one BH with mass $\geq 50M_{\odot}$ [32]. Even in the absence of migration traps, hierarchical mergers can constitute 20 – 45% of all mergers mediated by binary-single interactions and gaseous torques [33]. Nonetheless, the fraction of remnants in the high-end of the BH mass distribution is expected to remain generally low, around 3 – 11%, but can significantly vary depending on the adopted model [34]. The high occurrence of repeated mergers influences the mass ratio AGN mergers, whose distribution peaks at values around $q = 0.2 - 0.7$, depending on the models [31,502]. Similarly to quiescent nuclei, dynamical interactions can enable the formation of eccentric mergers also in AGNs via either binary-single interactions or GW captures. Given the flattened configuration of AGN discs, most of the mergers produced via binary-single scatterings are expected to produce eccentric binaries detectable by LISA [438]. Together with binary-single interactions, GW captures occurring within $O(\text{mpc})$ from the SMBH can be sufficiently energetic to trigger the formation of mergers preserving an eccentricity $e > 0.3$ in the LIGO-Virgo band with a probability of 20 – 70% [35,438].

Gaseous torques and accretion are expected to align both the BH spin vectors and the binary angular momentum, thus suggesting that BBHs in AGNs are characterised by either aligned or anti-aligned spins. BBHs moving on prograde orbits with respect to the AGN angular momentum are expected to rapidly accrete gas, spin up and align the spins over a timescale shorter than the AGN lifetime [503], whilst those on retrograde orbits are more likely to merge and leave behind a final BH with a spin antialigned with respect to the disc [25]. Given the alignment/antialignment of the orbital spins, AGN mergers are expected to have an effective spin distribution peaked at positive/negative values, likely around 0.4 [32]. The preponderance of hierarchical mergers would also favor the development of anti-/aligned mergers [32], thus possibly causing the formation of a sub-population of mergers characterised by large masses and $\chi_{\text{eff}} < 0$, a feature hardly reproducible through other channels. Nonetheless, even in AGNs is possible to generate low χ_{eff} mergers, depending on the efficiency of radial migration and the binary-single scattering rate [504], although the overall distribution could preserve a small excess toward positive values dominated by mergers among high generation BHs [502]. Gaseous accretion can also favour the formation of COs in the lower mass-gap, thus providing suitable explanation for GW sources like GW190425 or GW190814 [34,134].

As shown in some numerical models, in AGNs mergers a combination of the effective spin parameter and the precession parameter, namely $\chi_{\text{tot}} \equiv (\chi_{\text{eff}}^2 + \chi_p^2)^{1/2}$, increases with the merger chirp mass up to the maximum chirp mass allowed by the adopted, first-generation, mass spectrum, and then saturates toward a value $\chi_{\text{typ}} \sim 0.6$ [505]. Despite such typical quantity could represent an optimal parameter to identify AGN merger candidates, the precession spin parameter χ_p is often unconstrained in observed data, making it hard to place reliable constraints on χ_{typ} .

One of the most intriguing predictions of the AGN channel is the possible production of EM signatures associated with the merger event. A well known example is the GW190521 source, which has been proposed to be associated with an EM transient detected by the Zwicky Transient Facility [506], although it is rather hard to assess whether or not the GW and EM signals are truly associated [507,508], as GW190521 has a localization volume that likely contains $\sim 10^4$ AGNs [509]. Nonetheless, future follow-up campaigns targeting the most massive BBH mergers could establish their association to an EM counterpart, provided that the fraction of BBHs producing an AGN flare is substantial (> 0.1) [509].

Establishing whether a BBH merger has an AGN origin could be assessed statistically on the basis of spatial correlation, a technique that requires at least $f_{\text{AGN}} N_{\text{det}}$ detections, where f_{AGN} corresponds to the fraction of GWs coming from AGNs [510]. In principle, this implies that the missing evidence of a BBH-AGN connection in the light of 100 GW detections would suggest $f_{\text{AGN}} < 0.25$, although the number of required detections to assess their AGN origin hugely varies with the AGN number density [510].

8.2. Expected Merger Rate and Prediction

In the following, we retrieve from the literature merger rate estimates at redshift $z = 0$ for both BBH and NS-BH mergers induced by dynamics around a quiescent SMBH or in an AGN. When the authors provide the number of events per galaxy and per year [e.g. 265] we multiply this quantity by the local density of Milky Way equivalent galaxies $\rho_{\text{MWEG}} = 0.0116 \text{ Mpc}^{-3}$ [511,512]. Figures 14 and 15 show the merger rate density interval for BBH and NS-BH mergers at redshift $z \sim 0$ reported in the literature.

Broadly speaking, the inferred merger rates for mergers around quiescent SMBHs and AGNs cover a wide range of values, up to 3-4 order of magnitudes, owing to the large uncertainties affecting the models.

For AGNs, there are several sources of uncertainties [for a detailed discussion, see 33,513]: the number density of galactic nuclei hosting an AGN, ($10^{-3} - 10^{-2}$) Mpc^{-3} [e.g. 514], the BH number density in galactic nuclei (10^{4-6}) pc^{-3} [53,55,58], the AGN occupation fraction (0.01 – 0.3) [515], the BH binary fraction (0.01 – 0.2) [55,287,434,516], the AGN lifetime (0.1 – 100) Myr [517–519].

For quiescent SMBHs, instead, the uncertainties owe mostly to the number of BHs lurking in the galactic centre and the rate at which the BH population is replenished [277,291,399], the geometry of the NC surrounding the SMBH [291,392] and the SMBH mass [277,291,399], the properties of the BBH population [277,486].

Adopting Milky Way like conditions and assuming that the fraction of galaxies hosting a NC is ~ 0.5 yields a BBH merger rate of $\sim 1 - 20 \text{ Gpc}^{-3} \text{ yr}^{-1}$ [e.g. 59,358]. This rate is consistent with a simplified model that starts with objects at the BH stage [e.g. 291] and N-body calculations [277]. Vector resonant relaxation only slightly enhance the rate, for a Milky Way like conditions, but is much more effective for a smaller mass SMBH [e.g. 400]. On the other had, the EKL-derivative for a none spherical potential yields a rate of $\sim 1 - 15 \text{ Gpc}^{-3} \text{ yr}^{-1}$ [392]. Thus, combining these three effects, the merger rate from within inner few to ten parsecs at the centre of a galaxy is expected to be $1 - 50 \text{ Gpc}^{-3} \text{ yr}^{-1}$. The lower limit in this range is

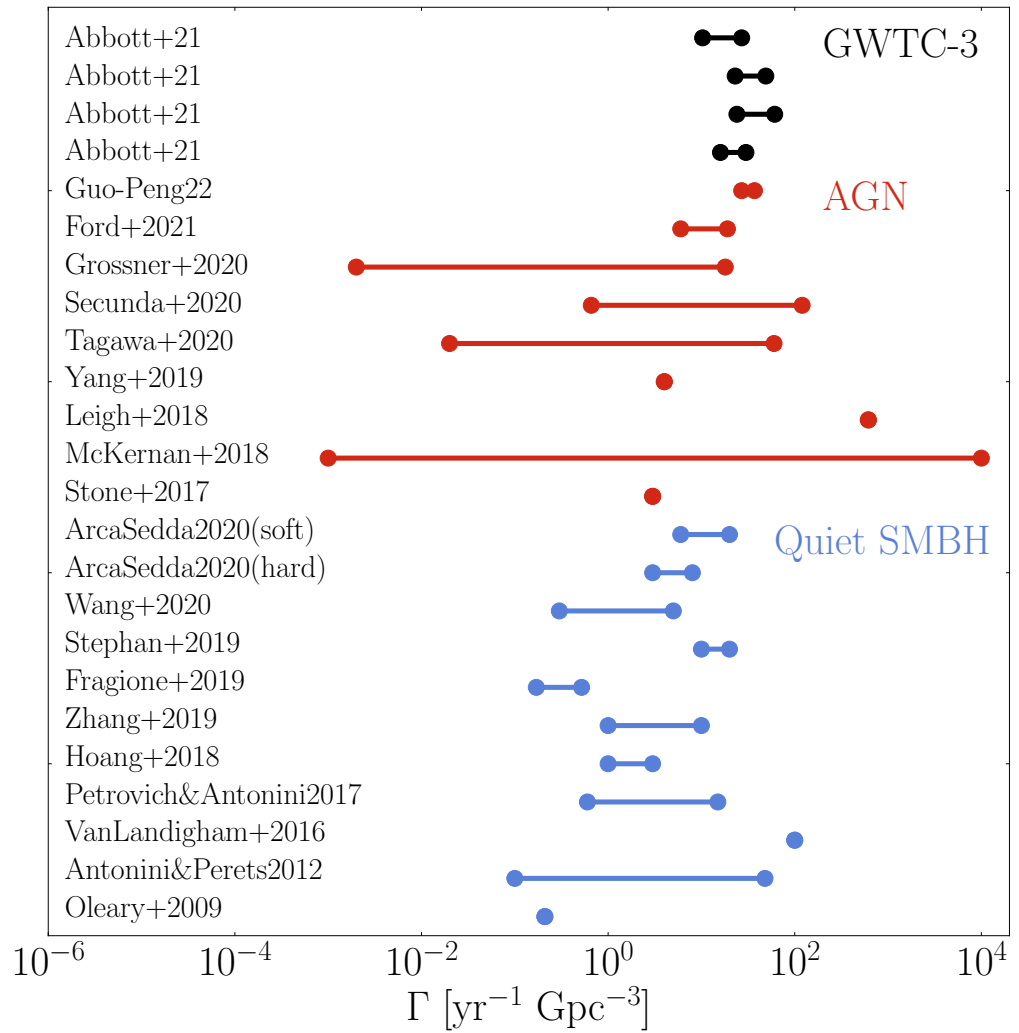


Figure 14. Merger rate density of BH-BH mergers in quiescent and active galactic nuclei at redshift $z = 0$.

taken to be from the lower limit of one of the channels, and the upper limit is taken from the combination of the three channels. 1211

Future detectors, like LISA or DECIGO, could shed light on the population of merging binaries in our Galactic Centre. For example, recent models of the Milky Way centre suggest that LISA could identify up to $1 - 20(15 - 150)$ BBH (WD-WD binaries) [358]. 1212 1213 1214 1215

Thus, the merger rate boundary limits for BBHs around quiescent SMBHs, $\mathcal{R}(0) \simeq (0.1 - 10^2)\text{yr}^{-1}\text{Gpc}^{-3}$, is somewhat narrower with respect to AGNs – whose rate spans up to 7 orders of magnitudes in some models. Future numerical simulations that account simultaneously for the evolution of the galactic nucleus and its stellar population could help to further reduce the uncertainties. 1216 1217 1218 1219 1220

Another interesting class of GW sources is represented by NS-BH mergers, which may also produce EM emission promptly after the merger. However, the formation of NS-BH binaries is strongly suppressed in dense stellar environments, owing to the fact that BHs have larger cross sections than other COs, thus favouring the interaction among themselves. This implies that the formation of NS-BH binaries either takes place on long timescales or is a byproduct of primordial binaries. Either way, merging NS-BH binaries in quiescent galactic nuclei can form via binary-single scatterings (rate $\mathcal{R} \sim 0.0001 - 0.01\text{yr}^{-1}\text{Gpc}^{-3}$) [130,136], similarly to what happens in globular and young clusters [132,133], possibly contributing to the formation of low-mass ratio systems like GW190814 [136]. 1221 1222 1223 1224 1225 1226 1227 1228 1229

Mergers can be triggered by EKL oscillations induced onto binaries formed via GW captures ($\mathcal{R} \sim (0.001 - 0.06)\text{yr}^{-1}\text{Gpc}^{-3}$) [310], dynamical interactions ($\mathcal{R} \sim 0.06 - 0.1\text{yr}^{-1}\text{Gpc}^{-3}$) [399], or binary stellar evolution – although likely with a rather low ($\sim 0.6\%$) probability ($\mathcal{R} \sim 0.2 - 2\text{yr}^{-1}\text{Gpc}^{-3}$ [59,358]). 1230 1231 1232 1233

In AGN discs, instead, the production of NS-BH mergers proceeds, in principle, similarly to BBHs, but their amount relative to BBHs is rather uncertain. In general, double NS (DNS) and NS-BH mergers constitute a relatively small fraction among all mergers developing in an AGN, namely $f_{\text{DNS}} \simeq (0.5 - 3) \times 10^{-4}$ (DNS) and $f_{\text{NSBH}} = (0.8 - 6) \times 10^{-4}$ (NS-BH) [34], although according to some models these quantities can be as large as $f_{\text{DNS}} = 0.01$ ($f_{\text{NSBH}} = 0.3$) for DNS(NS-BH) mergers [520]. These estimates corresponds to a merger rate density of $f_{\text{DNS}} = 400f_{\text{AGN}}\text{yr}^{-1}\text{Gpc}^{-3}$ (DNS) and $f_{\text{NS-BH}} = 10 - 300f_{\text{AGN}}\text{yr}^{-1}\text{Gpc}^{-3}$ (NS-BH) [520], although depending on the model assumptions these estimates can be up to 2-3 order of magnitude smaller [34]. 1234 1235 1236 1237 1238 1239 1240 1241 1242

A list of values for the BBH and NS-BH merger rate density is reported in Tables 1, 2. 1243

Comparing the modelled merger rate densities listed in Tables 1 and 2 with that inferred from GW observations [141] makes evident that the galactic nuclei channel for BBH mergers can contribute quite significantly to the overall population but are unlikely to contribute much to the global population of NS-BH mergers. 1244 1245 1246 1247

It is interesting to note that the estimated rates for BBH mergers galactic nuclei are comparable to those predicted for other channels [526, for a complete review on merger rates from different channels see]. Therefore, untangling the signatures of different formation channels in ground-based observations might be a quite hard task. 1248 1249 1250 1251

Future detectors might help unravelling how different channels contribute to the overall population of BBH mergers. An equal-mass binary with total mass m_{bin} emitting GWs at frequency f will merge in a timescale 1252 1253 1254

$$\tau \sim 5 \text{ yr} \left(\frac{f}{10 \text{ mHz}} \right)^{-8/3} \left(\frac{m_{\text{bin}}}{68M_{\odot}} \right)^{-8/3}, \quad (45)$$

thus combining LISA and ground-based observations has the potential to cover the full BBH frequency spectrum. Sources in the mass range between GW150914, the first GW sources ever detected [65], and GW190521 [76], emitting at 10 mHz could be observed in the last 5-1 yr prior 1255 1256 1257

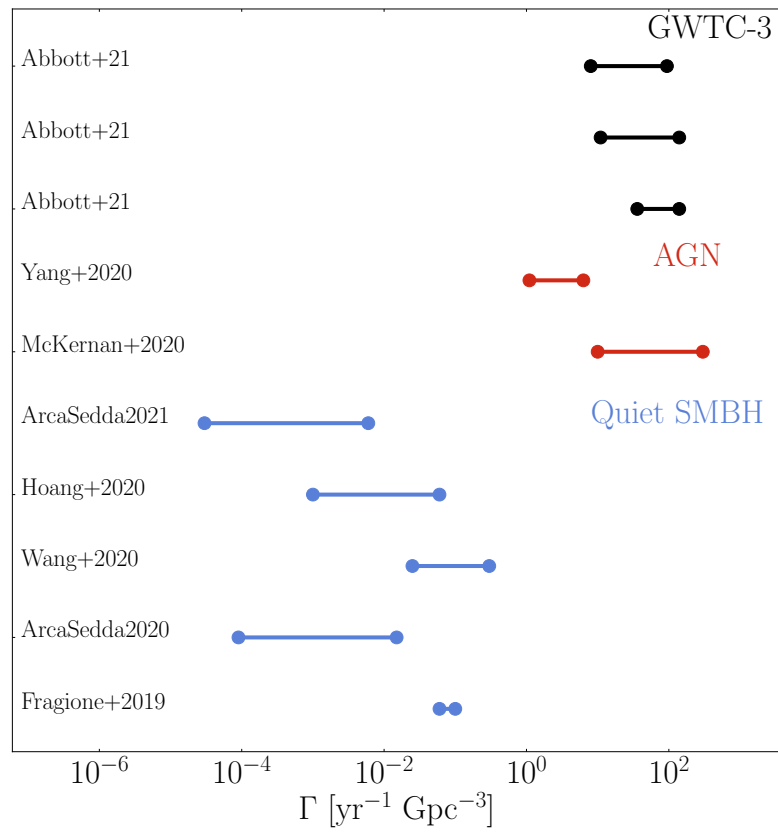


Figure 15. Same as in Figure 14, but for NS-BH mergers.

BBH merger rates		
Process	Γ [$\text{yr}^{-1}\text{Gpc}^{-3}$]	Ref.
GWTC-3		
-	17.9 – 44	The LIGO Scientific Collaboration <i>et al.</i> [141]
quiescent SMBH		
EKL+SEV	4 – 24	Wang <i>et al.</i> [358]
EKL+DYN	3 – 8	Arca Sedda [277]
EKL+DYN	6 – 20	Arca Sedda [277]
EKL+SEV	10 – 20	Stephan <i>et al.</i> [59]
EKL	0.17 – 0.52	Fragione <i>et al.</i> [399]
EKL+DYN	1 – 10	Zhang <i>et al.</i> [486]
EKL	1 – 3	Hoang <i>et al.</i> [291]
DYN	10^2 – 10^4	Leigh <i>et al.</i> [30]
EKL	0.6 – 15	Petrovich and Antonini [392]
EKL	< 100	VanLandingham <i>et al.</i> [521]
EKL	0.1 – 48	Antonini and Perets [378]
DYN	0.21	O’Leary <i>et al.</i> [265]
AGN		
GAS+TRP	27 – 37	Li [522]
DYN+GAS	6 – 19	Ford and McKernan [523]
MIG+TRP	0.66 – 120	Secunda <i>et al.</i> [524]
GAS	0.002 – 18	Gröbner <i>et al.</i> [525]
DYN+GAS	0.02 – 60	Tagawa <i>et al.</i> [33]
DYN+TRP	4	Yang <i>et al.</i> [31]
MIG	10^{-3} – 10^4	McKernan <i>et al.</i> [513]
TRP	10^2 – 10^4	Leigh <i>et al.</i> [30]
DYN+GAS	3	Stone <i>et al.</i> [440]

Table 1. BBH merger rate density for quiescent SMBHs and AGNs. Column 1: type of physical processes included – Kozai-Lidov (EKL), dynamical scatterings (single-single or binary-single, DYN), binary stellar evolution (SEV), gaseous capture via migration, and/or dynamical friction (GAS), migration (MIG), pairing in migration traps (TRP). Column 2: merger rate density. Column 3: reference. When a volumetric rate density was not provided in the referred paper, we adopted when required a local galaxy number density of $\rho_{\text{glx}} = 0.0116 \text{ Mpc}^{-3}$ [511,512] and an average number of BBH binaries in a MW-like nucleus of $N_{\text{BBH}} = 200$ [277,291].

NS-BH merger rates		
Process	Γ [$\text{yr}^{-1}\text{Gpc}^{-3}$]	Ref.
GWTC-3		
-	7.8 – 140	The LIGO Scientific Collaboration <i>et al.</i> [141]
quiescent SMBH		
DYN	3×10^{-5} – 0.006	Arca Sedda [136]
EKL+SEV	0.025 – 0.3	Wang <i>et al.</i> [358]
EKL	0.06 – 1	Fragione <i>et al.</i> [399]
DYN	9×10^{-5} – 0.015	Arca Sedda [130]
DYN	0.001 – 0.06	Hoang <i>et al.</i> [310]
AGN		
MIG+TRP	10 – 300	McKernan <i>et al.</i> [520]
DYN+GAS	1.1 – 6.3	Yang <i>et al.</i> [134]

Table 2. Same as in Table 1 but for NS-BH binaries. Note that the estimate from McKernan *et al.* [520] is obtained under the extreme assumption that all BBH mergers originate in AGNs.

to merger, enabling more precise measurement of localisation, eccentricity, spin amplitude and alignment, and binary mass [443,446]. More likely, ground based observations can be *reverse engineered* by seeking for the observed binaries in data previously acquired with LISA. Unfortunately, recent models suggest that LISA will observe only a few tens to a hundred BBHs, with only $\lesssim 10$ potentially observable as multi-band sources, depending on LISA mission lifetime and the adopted SNR threshold [443,446,488,527,528].

Deci-Hz observatories [450–453], filling the gap between space-borne and ground-based detectors, could permit us to pierce deeper in the cosmos and reconstruct BBH merger evolutionary history. A DECIGO-like detector [451,452] has the potentiality to observe merging BBHs up to a redshift $z \sim 10^3$ [453], well beyond the formation time of the first stars. More modest detector design, although still very ambitious, could still provide observation of stellar BBH mergers up to redshift $z = 3 - 100$ [453].

8.3. Imprint of galactic nuclei on the gravitational-wave emission from merging compact objects

An SMBH in the vicinity of a merging BBH can leave several imprints, some of which potentially measurable with future space-borne and third generation detectors.

8.3.1. Eccentricity variation encoded in the gravitational-wave signal of merging compact objects

LISA has the potential capability to track signatures of the EKL mechanism in our own Galactic Centre [489,529,530] – and closeby galactic centres [531] – and probe the very existence of compact BBHs orbiting around an SMBH. As we described in the previous sections, a triple system composed of an inner binary whose centre of mass orbits around a distant perturber can be subjected to secular oscillations of the orbital inclination and eccentricity of the inner orbit.

A compact binary with mass m_{bin} , semimajor axis a , and eccentricity e emits GWs characterised by a broad frequency spectrum peaked at [265]

$$f_{\text{peak}} = 7.6 \times 10^{-6} \text{ Hz} \frac{(1+e)^{1/2}}{(1-e)^{3/2}} \left(\frac{a}{0.1 \text{ AU}} \right)^{-3/2} \left(\frac{M}{50 M_{\odot}} \right)^{1/2} \sim 0.01 \text{ Hz}. \quad (46)$$

From the equation above it is apparent that a circular binary with mass $m_{\text{bin}} = (25 + 25) M_{\odot}$ and semimajor axis $a = 0.1 \text{ AU}$ – which implies a merging time of $t_{\text{GW}} = 1 \text{ Gyr}$ [386] – would be invisible to LISA until its semimajor axis reduces by a factor $O(10)$. However, the EKL mechanism at play can trigger eccentricity oscillations that can bring the GW peak frequency into the LISA band well before the binary shrinks, provided that the eccentricity peak reaches a sufficiently large value, $e_{\text{peak}} > 0.95$ in the aforementioned example. Additionally, EKL will shorten the binary lifetime by a factor 10^4 [378,490].

Such a binary moving about a SMBH like SgrA* will undergo a periodic shift of the frequency peak from 10^{-5} Hz up to 0.1 Hz [489], thus fully covering the LISA sensitivity band. The period of such shift – $\sim 1 \text{ month}$ – can be much shorter than the LISA mission lifetime, thus making possible the detection of such clear signature of a BBH-SMBH triple [see also 529,530]. EKL signatures could be observed also in closeby galactic nuclei, at a distance $1 - 10 \text{ Mpc}$, depending on the binary and SMBH masses and the orbital properties [489,530,531].

The same process might help spotting binaries containing an IMBH around an SMBH [531,532].

Detection (or not) of even one such signatures would provide crucial insights on the formation probability of BBHs around an SMBH and the possible contribute of galactic nuclei BBHs to the overall population of BBH mergers.

Several deci-Hz observatories, like DECIGO or the Big Bang Observatory, could enable an even more clear detection of such signatures [530]. Moreover, eventual synergies among

different detectors operating at the same time could enable a simultaneous tracking of the EKL mechanism at play, helping to remove any possible degeneracy in the parameter space [530].

8.3.2. Supermassive black hole acceleration encoded in the gravitational-wave signal of merging compact objects

In general, a merging BBH emits GWs at a frequency that is redshifted by a factor $(1 + z_C)^{-1}$, with z_C being the cosmological redshift. However, the signal emitted by the BBH while revolving around the SMBH suffers a time-dependent variation caused by its motion with respect to the observer.

The variation in the distance between the emitter and the observer causes a Doppler shift in the arrival time of GW pulses, the gravitational time dilation causes relativistic Doppler shift and gravitational redshift, whilst the SMBH gravitational field causes a delay in the time arrival of the GW signal. The aforementioned three effects, called Roemer, Einstein, and Shapiro delay [533], causes a shift in the measured GW signal that might be measurable in both low- [498,534–539] and high-frequency detectors [165,540,541].

For example, LVC detectors could measure such shift in BBH binaries with masses $m_{\text{bin}} \gtrsim 20M_\odot$ orbiting at $r \sim 1$ AU from an SMBH with mass $M_{\text{SMBH}} \sim 10^5 - 10^6 M_\odot$ [540].

The Doppler boost effect has potentially crucial implications for the interpretation of detected signals. In fact, aside the cosmological redshift, the signal emitted by a BBH revolving around an SMBH can suffer a Doppler shift,

$$(1 + z_D) \sim (1 - v^2/c^2)^{-1/2}(1 + v/c),$$

and a gravitational redshift [165,535,537,540–542]. Defining the SMBH Schwarzschild radius (R_S) and the semimajor axis of the BBH orbit around the SMBH (r) enables us to calculate the Doppler shift at pericentre through the relation $(v/c)^2 = (R_S/2r)(1 + e)/(1 - e)$ and the gravitational redshift as

$$(1 + z_G) \sim (1 - R_S/r)^{-1/2},$$

under the simplistic assumption that the GW emitter and receiver are on the same side with respect to the SMBH [541]. Thus, the total shift induced by the SMBH can be written as $(1 + z) = (1 + z_C)(1 + z_D)(1 + z_G)$ [165,541]. Since the measured BBH chirp mass scales with $\mathcal{M}_{\text{obs}} \propto f^{-11/5} \dot{f}^{3/5}$ and its luminosity distance $D_{\text{L,obs}} \propto f^{2/3}$, measured and intrinsic quantities are linked by the total redshift as

$$\mathcal{M}_{\text{obs}} = \mathcal{M}(1 + z_C)(1 + z_D)(1 + z_G) \quad (47)$$

$$D_{\text{L,obs}} = D_C(1 + z_C)(1 + z_D)(1 + z_G), \quad (48)$$

where D_C is the BBH comoving distance. Depending on the values of the additional corrections, the interpretation of observed sources might thus be biased toward larger values [541]. Note that this corrective factor depends only on the cosmological location of the merger, the SMBH mass, and the BBH-SMBH orbital semimajor axis and eccentricity. Figure 16 shows how the correction factor varies with the SMBH mass and the distance to the galactic centre assuming that the merger occurs at redshift $z_C = 0$ and the BBH-SMBH orbital eccentricity $e = 0 - 0.5 - 0.9$. Note that the spikes occurs when $R_S \sim r$ or $R_S \sim 2r(1 - e)/(1 + e)$. The picture makes evident that both the observed chirp mass and luminosity distance might overestimate the intrinsic properties of the merger by a factor up to 2 – 3 [541], and on average by around 10 – 30% [165].

It is worth noting that a BBH with mass $m_{\text{bin}} = 50M_\odot$ at a distance $r = 1$ mpc from an SMBH with mass $M_{\text{SMBH}} = 10^6(10^8)M_\odot$ revolves around the SMBH in a time $P_2 \simeq 3(0.3)$ yr, thus a detector with a mission lifetime (τ_{life}) longer than the BBH merging time and the

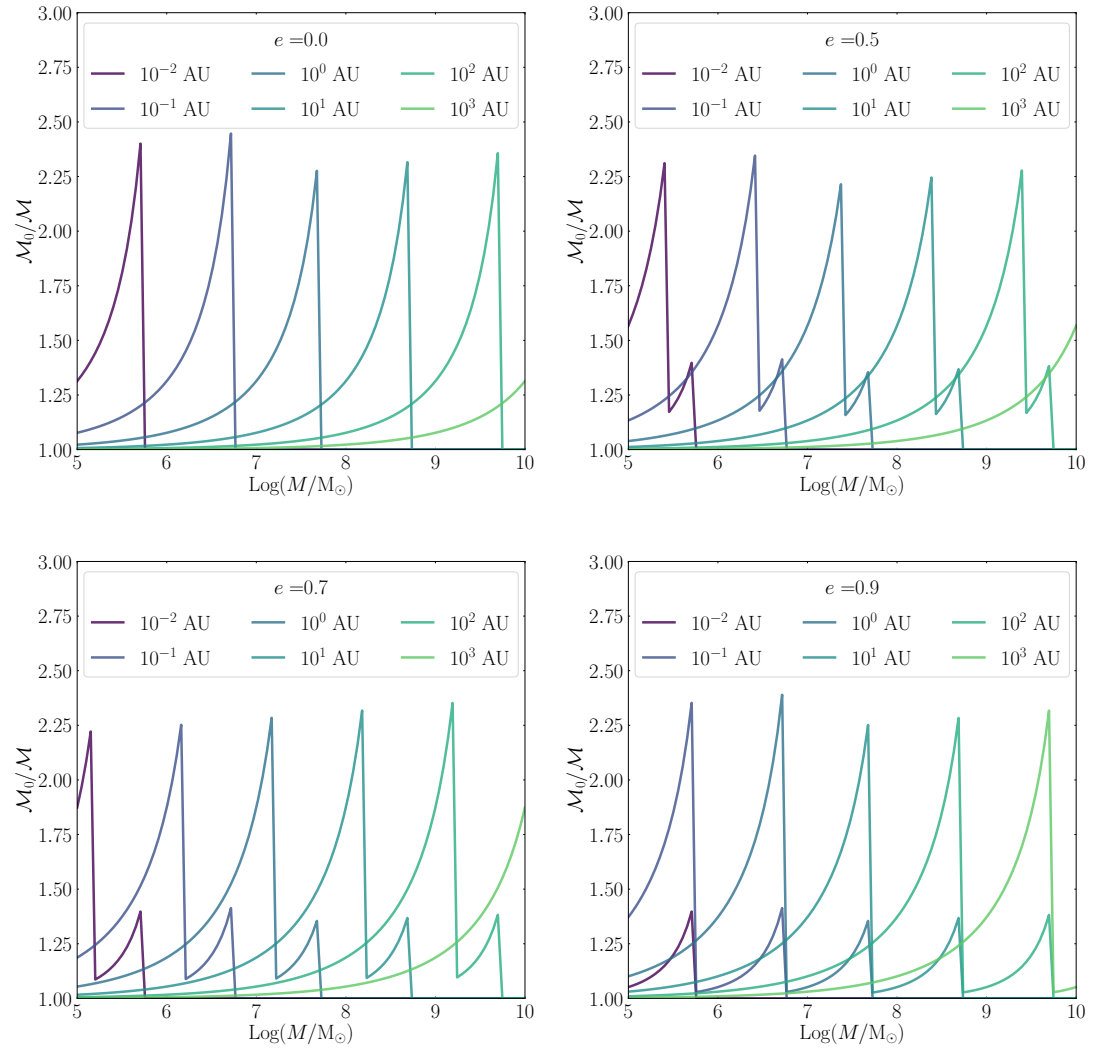


Figure 16. Total chirp mass correction factor as a function of the SMBH mass and for different values of the BBH-SMBH separation, assuming that the BBH undergoes merger at redshift $z = 0$ and moves around the SMBH on an orbit with eccentricity $e = 0 - 0.5 - 0.7 - 0.9$.

orbital period could measure the Doppler modulation in the source signal [534–536,539] and related-effects [498,538,542,543].

While revolving around the SMBH, the source will appear to change its redshift by a factor $\delta z \sim a_{\text{COM}} \tau_{\text{life}} / c$ [534,536]. The resulting progressive drift of the GW signal could be detected by LISA in principle, and since it is maximized in galactic nuclei, its detection could represent a strong indicator of the merger environment [534]. The effect of Doppler boost could be measurable up to a redshift $z < 0.05$, thus permitting to probe the BBH-SMBH interplay in the local Universe [535], but even in the case of no-detection the acceleration drift could be sufficient to bias the parameter estimation of future detected sources [536]. A sufficiently long monitoring of the source could also lead to detection of lensing signatures caused by the SMBH [538,542,544]. The probability to observe such an effect depends on the properties of BBHs forming around an SMBH and could be $O(1 - 3\%)$ with both LISA and TianGO [538,542], potentially enabling to measure the SMBH mass at a level of $0.01 - 1\%$ [538,539]. Similarly to electromagnetic wavelets, GWs from BBHs around an SMBH could be affected by aberration, an effect that can cause a shift in the GW signal as significant as the “standard” Doppler shift and potentially detectable by a LISA-like mission, provided that the BBH is orbiting within a few 10^3 Schwarzschild radii [543]. The detection of a few hundred BBHs should thus help us starting to unveil how different channels contribute to the formation of merging BBHs [542].

Furthermore, the GW signal emitted by the merging COB can be scattered by the central SMBH. This can produce a secondary signal, a sort of “GW echo”, which will have similar time-frequency evolution as the main signal but is delayed in time. For sources moving within $10 - 10^4$ Schwarzschild radii from the SMBH, around $10(90)\%$ of the detectable echo arrives within $\sim 1(100)\text{s}(M_{\text{SMBH}}/10^6 M_{\odot})$ after the primary signal [545].

In the case of Kerr SMBHs, there are three further effects that might leave an imprint on the BBH emitted signal, namely i) the precession of the BBH-SMBH angular momentum around the SMBH spin owing to spin-orbit coupling associated with the 1.5 PN effect [382,496,499], ii) the precession of the BBH angular momentum around the BBH-SMBH angular momentum, a geodesic de Sitter-like precession induced by GR [546,547], iii) precession of the BBH angular momentum around the SMBH spin owing to the Lens-Thirring precession. The coupling of these effects can lead to a modulation in the GW signal of inspiralling BBHs, possibly being observable with space-borne detectors like LISA if the precession period is shorter than the observation time [498,499].

Finally, if the BBH is traveling in an AGN disc, the gaseous medium can leave an imprint on the binary waveform that translates into an overestimate of the binary chirp mass by a factor $(1 + \tau_{\text{gw}}/\tau_{\text{gas}})^{3/5}$ and of the binary distance by a factor $(1 + \tau_{\text{gw}}/\tau_{\text{gas}})$, where τ_{gw} and τ_{gas} represents the GW and the hydrodynamical timescale, respectively [548].

9. Summary

Galactic nuclei likely represents the most intricate environments in the Universe, where dynamics is regulated by a complex interplay among stellar interactions powered by the high-densities of NCs, secular effects driven by central SMBHs, and gaseous-driven effects in AGNs.

Discoveries like the emission GWs emitted by merging COs, the high-energy emission from the Galactic Centre possibly triggered by COBs, the stellar motion in the immediate vicinity of SgrA*, the Galactic SMBH, recently revived the interest about how CO form, pair-up, and eventually merge in quiescent and active galactic nuclei harboring a NC, an SMBH.

In this review we provided an overlook of the plethora of mechanisms that can contribute to the formation, and possibly coalescence, of COB in both galactic nuclei with a quiescent SMBH and AGNs. These mechanisms rely upon different theoretical frameworks devised to represent different aspects – e.g., scatterings, EKL, gas torques – of the same environment.

We have highlighted the main imprints that one mechanism or another could leave in the population of COB it produces, and how they could be used to untangle the origin of some GW sources detectable with present-day or future GW observatories.

The main peculiarities of the most recent theoretical frameworks can be summarised as follows:

- Dynamics plays a crucial role in determining COB formation in galactic nuclei. Three-body scatterings, involving three initially unbound objects, are likely dominant in galaxies with a large NC-to-SMBH mass ratio, but become extremely inefficient close to the SMBH. Conversely, single-single interactions that form bound pairs via GW bremsstrahlung – or GW captures – are more efficient in the SMBH immediate vicinity and in the nuclei with the most massive SMBH. However, GW captures produce short-lived binaries that merge within days or hours from the formation and have a large chance to be highly eccentric when sweeping through high-frequency detectors.
- Galaxies dominated by a quiescent SMBH can efficiently replenish their population of COBs – particularly BHs – via accretion of massive star clusters that undergo inward migration owing to dynamical friction.
- A substantial population of primordial binaries can also play a crucial role in determining the properties of COBs in galactic nuclei, although most of them are likely destroyed by the SMBH tidal field.
- Once binaries start forming in galactic nuclei, their further evolution is regulated mostly by binary-single interactions, which generally promote the formation of tighter and more massive binaries but, depending on the binary properties, can lead to their evaporation well before GW emission start dominating the binary evolution.
- Owing to dynamical friction, or mass segregation, and dynamical interactions, COBs are expected to move through regions of the nucleus with different velocity dispersion and density. Variation of the environment structure can dramatically affect the COB fate: an initially hard binary moving inward can appear soft closer to the SMBH and eventually be disrupted by interaction with other stars and COs.
- Around 20 – 70% of COBs formed in galactic nuclei are expected to suffer the effect of the SMBH gravitational field, which can cause periodic oscillations of their eccentricity called eccentric-Kozai-Lidov resonances. This mechanism can significantly shorten the COB lifetime, possibly affecting the delay time of merging COs. The development of EKL oscillations strongly depends on the binary properties (e.g. general relativistic precession can suppress EKL), the distance to the SMBH, the eccentricity of the COB orbit about the SMBH.
- In AGNs, the formation of COBs is favored by both gaseous torques and dynamical scatterings, whose efficiency is boosted by the nearly planar configuration. The possible existence of migration traps, where inward and outward torques cancel out, makes AGNs potential factories of multiple-generation CO mergers and IMBHs.
- Mergers occurring in galactic nuclei features some peculiar traits: a significant fraction of mergers with one component in the upper mass-gap, a non-negligible fraction of multiple generation mergers that can affect the high-end of the BH mass distribution, fairly misaligned spins, although in AGNs a noticeable fraction of high-generation mergers might have mildly aligned spins, and a quite significant probability to preserve an eccentricity $e > 0.1$ whilst sweeping through the frequency bands of both low- and high-frequency detectors.
- The merger rate inferred for present-day GW detectors for BBH and NS-BH binary mergers in galactic nuclei is poorly constrained owing to the many model uncertainties. For BBH mergers, models for quiescent SMBHs and AGNs predicts similar estimates, which generally fall in the range $\mathcal{R}_{\text{BBH}} = 10^{-3} - 10^2 \text{yr}^{-1} \text{Gpc}^{-3}$. For NS-BH mergers, instead, there

are clear differences between the prediction for quiescent, $\mathcal{R}_{\text{BBH}} = 10^{-5} - 1\text{yr}^{-1}\text{Gpc}^{-3}$, and active nuclei models, $\mathcal{R}_{\text{BBH}} = 1 - 10^3\text{yr}^{-1}\text{Gpc}^{-3}$, partly owing to the relatively poor literature and the huge uncertainties.

- The presence of an SMBH in the vicinity of a merging COB can leave some imprints on the emitted GW signal that could, in principle, be detected with future detectors. Among others, a shift in the peak frequency for mergers occurring in the Milky Way centre, a variation in the measured redshift induced by the rapid motion of the binary around the SMBH, and the development of a GW echo produced by the scattering of the emitted GWs onto the SMBH.

Despite the current literature is very rich, and the amount of new work done in the field is constantly increasing, there are still a number of important elements that are missing in current models and deserve further development. Among others, we identify in the following some elements that may be key to place more stringent constraints on the model predictions:

- **Initial conditions:** probably the most important unknown that mostly affect all the models is the scarce knowledge of how stars form and pair in the extreme environment of a galactic nucleus. The initial binary fraction, the initial distribution of periods and masses, the metallicity spread in the galactic nucleus are all factors that crucially determine the COB properties: semimajor axis, eccentricity, component masses.
- **Interplay of mechanisms:** as we have seen throughout the review, COB formation is likely regulated by many mechanisms likely operating simultaneously. However, most theoretical models focus on one specific aspect at the time. Fully self-consistent N -body simulations capable of taking into account stellar evolution of single and binary stars, the SMBH tidal field, and potentially the effect of an AGN disc exists, but their resolution is still too low and their computational cost too large to permit a one-to-one representation of a Milky Way-like nucleus. Simpler models relying on semi-analytic assumptions or few-body (scattering) simulations represent a valid alternative, although they sometimes neglect potentially crucial elements, like the importance of flybys on the evolution of COBs undergoing EKL oscillations, the development of EKL resonances in binaries formed in AGNs, the role of star formation onto the actual population of COBs around an SMBH.
- **Observations:** from an observational perspective, the observation of young massive binaries in galactic nuclei, a larger number of GW detections, a more precise localization of GW sources, and the future detection of inspiralling binaries in the Milky Way centre can definitely help us improving our knowledge of the processes regulating COB formation in galactic nuclei.

Funding: MAS acknowledges funding from the European Union’s Horizon 2020 research and innovation programme under the Marie Skłodowska-Curie grant agreement No. 101025436 (project GRACE-BH, PI: Manuel Arca Sedda). SN acknowledges the partial support from NASA ATP 80NSSC20K0505, NSF through grant No. 2206428, and thanks Howard and Astrid Preston for their generous support. This work was supported by the Science and Technology Facilities Council Grant Number ST/W000903/1 (to BK).

Acknowledgments:

Conflicts of Interest: “The authors declare no conflict of interest.”

References

1. Georgiev, I.Y.; Böker, T.; Leigh, N.; Lützgendorf, N.; Neumayer, N. Masses and scaling relations for nuclear star clusters, and their co-existence with central black holes. *MNRAS* **2016**, *457*, 2122–2138, [arXiv:astro-ph.GA/1601.02613]. doi:10.1093/mnras/stw093. 1476
2. Pechetti, R.; Seth, A.; Neumayer, N.; Georgiev, I.; Kacharov, N.; den Brok, M. Luminosity Models and Density Profiles for Nuclear Star Clusters for a Nearby Volume-limited Sample of 29 Galaxies. *ApJ* **2020**, *900*, 32, [arXiv:astro-ph.GA/1911.09686]. doi:10.3847/1538-4357/abaaa7. 1477
3. Neumayer, N.; Seth, A.; Böker, T. Nuclear star clusters. *A&A Rev.* **2020**, *28*, 4, [arXiv:astro-ph.GA/2001.03626]. doi:10.1007/s00159-020-00125-0. 1478
4. Gültekin, K.; Richstone, D.O.; Gebhardt, K.; Lauer, T.R.; Tremaine, S.; Aller, M.C.; Bender, R.; Dressler, A.; Faber, S.M.; Filippenko, A.V.; et al. The M- σ and M-L Relations in Galactic Bulges, and Determinations of Their Intrinsic Scatter. *ApJ* **2009**, *698*, 198–221, [arXiv:astro-ph.GA/0903.4897]. doi:10.1088/0004-637X/698/1/198. 1479
5. Graham, A.W.; Scott, N. The M_{BH-L_{spheroid}} Relation at High and Low Masses, the Quadratic Growth of Black Holes, and Intermediate-mass Black Hole Candidates. *ApJ* **2013**, *764*, 151, [arXiv:astro-ph.CO/1211.3199]. doi:10.1088/0004-637X/764/2/151. 1480
6. Graham, A.W.; Spitler, L.R. Quantifying the coexistence of massive black holes and dense nuclear star clusters. *MNRAS* **2009**, *397*, 2148–2162, [arXiv:astro-ph.CO/0907.5250]. doi:10.1111/j.1365-2966.2009.15118.x. 1481
7. Neumayer, N.; Walcher, C.J. Are Nuclear Star Clusters the Precursors of Massive Black Holes? *Advances in Astronomy* **2012**, *2012*, 709038, [arXiv:astro-ph.CO/1201.4950]. doi:10.1155/2012/709038. 1482
8. Nguyen, D.D.; Seth, A.C.; Neumayer, N.; Kamann, S.; Voggel, K.T.; Cappellari, M.; Picotti, A.; Nguyen, P.M.; Böker, T.; Debattista, V.; et al. Nearby Early-type Galactic Nuclei at High Resolution: Dynamical Black Hole and Nuclear Star Cluster Mass Measurements. *ApJ* **2018**, *858*, 118, [arXiv:astro-ph.GA/1711.04314]. doi:10.3847/1538-4357/aabe28. 1483
9. Sánchez-Janssen, R.; Côté, P.; Ferrarese, L.; Peng, E.W.; Roediger, J.; Blakeslee, J.P.; Emsellem, E.; Puzia, T.H.; Spengler, C.; Taylor, J.; et al. The Next Generation Virgo Cluster Survey. XXIII. Fundamentals of Nuclear Star Clusters over Seven Decades in Galaxy Mass. *ApJ* **2019**, *878*, 18, [arXiv:astro-ph.GA/1812.01019]. doi:10.3847/1538-4357/aaf4fd. 1484
10. Walcher, C.J.; van der Marel, R.P.; McLaughlin, D.; Rix, H.W.; Böker, T.; Häring, N.; Ho, L.C.; Sarzi, M.; Shields, J.C. Masses of Star Clusters in the Nuclei of Bulgeless Spiral Galaxies. *ApJ* **2005**, *618*, 237–246, [arXiv:astro-ph/astro-ph/0409216]. doi:10.1086/425977. 1485
11. Goodman, J.; Hut, P. Binary–Single-Star Scattering. V. Steady State Binary Distribution in a Homogeneous Static Background of Single Stars. *ApJ* **1993**, *403*, 271. doi:10.1086/172200. 1486
12. Krabbe, A.; Genzel, R.; Eckart, A.; Najarro, F.; Lutz, D.; Cameron, M.; Kroker, H.; Tacconi-Garman, L.E.; Thatte, N.; Weitzel, L.; et al. The Nuclear Cluster of the Milky Way: Star Formation and Velocity Dispersion in the Central 0.5 Parsec. *ApJL* **1995**, *447*, L95. doi:10.1086/309579. 1487
13. Miller, M.C.; Lauburg, V.M. Mergers of Stellar-Mass Black Holes in Nuclear Star Clusters. *ApJ* **2009**, *692*, 917–923, [arXiv:astro-ph/0804.2783]. doi:10.1088/0004-637X/692/1/917. 1488
14. Kozai, Y. Secular perturbations of asteroids with high inclination and eccentricity. *AJ* **1962**, *67*, 591–598. doi:10.1086/108790. 1489
15. Lidov, M.L. The evolution of orbits of artificial satellites of planets under the action of gravitational perturbations of external bodies. *P&SS* **1962**, *9*, 719–759. doi:10.1016/0032-0633(62)90129-0. 1490
16. Harrington, R.S. Dynamical evolution of triple stars. *AJ* **1968**, *73*, 190–194. doi:10.1086/110614. 1491
17. Ford, E.B.; Kozinsky, B.; Rasio, F.A. Secular Evolution of Hierarchical Triple Star Systems. *ApJ* **2000**, *535*, 385–401. doi:10.1086/308815. 1492
18. Blaes, O.; Lee, M.H.; Socrates, A. The Kozai Mechanism and the Evolution of Binary Supermassive Black Holes. *ApJ* **2002**, *578*, 775–786, [arXiv:astro-ph/astro-ph/0203370]. doi:10.1086/342655. 1493
19. Lithwick, Y.; Naoz, S. The Eccentric Kozai Mechanism for a Test Particle. *ApJ* **2011**, *742*, 94, [arXiv:astro-ph.EP/1106.3329]. doi:10.1088/0004-637X/742/2/94. 1494
20. Naoz, S.; Kocsis, B.; Loeb, A.; Yunes, N. Resonant Post-Newtonian Eccentricity Excitation in Hierarchical Three-body Systems. *ApJ* **2013**, *773*, 187, [arXiv:astro-ph.SR/1206.4316]. doi:10.1088/0004-637X/773/2/187. 1495
21. Naoz, S. The Eccentric Kozai-Lidov Effect and Its Applications. *ARA&A* **2016**, *54*, 441–489, [arXiv:astro-ph.EP/1601.07175]. doi:10.1146/annurev-astro-081915-023315. 1496
22. Syer, D.; Clarke, C.J.; Rees, M.J. Star-disc interactions near a massive black hole. *MNRAS* **1991**, *250*, 505–512. doi:10.1093/mnras/250.3.505. 1497
23. Šubr, L.; Karas, V. On highly eccentric stellar trajectories interacting with a self-gravitating disc in Sgr A^{star}. *A&A* **2005**, *433*, 405–413, [arXiv:astro-ph/astro-ph/0501203]. doi:10.1051/0004-6361:20042089. 1498
24. McKernan, B.; Ford, K.E.S.; Lyra, W.; Perets, H.B.; Winter, L.M.; Yaqoob, T. On rapid migration and accretion within discs around supermassive black holes. *MNRAS* **2011**, *417*, L103–L107, [arXiv:astro-ph.CO/1108.1787]. doi:10.1111/j.1745-3933.2011.01132.x. 1499
25. Baruteau, C.; Cuadra, J.; Lin, D.N.C. Binaries Migrating in a Gaseous Disk: Where are the Galactic Center Binaries? *ApJ* **2011**, *726*, 28, [arXiv:astro-ph.GA/1011.0360]. doi:10.1088/0004-637X/726/1/28. 1500
26. McKernan, B.; Ford, K.E.S.; Lyra, W.; Perets, H.B. Intermediate mass black holes in AGN discs - I. Production and growth. *MNRAS* **2012**, *425*, 460–469, [arXiv:astro-ph.GA/1206.2309]. doi:10.1111/j.1365-2966.2012.21486.x. 1501

27. Kennedy, G.F.; Meiron, Y.; Shukirgaliyev, B.; Panamarev, T.; Berczik, P.; Just, A.; Spurzem, R. Star-disc interaction in galactic nuclei: orbits and rates of accreted stars. *MNRAS* **2016**, *460*, 240–255, [arXiv:astro-ph.GA/1604.05309]. doi:10.1093/mnras/stw908. 1529
28. Bartos, I.; Kocsis, B.; Haiman, Z.; Márka, S. Rapid and Bright Stellar-mass Binary Black Hole Mergers in Active Galactic Nuclei. *ApJ* **2017**, *835*, 165, [arXiv:astro-ph.HE/1602.03831]. doi:10.3847/1538-4357/835/2/165. 1530
29. Panamarev, T.; Shukirgaliyev, B.; Meiron, Y.; Berczik, P.; Just, A.; Spurzem, R.; Omarov, C.; Vilkoviskij, E. Star-disc interaction in galactic nuclei: formation of a central stellar disc. *MNRAS* **2018**, *476*, 4224–4233, [arXiv:astro-ph.GA/1802.03027]. doi:10.1093/mnras/sty459. 1533
30. Leigh, N.W.C.; Geller, A.M.; McKernan, B.; Ford, K.E.S.; Mac Low, M.M.; Bellovary, J.; Haiman, Z.; Lyra, W.; Samsing, J.; O’Dowd, M.; et al. On the rate of black hole binary mergers in galactic nuclei due to dynamical hardening. *MNRAS* **2018**, *474*, 5672–5683, [arXiv:astro-ph.GA/1711.10494]. doi:10.1093/mnras/stx3134. 1536
31. Yang, Y.; Bartos, I.; Haiman, Z.; Kocsis, B.; Márka, Z.; Stone, N.C.; Márka, S. AGN Disks Harden the Mass Distribution of Stellar-mass Binary Black Hole Mergers. *ApJ* **2019**, *876*, 122, [arXiv:astro-ph.HE/1903.01405]. doi:10.3847/1538-4357/ab16e3. 1539
32. Yang, Y.; Bartos, I.; Gayathri, V.; Ford, K.E.S.; Haiman, Z.; Klimentko, S.; Kocsis, B.; Márka, S.; Márka, Z.; McKernan, B.; et al. Hierarchical Black Hole Mergers in Active Galactic Nuclei. *Phys. Rev. Lett.* **2019**, *123*, 181101, [arXiv:astro-ph.HE/1906.09281]. doi:10.1103/PhysRevLett.123.181101. 1541
33. Tagawa, H.; Haiman, Z.; Kocsis, B. Formation and Evolution of Compact-object Binaries in AGN Disks. *ApJ* **2020**, *898*, 25, [arXiv:astro-ph.GA/1912.08218]. doi:10.3847/1538-4357/ab9b8c. 1544
34. Tagawa, H.; Kocsis, B.; Haiman, Z.; Bartos, I.; Omukai, K.; Samsing, J. Mass-gap Mergers in Active Galactic Nuclei. *ApJ* **2021**, *908*, 194, [arXiv:astro-ph.HE/2012.00011]. doi:10.3847/1538-4357/abd555. 1545
35. Samsing, J.; Bartos, I.; D’Orazio, D.J.; Haiman, Z.; Kocsis, B.; Leigh, N.W.C.; Liu, B.; Pessah, M.E.; Tagawa, H. AGN as potential factories for eccentric black hole mergers. *Nature* **2022**, *603*, 237–240. doi:10.1038/s41586-021-04333-1. 1546
36. Ghez, A.M.; Salim, S.; Weinberg, N.N.; Lu, J.R.; Do, T.; Dunn, J.K.; Matthews, K.; Morris, M.R.; Yelda, S.; Becklin, E.E.; et al. Measuring Distance and Properties of the Milky Way’s Central Supermassive Black Hole with Stellar Orbits. *ApJ* **2008**, *689*, 1044–1062, [arXiv:astro-ph/0808.2870]. doi:10.1086/592738. 1547
37. Gillessen, S.; Eisenhauer, F.; Trippe, S.; Alexander, T.; Genzel, R.; Martins, F.; Ott, T. Monitoring Stellar Orbits Around the Massive Black Hole in the Galactic Center. *ApJ* **2009**, *692*, 1075–1109, [arXiv:astro-ph/0810.4674]. doi:10.1088/0004-637X/692/2/1075. 1548
38. Gillessen, S.; Plewa, P.M.; Eisenhauer, F.; Sari, R.; Waisberg, I.; Habibi, M.; Pfuhl, O.; George, E.; Dexter, J.; von Fellenberg, S.; et al. An Update on Monitoring Stellar Orbits in the Galactic Center. *ApJ* **2017**, *837*, 30, [arXiv:astro-ph.GA/1611.09144]. doi:10.3847/1538-4357/aa5c41. 1549
39. Gravity Collaboration.; Abuter, R.; Aymar, N.; Amorim, A.; Ball, J.; Bauböck, M.; Berger, J.P.; Bonnet, H.; Bourdarot, G.; Brandner, W.; et al. Mass distribution in the Galactic Center based on interferometric astrometry of multiple stellar orbits. *A&A* **2022**, *657*, L12. doi:10.1051/0004-6361/202142465. 1550
40. Pfuhl, O.; Fritz, T.K.; Zilka, M.; Maness, H.; Eisenhauer, F.; Genzel, R.; Gillessen, S.; Ott, T.; Dodds-Eden, K.; Sternberg, A. The Star Formation History of the Milky Way’s Nuclear Star Cluster. *ApJ* **2011**, *741*, 108, [arXiv:astro-ph.GA/1110.1633]. doi:10.1088/0004-637X/741/2/108. 1551
41. Schödel, R.; Feldmeier, A.; Kunneriath, D.; Stolovy, S.; Neumayer, N.; Amaro-Seoane, P.; Nishiyama, S. Surface brightness profile of the Milky Way’s nuclear star cluster. *A&A* **2014**, *566*, A47, [arXiv:astro-ph.GA/1403.6657]. doi:10.1051/0004-6361/201423481. 1552
42. Fritz, T.K.; Chatzopoulos, S.; Gerhard, O.; Gillessen, S.; Genzel, R.; Pfuhl, O.; Tacchella, S.; Eisenhauer, F.; Ott, T. The Nuclear Cluster of the Milky Way: Total Mass and Luminosity. *ApJ* **2016**, *821*, 44, [arXiv:astro-ph.GA/1406.7568]. doi:10.3847/0004-637X/821/1/44. 1553
43. Gravity Collaboration.; Abuter, R.; Amorim, A.; Anugu, N.; Bauböck, M.; Benisty, M.; Berger, J.P.; Blind, N.; Bonnet, H.; Brandner, W.; et al. Detection of the gravitational redshift in the orbit of the star S2 near the Galactic centre massive black hole. *A&A* **2018**, *615*, L15, [arXiv:astro-ph.GA/1807.09409]. doi:10.1051/0004-6361/201833718. 1554
44. Do, T.; Hees, A.; Ghez, A.; Martinez, G.D.; Chu, D.S.; Jia, S.; Sakai, S.; Lu, J.R.; Gautam, A.K.; O’Neil, K.K.; et al. Relativistic redshift of the star S0-2 orbiting the Galactic Center supermassive black hole. *Science* **2019**, *365*, 664–668, [arXiv:astro-ph.GA/1907.10731]. doi:10.1126/science.aav8137. 1555
45. GRAVITY Collaboration.; Abuter, R.; Amorim, A.; Bauböck, M.; Berger, J.P.; Bonnet, H.; Brandner, W.; Cardoso, V.; Clénet, Y.; de Zeeuw, P.T.; et al. Detection of the Schwarzschild precession in the orbit of the star S2 near the Galactic centre massive black hole. *A&A* **2020**, *636*, L5, [arXiv:astro-ph.GA/2004.07187]. doi:10.1051/0004-6361/202037813. 1556
46. Gualandris, A.; Merritt, D. Perturbations of Intermediate-mass Black Holes on Stellar Orbits in the Galactic Center. *ApJ* **2009**, *705*, 361–371, [arXiv:astro-ph.GA/0905.4514]. doi:10.1088/0004-637X/705/1/361. 1557
47. Gualandris, A.; Gillessen, S.; Merritt, D. The Galactic Centre star S2 as a dynamical probe for intermediate-mass black holes. *MNRAS* **2010**, *409*, 1146–1154, [arXiv:astro-ph.GA/1006.3563]. doi:10.1111/j.1365-2966.2010.17373.x. 1558
48. Arca-Sedda, M.; Gualandris, A. Gravitational wave sources from inspiralling globular clusters in the Galactic Centre and similar environments. *MNRAS* **2018**, *477*, 4423–4442, [arXiv:astro-ph.GA/1804.06116]. doi:10.1093/mnras/sty922. 1559

49. Arca Sedda, M. The connection between stellar and nuclear clusters: Can an IMBH be sitting at the heart of the Milky Way? *Star Clusters: From the Milky Way to the Early Universe*; Bragaglia, A.; Davies, M.; Sills, A.; Vesperini, E., Eds., 2020, Vol. 351, pp. 51–55. doi:10.1017/S1743921319007324. 1583
1584
50. Naoz, S.; Will, C.M.; Ramirez-Ruiz, E.; Hees, A.; Ghez, A.M.; Do, T. A Hidden Friend for the Galactic Center Black Hole, Sgr A*. *ApJL* **2020**, *888*, L8, [arXiv:astro-ph.GA/1912.04910]. doi:10.3847/2041-8213/ab5e3b. 1586
1587
51. Rose, S.C.; Naoz, S.; Sari, R.; Linial, I. The Formation of Intermediate-mass Black Holes in Galactic Nuclei. *ApJL* **2022**, *929*, L22, [arXiv:astro-ph.GA/2201.00022]. doi:10.3847/2041-8213/ac6426. 1588
1589
52. Zhang, E.; Naoz, S.; Will, C.M. A Stability Timescale for Non-Hierarchical Three-Body Systems. *arXiv e-prints* **2023**, p. arXiv:2301.08271, [arXiv:astro-ph.GA/2301.08271]. doi:10.48550/arXiv.2301.08271. 1590
1591
53. Hailey, C.J.; Mori, K.; Bauer, F.E.; Berkowitz, M.E.; Hong, J.; Hord, B.J. A density cusp of quiescent X-ray binaries in the central parsec of the Galaxy. *Nature* **2018**, *556*, 70–73. doi:10.1038/nature25029. 1592
1593
54. Maccarone, T.J.; Degenaar, N.; Tetarenko, B.E.; Heinke, C.O.; Wijnands, R.; Sivakoff, G.R. On the recurrence times of neutron star X-ray binary transients and the nature of the Galactic Centre quiescent X-ray binaries. *MNRAS* **2022**, *512*, 2365–2370, [arXiv:astro-ph.HE/2202.09503]. doi:10.1093/mnras/stac506. 1594
1595
1596
55. Antonini, F. On the Distribution of Stellar Remnants around Massive Black Holes: Slow Mass Segregation, Star Cluster Inspirals, and Correlated Orbits. *ApJ* **2014**, *794*, 106, [arXiv:astro-ph.GA/1402.4865]. doi:10.1088/0004-637X/794/2/106. 1597
1598
56. Arca-Sedda, M.; Kocsis, B.; Brandt, T.D. Gamma-ray and X-ray emission from the Galactic centre: hints on the nuclear star cluster formation history. *MNRAS* **2018**, *479*, 900–916, [arXiv:astro-ph.GA/1709.03119]. doi:10.1093/mnras/sty1454. 1599
1600
57. Generozov, A.; Stone, N.C.; Metzger, B.D.; Ostriker, J.P. An overabundance of black hole X-ray binaries in the Galactic Centre from tidal captures. *MNRAS* **2018**, *478*, 4030–4051, [arXiv:astro-ph.HE/1804.01543]. doi:10.1093/mnras/sty1262. 1601
1602
58. Miralda-Escudé, J.; Gould, A. A Cluster of Black Holes at the Galactic Center. *ApJ* **2000**, *545*, 847–853, [arXiv:astro-ph/astro-ph/0003269]. doi:10.1086/317837. 1603
1604
59. Stephan, A.P.; Naoz, S.; Ghez, A.M.; Morris, M.R.; Ciurlo, A.; Do, T.; Breivik, K.; Coughlin, S.; Rodriguez, C.L. The Fate of Binaries in the Galactic Center: The Mundane and the Exotic. *ApJ* **2019**, *878*, 58, [arXiv:astro-ph.SR/1903.00010]. doi:10.3847/1538-4357/ab1e4d. 1605
1606
60. Giesers, B.; Dreizler, S.; Husser, T.O.; Kamann, S.; Anglada Escudé, G.; Brinchmann, J.; Carollo, C.M.; Roth, M.M.; Weilbacher, P.M.; Wisotzki, L. A detached stellar-mass black hole candidate in the globular cluster NGC 3201. *MNRAS* **2018**, *475*, L15–L19, [arXiv:astro-ph.SR/1801.05642]. doi:10.1093/mnrasl/slx203. 1607
1608
1609
61. Giesers, B.; Kamann, S.; Dreizler, S.; Husser, T.O.; Askar, A.; Göttgens, F.; Brinchmann, J.; Latour, M.; Weilbacher, P.M.; Wendt, M.; et al. A stellar census in globular clusters with MUSE: Binaries in NGC 3201. *A&A* **2019**, *632*, A3, [arXiv:astro-ph.SR/1909.04050]. doi:10.1051/0004-6361/201936203. 1610
1611
1612
62. El-Badry, K.; Rix, H.W.; Quataert, E.; Howard, A.W.; Isaacson, H.; Fuller, J.; Hawkins, K.; Breivik, K.; Wong, K.W.K.; Rodriguez, A.C.; et al. A Sun-like star orbiting a black hole. *arXiv e-prints* **2022**, p. arXiv:2209.06833, [arXiv:astro-ph.SR/2209.06833]. 1613
1614
63. Maccarone, T.J.; Kundu, A.; Zepf, S.E.; Rhode, K.L. A black hole in a globular cluster. *Nature* **2007**, *445*, 183–185, [arXiv:astro-ph/astro-ph/0701310]. doi:10.1038/nature05434. 1615
1616
64. Strader, J.; Chomiuk, L.; Maccarone, T.J.; Miller-Jones, J.C.A.; Seth, A.C. Two stellar-mass black holes in the globular cluster M22. *Nature* **2012**, *490*, 71–73, [arXiv:astro-ph.HE/1210.0901]. doi:10.1038/nature11490. 1617
1618
65. Abbott, B.P.; Abbott, R.; Abbott, T.D.; Abernathy, M.R.; Acernese, F.; Ackley, K.; Adams, C.; Adams, T.; Addesso, P.; Adhikari, R.X.; et al. Observation of Gravitational Waves from a Binary Black Hole Merger. *Phys. Rev. Lett.* **2016**, *116*, 061102, [arXiv:gr-qc/1602.03837]. doi:10.1103/PhysRevLett.116.061102. 1619
1620
1621
66. Abbott, B.P.; Abbott, R.; Abbott, T.D.; Acernese, F.; Ackley, K.; Adams, C.; Adams, T.; Addesso, P.; Adhikari, R.X.; Adya, V.B.; et al. GW170817: Observation of Gravitational Waves from a Binary Neutron Star Inspiral. *Phys. Rev. Lett.* **2017**, *119*, 161101, [arXiv:gr-qc/1710.05832]. doi:10.1103/PhysRevLett.119.161101. 1622
1623
1624
67. Abbott, B.P.; Abbott, R.; Abbott, T.D.; Abernathy, M.R.; Acernese, F.; Ackley, K.; Adams, C.; Adams, T.; Addesso, P.; Adhikari, R.X.; et al. GW151226: Observation of Gravitational Waves from a 22-Solar-Mass Binary Black Hole Coalescence. *Phys. Rev. Lett.* **2016**, *116*, 241103, [arXiv:gr-qc/1606.04855]. doi:10.1103/PhysRevLett.116.241103. 1625
1626
1627
68. Abbott, B.P.; Abbott, R.; Abbott, T.D.; Abraham, S.; Acernese, F.; Ackley, K.; Adams, C.; Adhikari, R.X.; Adya, V.B.; Affeldt, C.; et al. GWTC-1: A Gravitational-Wave Transient Catalog of Compact Binary Mergers Observed by LIGO and Virgo during the First and Second Observing Runs. *Physical Review X* **2019**, *9*, 031040, [arXiv:astro-ph.HE/1811.12907]. doi:10.1103/PhysRevX.9.031040. 1628
1629
1630
69. Abbott, B.P.; Abbott, R.; Abbott, T.D.; Acernese, F.; Ackley, K.; Adams, C.; Adams, T.; Addesso, P.; Adhikari, R.X.; Adya, V.B.; et al. GW170104: Observation of a 50-Solar-Mass Binary Black Hole Coalescence at Redshift 0.2. *Phys. Rev. Lett.* **2017**, *118*, 221101, [arXiv:gr-qc/1706.01812]. doi:10.1103/PhysRevLett.118.221101. 1631
1632
1633
70. Abbott, B.P.; Abbott, R.; Abbott, T.D.; Acernese, F.; Ackley, K.; Adams, C.; Adams, T.; Addesso, P.; Adhikari, R.X.; Adya, V.B.; et al. GW170814: A Three-Detector Observation of Gravitational Waves from a Binary Black Hole Coalescence. *Phys. Rev. Lett.* **2017**, *119*, 141101, [arXiv:gr-qc/1709.09660]. doi:10.1103/PhysRevLett.119.141101. 1634
1635
1636

71. Abbott, B.P.; Abbott, R.; Abbott, T.D.; Acernese, F.; Ackley, K.; Adams, C.; Adams, T.; Addesso, P.; Adhikari, R.X.; Adya, V.B.; et al. GW170608: Observation of a 19 Solar-mass Binary Black Hole Coalescence. *ApJL* **2017**, *851*, L35, [arXiv:astro-ph.HE/1711.05578]. doi:10.3847/2041-8213/aa9f0c. 1637
1638
72. Abbott, R.; Abbott, T.D.; Abraham, S.; Acernese, F.; Ackley, K.; Adams, A.; Adams, C.; Adhikari, R.X.; Adya, V.B.; Affeldt, C.; et al. GWTC-2: Compact Binary Coalescences Observed by LIGO and Virgo during the First Half of the Third Observing Run. *Physical Review X* **2021**, *11*, 021053, [arXiv:gr-qc/2010.14527]. doi:10.1103/PhysRevX.11.021053. 1640
1641
1642
73. Abbott, B.P.; Abbott, R.; Abbott, T.D.; Abraham, S.; Acernese, F.; Ackley, K.; Adams, C.; Adhikari, R.X.; Adya, V.B.; Affeldt, C.; et al. GW190425: Observation of a Compact Binary Coalescence with Total Mass $\sim 3.4 M_{\odot}$. *ApJL* **2020**, *892*, L3, [arXiv:astro-ph.HE/2001.01761]. doi:10.3847/2041-8213/ab75f5. 1643
1644
1645
74. Abbott, R.; Abbott, T.D.; Abraham, S.; Acernese, F.; Ackley, K.; Adams, C.; Adhikari, R.X.; Adya, V.B.; Affeldt, C.; Agathos, M.; et al. GW190814: Gravitational Waves from the Coalescence of a 23 Solar Mass Black Hole with a 2.6 Solar Mass Compact Object. *ApJL* **2020**, *896*, L44, [arXiv:astro-ph.HE/2006.12611]. doi:10.3847/2041-8213/ab960f. 1646
1647
1648
75. Abbott, B.P.; Abbott, R.; Abbott, T.D.; Abraham, S.; Acernese, F.; Ackley, K.; Adams, C.; Adhikari, R.X.; Adya, V.B.; Affeldt, C.; et al. Binary Black Hole Population Properties Inferred from the First and Second Observing Runs of Advanced LIGO and Advanced Virgo. *ApJL* **2019**, *882*, L24, [arXiv:astro-ph.HE/1811.12940]. doi:10.3847/2041-8213/ab3800. 1649
1650
1651
76. Abbott, R.; Abbott, T.D.; Abraham, S.; Acernese, F.; Ackley, K.; Adams, C.; Adhikari, R.X.; Adya, V.B.; Affeldt, C.; Agathos, M.; et al. GW190521: A Binary Black Hole Merger with a Total Mass of $150 M_{\odot}$. *Phys. Rev. Lett.* **2020**, *125*, 101102, [arXiv:gr-qc/2009.01075]. doi:10.1103/PhysRevLett.125.101102. 1652
1653
1654
77. Abbott, R.; Abbott, T.D.; Abraham, S.; Acernese, F.; Ackley, K.; Adams, A.; Adams, C.; Adhikari, R.X.; Adya, V.B.; Affeldt, C.; et al. Population Properties of Compact Objects from the Second LIGO-Virgo Gravitational-Wave Transient Catalog. *ApJL* **2021**, *913*, L7, [arXiv:astro-ph.HE/2010.14533]. doi:10.3847/2041-8213/abe949. 1655
1656
1657
78. Abbott, R.; Abbott, T.D.; Abraham, S.; Acernese, F.; Ackley, K.; Adams, C.; Adhikari, R.X.; Adya, V.B.; Affeldt, C.; Agathos, M.; et al. GW190412: Observation of a binary-black-hole coalescence with asymmetric masses. *Phys. Rev. D* **2020**, *102*, 043015, [arXiv:astro-ph.HE/2004.08342]. doi:10.1103/PhysRevD.102.043015. 1658
1659
1660
79. Spera, M.; Trani, A.A.; Mencagli, M. Compact Binary Coalescences: Astrophysical Processes and Lessons Learned. *Galaxies* **2022**, *10*, 76, [arXiv:astro-ph.HE/2206.15392]. doi:10.3390/galaxies10040076. 1661
1662
80. Fryer, C.L.; Belczynski, K.; Wiktorowicz, G.; Dominik, M.; Kalogera, V.; Holz, D.E. Compact Remnant Mass Function: Dependence on the Explosion Mechanism and Metallicity. *ApJ* **2012**, *749*, 91, [arXiv:astro-ph.SR/1110.1726]. doi:10.1088/0004-637X/749/1/91. 1663
1664
81. Wyrzykowski, L.; Mandel, I. Constraining the masses of microlensing black holes and the mass gap with Gaia DR2. *A&A* **2020**, *636*, A20, [arXiv:astro-ph.SR/1904.07789]. doi:10.1051/0004-6361/201935842. 1665
1666
82. Lam, C.Y.; Lu, J.R.; Udalski, A.; Bond, I.; Bennett, D.P.; Skowron, J.; Mróz, P.; Poleski, R.; Sumi, T.; Szymański, M.K.; et al. An Isolated Mass-gap Black Hole or Neutron Star Detected with Astrometric Microlensing. *ApJL* **2022**, *933*, L23, [arXiv:astro-ph.GA/2202.01903]. doi:10.3847/2041-8213/ac7442. 1667
1668
1669
83. Fowler, W.A.; Hoyle, F. Neutrino Processes and Pair Formation in Massive Stars and Supernovae. *ApJS* **1964**, *9*, 201. doi:10.1086/190103. 1670
1671
84. Woosley, S.E.; Blinnikov, S.; Heger, A. Pulsational pair instability as an explanation for the most luminous supernovae. *Nature* **2007**, *450*, 390–392, [arXiv:astro-ph/0710.3314]. doi:10.1038/nature06333. 1672
1673
85. Woosley, S.E. Pulsational Pair-instability Supernovae. *ApJ* **2017**, *836*, 244, [arXiv:astro-ph.HE/1608.08939]. doi:10.3847/1538-4357/836/2/244. 1674
1675
86. Bellovary, J.M.; Mac Low, M.M.; McKernan, B.; Ford, K.E.S. Migration Traps in Disks around Supermassive Black Holes. *ApJL* **2016**, *819*, L17, [arXiv:astro-ph.GA/1511.00005]. doi:10.3847/2041-8205/819/2/L17. 1676
1677
87. Spera, M.; Mapelli, M. Very massive stars, pair-instability supernovae and intermediate-mass black holes with the sevsn code. *MNRAS* **2017**, *470*, 4739–4749, [arXiv:astro-ph.SR/1706.06109]. doi:10.1093/mnras/stx1576. 1678
1679
88. Farmer, R.; Renzo, M.; de Mink, S.E.; Marchant, P.; Justham, S. Mind the Gap: The Location of the Lower Edge of the Pair-instability Supernova Black Hole Mass Gap. *ApJ* **2019**, *887*, 53, [arXiv:astro-ph.SR/1910.12874]. doi:10.3847/1538-4357/ab518b. 1680
1681
89. Woosley, S.E. The Evolution of Massive Helium Stars, Including Mass Loss. *ApJ* **2019**, *878*, 49, [arXiv:astro-ph.SR/1901.00215]. doi:10.3847/1538-4357/ab1b41. 1682
1683
90. Stevenson, S.; Sampson, M.; Powell, J.; Vigna-Gómez, A.; Neijssel, C.J.; Szécsi, D.; Mandel, I. The Impact of Pair-instability Mass Loss on the Binary Black Hole Mass Distribution. *ApJ* **2019**, *882*, 121, [arXiv:astro-ph.HE/1904.02821]. doi:10.3847/1538-4357/ab3981. 1684
1685
91. Farmer, R.; Renzo, M.; de Mink, S.E.; Fishbach, M.; Justham, S. Constraints from Gravitational-wave Detections of Binary Black Hole Mergers on the $^{12}\text{C}(\alpha, \gamma)^{16}\text{O}$ Rate. *ApJL* **2020**, *902*, L36, [arXiv:astro-ph.HE/2006.06678]. doi:10.3847/2041-8213/abbadd. 1686
1687
92. Marchant, P.; Moriya, T.J. The impact of stellar rotation on the black hole mass-gap from pair-instability supernovae. *A&A* **2020**, *640*, L18, [arXiv:astro-ph.HE/2007.06220]. doi:10.1051/0004-6361/202038902. 1688
1689

93. van Son, L.A.C.; De Mink, S.E.; Broekgaarden, F.S.; Renzo, M.; Justham, S.; Laplace, E.; Morán-Fraile, J.; Hendriks, D.D.; Farmer, R. Polluting the Pair-instability Mass Gap for Binary Black Holes through Super-Eddington Accretion in Isolated Binaries. *ApJ* **2020**, *897*, 100, [arXiv:astro-ph.HE/2004.05187]. doi:10.3847/1538-4357/ab9809. 1690
1691
94. Costa, G.; Bressan, A.; Mapelli, M.; Marigo, P.; Iorio, G.; Spera, M. Formation of GW190521 from stellar evolution: the impact of the hydrogen-rich envelope, dredge-up, and $^{12}\text{C}(\alpha, \gamma)^{16}\text{O}$ rate on the pair-instability black hole mass gap. *MNRAS* **2021**, *501*, 4514–4533, [arXiv:astro-ph.SR/2010.02242]. doi:10.1093/mnras/staa3916. 1693
1694
1695
95. Vink, J.S.; Higgins, E.R.; Sander, A.A.C.; Sabhahit, G.N. Maximum black hole mass across cosmic time. *MNRAS* **2021**, *504*, 146–154, [arXiv:astro-ph.HE/2010.11730]. doi:10.1093/mnras/stab842. 1696
1697
96. Arca Sedda, M.; Benacquista, M. Using final black hole spins and masses to infer the formation history of the observed population of gravitational wave sources. *MNRAS* **2019**, *482*, 2991–3010, [arXiv:astro-ph.GA/1806.01285]. doi:10.1093/mnras/sty2764. 1698
1699
97. Bavera, S.S.; Fragos, T.; Qin, Y.; Zapartas, E.; Neijssel, C.J.; Mandel, I.; Batta, A.; Gaebel, S.M.; Kimball, C.; Stevenson, S. The origin of spin in binary black holes. Predicting the distributions of the main observables of Advanced LIGO. *A&A* **2020**, *635*, A97, [arXiv:astro-ph.HE/1906.12257]. doi:10.1051/0004-6361/201936204. 1700
1701
1702
98. Arca Sedda, M.; Mapelli, M.; Spera, M.; Benacquista, M.; Giacobbo, N. Fingerprints of Binary Black Hole Formation Channels Encoded in the Mass and Spin of Merger Remnants. *ApJ* **2020**, *894*, 133, [arXiv:astro-ph.GA/2003.07409]. doi:10.3847/1538-4357/ab88b2. 1703
1704
99. Arca Sedda, M.; Mapelli, M.; Benacquista, M.; Spera, M. Population synthesis of black hole mergers with B-POP: the impact of dynamics, natal spins, and intermediate-mass black holes on the population of gravitational wave sources. *arXiv e-prints* **2021**, p. arXiv:2109.12119, [arXiv:astro-ph.GA/2109.12119]. 1705
1706
1707
100. Zevin, M.; Spera, M.; Berry, C.P.L.; Kalogera, V. Exploring the Lower Mass Gap and Unequal Mass Regime in Compact Binary Evolution. *ApJL* **2020**, *899*, L1, [arXiv:astro-ph.HE/2006.14573]. doi:10.3847/2041-8213/aba74e. 1708
1709
101. Zevin, M.; Bavera, S.S.; Berry, C.P.L.; Kalogera, V.; Fragos, T.; Marchant, P.; Rodriguez, C.L.; Antonini, F.; Holz, D.E.; Pankow, C. One Channel to Rule Them All? Constraining the Origins of Binary Black Holes Using Multiple Formation Pathways. *ApJ* **2021**, *910*, 152, [arXiv:astro-ph.HE/2011.10057]. doi:10.3847/1538-4357/abe40e. 1710
1711
1712
102. Mapelli, M.; Bouffanais, Y.; Santoliquido, F.; Arca Sedda, M.; Artale, M.C. The cosmic evolution of binary black holes in young, globular, and nuclear star clusters: rates, masses, spins, and mixing fractions. *MNRAS* **2022**, *511*, 5797–5816, [arXiv:astro-ph.HE/2109.06222]. doi:10.1093/mnras/stac422. 1713
1714
1715
103. Spera, M.; Mapelli, M.; Giacobbo, N.; Trani, A.A.; Bressan, A.; Costa, G. Merging black hole binaries with the SEVN code. *MNRAS* **2019**, *485*, 889–907, [arXiv:astro-ph.HE/1809.04605]. doi:10.1093/mnras/stz359. 1716
1717
104. Di Carlo, U.N.; Mapelli, M.; Bouffanais, Y.; Giacobbo, N.; Santoliquido, F.; Bressan, A.; Spera, M.; Haardt, F. Binary black holes in the pair instability mass gap. *MNRAS* **2020**, *497*, 1043–1049, [arXiv:astro-ph.HE/1911.01434]. doi:10.1093/mnras/staa1997. 1718
1719
105. Arca-Sedda, M.; Rizzuto, F.P.; Naab, T.; Ostriker, J.; Giersz, M.; Spurzem, R. Breaching the Limit: Formation of GW190521-like and IMBH Mergers in Young Massive Clusters. *ApJ* **2021**, *920*, 128, [arXiv:astro-ph.GA/2105.07003]. doi:10.3847/1538-4357/ac1419. 1720
1721
106. Rizzuto, F.P.; Naab, T.; Spurzem, R.; Arca-Sedda, M.; Giersz, M.; Ostriker, J.P.; Banerjee, S. Black hole mergers in compact star clusters and massive black hole formation beyond the mass gap. *MNRAS* **2022**, *512*, 884–898, [arXiv:astro-ph.GA/2108.11457]. doi:10.1093/mnras/stac231. 1722
1723
1724
107. Rizzuto, F.P.; Naab, T.; Spurzem, R.; Giersz, M.; Ostriker, J.P.; Stone, N.C.; Wang, L.; Berczik, P.; Rampp, M. Intermediate mass black hole formation in compact young massive star clusters. *MNRAS* **2021**, *501*, 5257–5273, [arXiv:astro-ph.GA/2008.09571]. doi:10.1093/mnras/staa3634. 1725
1726
1727
108. Kremer, K.; Spera, M.; Becker, D.; Chatterjee, S.; Di Carlo, U.N.; Fragione, G.; Rodriguez, C.L.; Ye, C.S.; Rasio, F.A. Populating the Upper Black Hole Mass Gap through Stellar Collisions in Young Star Clusters. *ApJ* **2020**, *903*, 45, [arXiv:astro-ph.HE/2006.10771]. doi:10.3847/1538-4357/abb945. 1728
1729
1730
109. Costa, G.; Ballone, A.; Mapelli, M.; Bressan, A. Formation of black holes in the pair-instability mass gap: Evolution of a post-collision star. *MNRAS* **2022**, *516*, 1072–1080, [arXiv:astro-ph.SR/2204.03492]. doi:10.1093/mnras/stac222. 1731
1732
110. Ballone, A.; Costa, G.; Mapelli, M.; MacLeod, M. Formation of black holes in the pair-instability mass gap: Hydrodynamical simulation of a head-on massive star collision. *arXiv e-prints* **2022**, p. arXiv:2204.03493, [arXiv:astro-ph.SR/2204.03493]. 1733
1734
111. O’Leary, R.M.; Meiron, Y.; Kocsis, B. Dynamical Formation Signatures of Black Hole Binaries in the First Detected Mergers by LIGO. *ApJL* **2016**, *824*, L12, [arXiv:astro-ph.HE/1602.02809]. doi:10.3847/2041-8205/824/1/L12. 1735
1736
112. Gerosa, D.; Berti, E. Are merging black holes born from stellar collapse or previous mergers? *Phys. Rev. D* **2017**, *95*, 124046, [arXiv:gr-qc/1703.06223]. doi:10.1103/PhysRevD.95.124046. 1737
1738
113. Rodriguez, C.L.; Zevin, M.; Amaro-Seoane, P.; Chatterjee, S.; Kremer, K.; Rasio, F.A.; Ye, C.S. Black holes: The next generation—repeated mergers in dense star clusters and their gravitational-wave properties. *Phys. Rev. D* **2019**, *100*, 043027, [arXiv:astro-ph.HE/1906.10260]. doi:10.1103/PhysRevD.100.043027. 1739
1740
1741
114. Antonini, F.; Gieles, M.; Gualandris, A. Black hole growth through hierarchical black hole mergers in dense star clusters: implications for gravitational wave detections. *MNRAS* **2019**, *486*, 5008–5021, [arXiv:astro-ph.HE/1811.03640]. doi:10.1093/mnras/stz1149. 1742
1743

115. Mapelli, M.; Santoliquido, F.; Bouffanais, Y.; Arca Sedda, M.A.; Artale, M.C.; Ballone, A. Mass and Rate of Hierarchical Black Hole Mergers in Young, Globular and Nuclear Star Clusters. *Symmetry* **2021**, *13*, 1678, [arXiv:astro-ph.HE/2007.15022]. doi:10.3390/sym13091678. 1744
116. Mapelli, M.; Dall'Amico, M.; Bouffanais, Y.; Giacobbo, N.; Arca Sedda, M.; Artale, M.C.; Ballone, A.; Di Carlo, U.N.; Iorio, G.; Santoliquido, F.; et al. Hierarchical black hole mergers in young, globular and nuclear star clusters: the effect of metallicity, spin and cluster properties. *MNRAS* **2021**, *505*, 339–358, [arXiv:astro-ph.HE/2103.05016]. doi:10.1093/mnras/stab1334. 1745
117. Guillochon, J.; Ramirez-Ruiz, E. Hydrodynamical Simulations to Determine the Feeding Rate of Black Holes by the Tidal Disruption of Stars: The Importance of the Impact Parameter and Stellar Structure. *ApJ* **2013**, *767*, 25, [arXiv:astro-ph.HE/1206.2350]. doi:10.1088/0004-637X/767/1/25. 1746
118. Glebbeek, E.; Gaburov, E.; de Mink, S.E.; Pols, O.R.; Portegies Zwart, S.F. The evolution of runaway stellar collision products. *A&A* **2009**, *497*, 255–264, [arXiv:astro-ph.SR/0902.1753]. doi:10.1051/0004-6361/200810425. 1747
119. Shiokawa, H.; Krolik, J.H.; Cheng, R.M.; Piran, T.; Noble, S.C. General Relativistic Hydrodynamic Simulation of Accretion Flow from a Stellar Tidal Disruption. *ApJ* **2015**, *804*, 85, [arXiv:astro-ph.HE/1501.04365]. doi:10.1088/0004-637X/804/2/85. 1748
120. Law-Smith, J.; Guillochon, J.; Ramirez-Ruiz, E. The Tidal Disruption of Sun-like Stars by Massive Black Holes. *ApJL* **2019**, *882*, L25, [arXiv:astro-ph.HE/1907.04859]. doi:10.3847/2041-8213/ab379a. 1749
121. Schröder, S.L.; MacLeod, M.; Loeb, A.; Vigna-Gómez, A.; Mandel, I. Explosions Driven by the Coalescence of a Compact Object with the Core of a Massive-star Companion inside a Common Envelope: Circumstellar Properties, Light Curves, and Population Statistics. *ApJ* **2020**, *892*, 13, [arXiv:astro-ph.HE/1906.04189]. doi:10.3847/1538-4357/ab7014. 1750
122. Cruz-Orsorio, A.; Rezzolla, L. Common-envelope Dynamics of a Stellar-mass Black Hole: General Relativistic Simulations. *ApJ* **2020**, *894*, 147, [arXiv:gr-qc/2004.13782]. doi:10.3847/1538-4357/ab89aa. 1751
123. Campanelli, M.; Lousto, C.O.; Zlochower, Y.; Merritt, D. Maximum Gravitational Recoil. *Phys. Rev. Lett.* **2007**, *98*, 231102, [arXiv:gr-qc/gr-qc/0702133]. doi:10.1103/PhysRevLett.98.231102. 1752
124. Lousto, C.O.; Zlochower, Y. Further insight into gravitational recoil. *Phys. Rev. D* **2008**, *77*, 044028, [arXiv:gr-qc/0708.4048]. doi:10.1103/PhysRevD.77.044028. 1753
125. Lousto, C.O.; Zlochower, Y.; Dotti, M.; Volonteri, M. Gravitational recoil from accretion-aligned black-hole binaries. *Phys. Rev. D* **2012**, *85*, 084015, [arXiv:gr-qc/1201.1923]. doi:10.1103/PhysRevD.85.084015. 1754
126. Holley-Bockelmann, K.; Gültekin, K.; Shoemaker, D.; Yunes, N. Gravitational Wave Recoil and the Retention of Intermediate-Mass Black Holes. *ApJ* **2008**, *686*, 829–837, [arXiv:astro-ph/0707.1334]. doi:10.1086/591218. 1755
127. Antonini, F.; Rasio, F.A. Merging Black Hole Binaries in Galactic Nuclei: Implications for Advanced-LIGO Detections. *ApJ* **2016**, *831*, 187, [arXiv:astro-ph.HE/1606.04889]. doi:10.3847/0004-637X/831/2/187. 1756
128. Fragione, G.; Kocsis, B.; Rasio, F.A.; Silk, J. Repeated Mergers, Mass-gap Black Holes, and Formation of Intermediate-mass Black Holes in Dense Massive Star Clusters. *ApJ* **2022**, *927*, 231, [arXiv:astro-ph.GA/2107.04639]. doi:10.3847/1538-4357/ac5026. 1757
129. Arca Sedda, M.; Amaro Seoane, P.; Chen, X. Merging stellar and intermediate-mass black holes in dense clusters: implications for LIGO, LISA, and the next generation of gravitational wave detectors. *A&A* **2021**, *652*, A54, [arXiv:astro-ph.GA/2007.13746]. doi:10.1051/0004-6361/202037785. 1758
130. Arca Sedda, M. Dissecting the properties of neutron star-black hole mergers originating in dense star clusters. *Communications Physics* **2020**, *3*, 43, [arXiv:astro-ph.GA/2003.02279]. doi:10.1038/s42005-020-0310-x. 1759
131. Gupta, A.; Gerosa, D.; Arun, K.G.; Berti, E.; Farr, W.M.; Sathyaprakash, B.S. Black holes in the low-mass gap: Implications for gravitational-wave observations. *Phys. Rev. D* **2020**, *101*, 103036, [arXiv:gr-qc/1909.05804]. doi:10.1103/PhysRevD.101.103036. 1760
132. Rastello, S.; Mapelli, M.; Di Carlo, U.N.; Giacobbo, N.; Santoliquido, F.; Spera, M.; Ballone, A.; Iorio, G. Dynamics of black hole-neutron star binaries in young star clusters. *MNRAS* **2020**, *497*, 1563–1570, [arXiv:astro-ph.HE/2003.02277]. doi:10.1093/mnras/staa2018. 1761
133. Ye, C.S.; Fong, W.f.; Kremer, K.; Rodriguez, C.L.; Chatterjee, S.; Fragione, G.; Rasio, F.A. On the Rate of Neutron Star Binary Mergers from Globular Clusters. *ApJL* **2020**, *888*, L10, [arXiv:astro-ph.HE/1910.10740]. doi:10.3847/2041-8213/ab5dc5. 1762
134. Yang, Y.; Gayathri, V.; Bartos, I.; Haiman, Z.; Safarzadeh, M.; Tagawa, H. Black Hole Formation in the Lower Mass Gap through Mergers and Accretion in AGN Disks. *ApJL* **2020**, *901*, L34, [arXiv:astro-ph.HE/2007.04781]. doi:10.3847/2041-8213/abb940. 1763
135. Kritos, K.; Cholis, I. Black holes merging with low mass gap objects inside globular clusters. *Phys. Rev. D* **2021**, *104*, 043004, [arXiv:astro-ph.GA/2104.02073]. doi:10.1103/PhysRevD.104.043004. 1764
136. Arca Sedda, M. Dynamical Formation of the GW190814 Merger. *ApJL* **2021**, *908*, L38, [arXiv:astro-ph.HE/2102.03364]. doi:10.3847/2041-8213/abdfcd. 1765
137. Mandel, I.; de Mink, S.E. Merging binary black holes formed through chemically homogeneous evolution in short-period stellar binaries. *MNRAS* **2016**, *458*, 2634–2647, [arXiv:astro-ph.HE/1601.00007]. doi:10.1093/mnras/stw379. 1766
138. Rodriguez, C.L.; Zevin, M.; Pankow, C.; Kalogera, V.; Rasio, F.A. Illuminating Black Hole Binary Formation Channels with Spins in Advanced LIGO. *ApJL* **2016**, *832*, L2, [arXiv:astro-ph.HE/1609.05916]. doi:10.3847/2041-8205/832/1/L2. 1767
139. Gerosa, D.; Berti, E.; O'Shaughnessy, R.; Belczynski, K.; Kesden, M.; Wysocki, D.; Gladysz, W. Spin orientations of merging black holes formed from the evolution of stellar binaries. *Phys. Rev. D* **2018**, *98*, 084036, [arXiv:astro-ph.HE/1808.02491]. doi:10.1103/PhysRevD.98.084036. 1768

140. Talbot, C.; Thrane, E. Determining the population properties of spinning black holes. *Phys. Rev. D* **2017**, *96*, 023012, [arXiv:astro-ph.HE/1704.08370]. doi:10.1103/PhysRevD.96.023012. 1799
1800
141. The LIGO Scientific Collaboration.; the Virgo Collaboration.; the KAGRA Collaboration.; Abbott, R.; Abbott, T.D.; Acernese, F.; Ackley, K.; Adams, C.; Adhikari, N.; Adhikari, R.X.; et al. The population of merging compact binaries inferred using gravitational waves through GWTC-3. *arXiv e-prints* **2021**, p. arXiv:2111.03634, [arXiv:astro-ph.HE/2111.03634]. 1801
1802
1803
142. Gerosa, D.; Fishbach, M. Hierarchical mergers of stellar-mass black holes and their gravitational-wave signatures. *Nature Astronomy* **2021**, *5*, 749–760, [arXiv:astro-ph.HE/2105.03439]. doi:10.1038/s41550-021-01398-w. 1804
1805
143. Damour, T.; Nagar, A. New effective-one-body description of coalescing nonprecessing spinning black-hole binaries. *Phys. Rev. D* **2014**, *90*, 044018, [arXiv:gr-qc/1406.6913]. doi:10.1103/PhysRevD.90.044018. 1806
1807
144. Cao, Z.; Han, W.B. Waveform model for an eccentric binary black hole based on the effective-one-body-numerical-relativity formalism. *Phys. Rev. D* **2017**, *96*, 044028, [arXiv:gr-qc/1708.00166]. doi:10.1103/PhysRevD.96.044028. 1808
1809
145. Liu, X.; Cao, Z.; Shao, L. Validating the effective-one-body numerical-relativity waveform models for spin-aligned binary black holes along eccentric orbits. *Phys. Rev. D* **2020**, *101*, 044049, [arXiv:gr-qc/1910.00784]. doi:10.1103/PhysRevD.101.044049. 1810
1811
146. Knee, A.M.; Romero-Shaw, I.M.; Lasky, P.D.; McIver, J.; Thrane, E. A Rosetta Stone for Eccentric Gravitational Waveform Models. *ApJ* **2022**, *936*, 172, [arXiv:gr-qc/2207.14346]. doi:10.3847/1538-4357/ac8b02. 1812
1813
147. Gayathri, V.; Healy, J.; Lange, J.; O’Brien, B.; Szczepanczyk, M.; Bartos, I.; Campanelli, M.; Klimenko, S.; Lousto, C.; O’Shaughnessy, R. Eccentricity Estimate for Black Hole Mergers with Numerical Relativity Simulations. *arXiv e-prints* **2020**, p. arXiv:2009.05461, [arXiv:astro-ph.HE/2009.05461]. 1814
1815
1816
148. Romero-Shaw, I.; Lasky, P.D.; Thrane, E.; Calderón Bustillo, J. GW190521: Orbital Eccentricity and Signatures of Dynamical Formation in a Binary Black Hole Merger Signal. *ApJL* **2020**, *903*, L5, [arXiv:astro-ph.HE/2009.04771]. doi:10.3847/2041-8213/abbe26. 1817
1818
149. Romero-Shaw, I.; Lasky, P.D.; Thrane, E. Signs of Eccentricity in Two Gravitational-wave Signals May Indicate a Subpopulation of Dynamically Assembled Binary Black Holes. *ApJL* **2021**, *921*, L31, [arXiv:astro-ph.HE/2108.01284]. doi:10.3847/2041-8213/ac3138. 1819
1820
150. Romero-Shaw, I.M.; Lasky, P.D.; Thrane, E. Four eccentric mergers increase the evidence that LIGO–Virgo–KAGRA’s binary black holes form dynamically. *arXiv e-prints* **2022**, p. arXiv:2206.14695, [arXiv:astro-ph.HE/2206.14695]. 1821
1822
151. Gondán, L.; Kocsis, B.; Raffai, P.; Frei, Z. Accuracy of Estimating Highly Eccentric Binary Black Hole Parameters with Gravitational-wave Detections. *ApJ* **2018**, *855*, 34, [arXiv:astro-ph.HE/1705.10781]. doi:10.3847/1538-4357/aaad0e. 1823
1824
152. Gondán, L.; Kocsis, B. Measurement Accuracy of Inspiring Eccentric Neutron Star and Black Hole Binaries Using Gravitational Waves. *ApJ* **2019**, *871*, 178, [arXiv:astro-ph.HE/1809.00672]. doi:10.3847/1538-4357/aaf893. 1825
1826
153. Portegies Zwart, S.F.; Verbunt, F. Population synthesis of high-mass binaries. *A&A* **1996**, *309*, 179–196. 1827
154. Hurley, J.R.; Tout, C.A.; Pols, O.R. Evolution of binary stars and the effect of tides on binary populations. *MNRAS* **2002**, *329*, 897–928, [arXiv:astro-ph/astro-ph/0201220]. doi:10.1046/j.1365-8711.2002.05038.x. 1828
1829
155. Marchant, P.; Langer, N.; Podsiadlowski, P.; Tauris, T.M.; Moriya, T.J. A new route towards merging massive black holes. *A&A* **2016**, *588*, A50, [arXiv:astro-ph.SR/1601.03718]. doi:10.1051/0004-6361/201628133. 1830
1831
156. Neijssel, C.J.; Vigna-Gómez, A.; Stevenson, S.; Barrett, J.W.; Gaebel, S.M.; Broekgaarden, F.S.; de Mink, S.E.; Szécsi, D.; Vinciguerra, S.; Mandel, I. The effect of the metallicity-specific star formation history on double compact object mergers. *MNRAS* **2019**, *490*, 3740–3759, [arXiv:astro-ph.SR/1906.08136]. doi:10.1093/mnras/stz2840. 1832
1833
1834
157. Dorozmaï, A.; Toonen, S. Importance of stable mass transfer and stellar winds for the formation of gravitational wave sources. *arXiv e-prints* **2022**, p. arXiv:2207.08837, [arXiv:astro-ph.SR/2207.08837]. 1835
1836
158. Trani, A.A.; Rieder, S.; Tanikawa, A.; Iorio, G.; Martini, R.; Karelin, G.; Glanz, H.; Portegies Zwart, S. Revisiting the common envelope evolution in binary stars: A new semianalytic model for N -body and population synthesis codes. *Phys. Rev. D* **2022**, *106*, 043014, [arXiv:astro-ph.SR/2205.13537]. doi:10.1103/PhysRevD.106.043014. 1837
1838
1839
159. Zevin, M.; Samsing, J.; Rodriguez, C.; Haster, C.J.; Ramirez-Ruiz, E. Eccentric Black Hole Mergers in Dense Star Clusters: The Role of Binary-Binary Encounters. *ApJ* **2019**, *871*, 91, [arXiv:astro-ph.HE/1810.00901]. doi:10.3847/1538-4357/aaf6ec. 1840
1841
160. Samsing, J.; Ramirez-Ruiz, E. On the Assembly Rate of Highly Eccentric Binary Black Hole Mergers. *ApJL* **2017**, *840*, L14, [arXiv:astro-ph.HE/1703.09703]. doi:10.3847/2041-8213/aa6f0b. 1842
1843
161. Kocsis, B. Dynamical Formation of Merging Stellar-Mass Binary Black Holes. In *Handbook of Gravitational Wave Astronomy. Edited by C. Bambi*; 2022; p. 15. doi:10.1007/978-981-15-4702-7_15-1. 1844
1845
162. Samsing, J.; D’Orazio, D.J. Black Hole Mergers From Globular Clusters Observable by LISA I: Eccentric Sources Originating From Relativistic N-body Dynamics. *MNRAS* **2018**, *481*, 5445–5450, [arXiv:astro-ph.HE/1804.06519]. doi:10.1093/mnras/sty2334. 1846
1847
163. Arca Sedda, M.; Li, G.; Kocsis, B. Order in the chaos. Eccentric black hole binary mergers in triples formed via strong binary-binary scatterings. *A&A* **2021**, *650*, A189, [arXiv:astro-ph.HE/1805.06458]. doi:10.1051/0004-6361/202038795. 1848
1849
164. Nishizawa, A.; Berti, E.; Klein, A.; Sesana, A. eLISA eccentricity measurements as tracers of binary black hole formation. *Phys. Rev. D* **2016**, *94*, 064020, [arXiv:gr-qc/1605.01341]. doi:10.1103/PhysRevD.94.064020. 1850
1851
165. Arca-Sedda, M.; Capuzzo-Dolcetta, R. The MEGaN project II. Gravitational waves from intermediate-mass and binary black holes around a supermassive black hole. *MNRAS* **2019**, *483*, 152–171, [arXiv:astro-ph.GA/1709.05567]. doi:10.1093/mnras/sty3096. 1852
1853

166. Raghavan, D.; McAlister, H.A.; Henry, T.J.; Latham, D.W.; Marcy, G.W.; Mason, B.D.; Gies, D.R.; White, R.J.; ten Brummelaar, T.A. A Survey of Stellar Families: Multiplicity of Solar-type Stars. *ApJS* **2010**, *190*, 1–42, [arXiv:astro-ph.SR/1007.0414]. doi:10.1088/0067-0049/190/1/1. 1854
1855
1856
167. Sana, H.; Evans, C.J. The multiplicity of massive stars. Active OB Stars: Structure, Evolution, Mass Loss, and Critical Limits; Neiner, C.; Wade, G.; Meynet, G.; Peters, G., Eds., 2011, Vol. 272, pp. 474–485, [arXiv:astro-ph.SR/1009.4197]. doi:10.1017/S1743921311011124. 1857
1858
168. Sana, H.; de Mink, S.E.; de Koter, A.; Langer, N.; Evans, C.J.; Gieles, M.; Gosset, E.; Izzard, R.G.; Le Bouquin, J.B.; Schneider, F.R.N. Binary Interaction Dominates the Evolution of Massive Stars. *Science* **2012**, *337*, 444, [arXiv:astro-ph.SR/1207.6397]. doi:10.1126/science.1223344. 1859
1860
1861
169. Moe, M.; Di Stefano, R. Mind Your Ps and Qs: The Interrelation between Period (P) and Mass-ratio (Q) Distributions of Binary Stars. *ApJS* **2017**, *230*, 15, [arXiv:astro-ph.SR/1606.05347]. doi:10.3847/1538-4365/aa6fb6. 1862
1863
170. Ott, T.; Eckart, A.; Genzel, R. Variable and Embedded Stars in the Galactic Center. *ApJ* **1999**, *523*, 248–264. doi:10.1086/307712. 1864
171. Martins, F.; Trippe, S.; Paumard, T.; Ott, T.; Genzel, R.; Rauw, G.; Eisenhauer, F.; Gillessen, S.; Maness, H.; Abuter, R. GCIRS 16SW: A Massive Eclipsing Binary in the Galactic Center. *ApJL* **2006**, *649*, L103–L106, [arXiv:astro-ph/astro-ph/0608215]. doi:10.1086/508328. 1865
1866
172. Rafelski, M.; Ghez, A.M.; Hornstein, S.D.; Lu, J.R.; Morris, M. Photometric Stellar Variability in the Galactic Center. *ApJ* **2007**, *659*, 1241–1256, [arXiv:astro-ph/astro-ph/0701082]. doi:10.1086/512062. 1867
1868
173. Pfuhl, O.; Alexander, T.; Gillessen, S.; Martins, F.; Genzel, R.; Eisenhauer, F.; Fritz, T.K.; Ott, T. Massive Binaries in the Vicinity of Sgr A*. *ApJ* **2014**, *782*, 101, [arXiv:astro-ph.GA/1307.7996]. doi:10.1088/0004-637X/782/2/101. 1869
1870
174. Gautam, A.K.; Do, T.; Ghez, A.M.; Morris, M.R.; Martinez, G.D.; Hosek, Matthew W., J.; Lu, J.R.; Sakai, S.; Witzel, G.; Jia, S.; et al. An Adaptive Optics Survey of Stellar Variability at the Galactic Center. *ApJ* **2019**, *871*, 103, [arXiv:astro-ph.SR/1811.04898]. doi:10.3847/1538-4357/aaf103. 1871
1872
1873
175. Zhu, Z.; Li, Z.; Morris, M.R. An Ultradeep Chandra Catalog of X-Ray Point Sources in the Galactic Center Star Cluster. *ApJS* **2018**, *235*, 26, [arXiv:astro-ph.HE/1802.05073]. doi:10.3847/1538-4365/aab14f. 1874
1875
176. Munro, M.P.; Lu, J.R.; Baganoff, F.K.; Brandt, W.N.; Garmire, G.P.; Ghez, A.M.; Hornstein, S.D.; Morris, M.R. A Remarkable Low-Mass X-Ray Binary within 0.1 Parsecs of the Galactic Center. *ApJ* **2005**, *633*, 228–239, [arXiv:astro-ph/astro-ph/0503572]. doi:10.1086/444586. 1876
1877
1878
177. Munro, M.P.; Bauer, F.E.; Bandyopadhyay, R.M.; Wang, Q.D. A Chandra Catalog of X-Ray Sources in the Central 150 pc of the Galaxy. *ApJS* **2006**, *165*, 173–187, [arXiv:astro-ph/astro-ph/0601627]. doi:10.1086/504798. 1879
1880
178. Munro, M.P.; Bauer, F.E.; Baganoff, F.K.; Bandyopadhyay, R.M.; Bower, G.C.; Brandt, W.N.; Broos, P.S.; Cotera, A.; Eikenberry, S.S.; Garmire, G.P.; et al. A Catalog of X-Ray Point Sources from Two Megaseconds of Chandra Observations of the Galactic Center. *ApJS* **2009**, *181*, 110–128, [arXiv:astro-ph/0809.1105]. doi:10.1088/0067-0049/181/1/110. 1881
1882
1883
179. Abazajian, K.N. The consistency of Fermi-LAT observations of the galactic center with a millisecond pulsar population in the central stellar cluster. *JCP* **2011**, *2011*, 010, [arXiv:astro-ph.HE/1011.4275]. doi:10.1088/1475-7516/2011/03/010. 1884
1885
180. Bartels, R.; Krishnamurthy, S.; Weniger, C. Strong Support for the Millisecond Pulsar Origin of the Galactic Center GeV Excess. *Phys. Rev. Lett.* **2016**, *116*, 051102, [arXiv:astro-ph.HE/1506.05104]. doi:10.1103/PhysRevLett.116.051102. 1886
1887
181. Hooper, D.; Goodenough, L. Dark matter annihilation in the Galactic Center as seen by the Fermi Gamma Ray Space Telescope. *Physics Letters B* **2011**, *697*, 412–428, [arXiv:hep-ph/1010.2752]. doi:10.1016/j.physletb.2011.02.029. 1888
1889
182. Macquart, J.P.; Kanekar, N. On Detecting Millisecond Pulsars at the Galactic Center. *ApJ* **2015**, *805*, 172, [arXiv:astro-ph.HE/1504.02492]. doi:10.1088/0004-637X/805/2/172. 1890
1891
183. Zhao, J.H.; Morris, M.R.; Goss, W.M. Detection of a Dense Group of Hypercompact Radio Sources in the Central Parsec of the Galaxy. *ApJL* **2022**, *927*, L6, [arXiv:astro-ph.GA/2202.05300]. doi:10.3847/2041-8213/ac54be. 1892
1893
184. Bartels, R.; Calore, F.; Storm, E.; Weniger, C. Galactic binaries can explain the Fermi Galactic centre excess and 511 keV emission. *MNRAS* **2018**, *480*, 3826–3841, [arXiv:astro-ph.HE/1803.04370]. doi:10.1093/mnras/sty2135. 1894
1895
185. Guépin, C.; Rinchiuso, L.; Kotera, K.; Moulin, E.; Pierog, T.; Silk, J. Pevatron at the Galactic Center: multi-wavelength signatures from millisecond pulsars. *JCP* **2018**, *2018*, 042, [arXiv:astro-ph.HE/1806.03307]. doi:10.1088/1475-7516/2018/07/042. 1896
1897
186. Eckner, C.; Hou, X.; Serpico, P.D.; Winter, M.; Zaharijas, G.; Martin, P.; di Mauro, M.; Mirabal, N.; Petrovic, J.; Prodanovic, T.; et al. Millisecond Pulsar Origin of the Galactic Center Excess and Extended Gamma-Ray Emission from Andromeda: A Closer Look. *ApJ* **2018**, *862*, 79, [arXiv:astro-ph.HE/1711.05127]. doi:10.3847/1538-4357/aac029. 1898
1899
1900
187. Brandt, T.D.; Kocsis, B. Disrupted Globular Clusters Can Explain the Galactic Center Gamma-Ray Excess. *ApJ* **2015**, *812*, 15, [arXiv:astro-ph.HE/1507.05616]. doi:10.1088/0004-637X/812/1/15. 1901
1902
188. Naoz, S.; Fragos, T.; Geller, A.; Stephan, A.P.; Rasio, F.A. Formation of Black Hole Low-mass X-Ray Binaries in Hierarchical Triple Systems. *ApJL* **2016**, *822*, L24, [arXiv:astro-ph.HE/1510.02093]. doi:10.3847/2041-8205/822/2/L24. 1903
1904
189. Levin, Y. Starbursts near supermassive black holes: young stars in the Galactic Centre, and gravitational waves in LISA band. *MNRAS* **2007**, *374*, 515–524, [arXiv:astro-ph/astro-ph/0603583]. doi:10.1111/j.1365-2966.2006.11155.x. 1905
1906
190. Alexander, R.D.; Armitage, P.J.; Cuadra, J. Binary formation and mass function variations in fragmenting discs with short cooling times. *MNRAS* **2008**, *389*, 1655–1664, [arXiv:astro-ph/0807.1731]. doi:10.1111/j.1365-2966.2008.13706.x. 1907
1908

191. Brown, W.R.; Geller, M.J.; Kenyon, S.J.; Kurtz, M.J. Discovery of an Unbound Hypervelocity Star in the Milky Way Halo. *ApJL* **2005**, *622*, L33–L36, [arXiv:astro-ph/astro-ph/0501177]. doi:10.1086/429378. 1910
192. Brown, W.R.; Geller, M.J.; Kenyon, S.J.; Kurtz, M.J. Hypervelocity Stars. I. The Spectroscopic Survey. *ApJ* **2006**, *647*, 303–311, [arXiv:astro-ph/astro-ph/0604111]. doi:10.1086/505165. 1911
193. Brown, W.R.; Geller, M.J.; Kenyon, S.J.; Kurtz, M.J.; Bromley, B.C. Hypervelocity Stars. III. The Space Density and Ejection History of Main-Sequence Stars from the Galactic Center. *ApJ* **2007**, *671*, 1708–1716, [arXiv:astro-ph/0709.1471]. doi:10.1086/523642. 1912
194. Brown, W.R. Hypervelocity Stars. *ARA&A* **2015**, *53*, 15–49. doi:10.1146/annurev-astro-082214-122230. 1913
195. Brown, W.R.; Lattanzi, M.G.; Kenyon, S.J.; Geller, M.J. Gaia and the Galactic Center Origin of Hypervelocity Stars. *ApJ* **2018**, *866*, 39, [arXiv:astro-ph.SR/1805.04184]. doi:10.3847/1538-4357/aadb8e. 1914
196. Hills, J.G. Hyper-velocity and tidal stars from binaries disrupted by a massive Galactic black hole. *Nature* **1988**, *331*, 687–689. doi:10.1038/331687a0. 1915
197. Yu, Q.; Tremaine, S. Ejection of Hypervelocity Stars by the (Binary) Black Hole in the Galactic Center. *ApJ* **2003**, *599*, 1129–1138, [arXiv:astro-ph/astro-ph/0309084]. doi:10.1086/379546. 1916
198. Gould, A.; Quillen, A.C. Sagittarius A* Companion S0-2: A Probe of Very High Mass Star Formation. *ApJ* **2003**, *592*, 935–940, [arXiv:astro-ph/astro-ph/0302437]. doi:10.1086/375840. 1917
199. Perets, H.B.; Hopman, C.; Alexander, T. Massive Perturber-driven Interactions between Stars and a Massive Black Hole. *ApJ* **2007**, *656*, 709–720, [arXiv:astro-ph/astro-ph/0606443]. doi:10.1086/510377. 1918
200. O’Leary, R.M.; Loeb, A. Production of hypervelocity stars through encounters with stellar-mass black holes in the Galactic Centre. *MNRAS* **2008**, *383*, 86–92, [arXiv:astro-ph/astro-ph/0609046]. doi:10.1111/j.1365-2966.2007.12531.x. 1919
201. Perets, H.B. Runaway and Hypervelocity Stars in the Galactic Halo: Binary Rejuvenation and Triple Disruption. *ApJ* **2009**, *698*, 1330–1340, [arXiv:astro-ph/0802.1004]. doi:10.1088/0004-637X/698/2/1330. 1920
202. Brown, H.; Kobayashi, S.; Rossi, E.M.; Sari, R. Tidal disruption of inclined or eccentric binaries by massive black holes. *MNRAS* **2018**, *477*, 5682–5691, [arXiv:astro-ph.HE/1804.02911]. doi:10.1093/mnras/sty1069. 1921
203. Rose, S.C.; Naoz, S.; Gautam, A.K.; Ghez, A.M.; Do, T.; Chu, D.; Becklin, E. On Socially Distant Neighbors: Using Binaries to Constrain the Density of Objects in the Galactic Center. *ApJ* **2020**, *904*, 113, [arXiv:astro-ph.SR/2008.06512]. doi:10.3847/1538-4357/abc557. 1922
204. Lu, J.R.; Do, T.; Ghez, A.M.; Morris, M.R.; Yelda, S.; Matthews, K. Stellar Populations in the Central 0.5 pc of the Galaxy. II. The Initial Mass Function. *ApJ* **2013**, *764*, 155, [arXiv:astro-ph.SR/1301.0540]. doi:10.1088/0004-637X/764/2/155. 1923
205. Stephan, A.P.; Naoz, S.; Ghez, A.M.; Witzel, G.; Sitarski, B.N.; Do, T.; Kocsis, B. Merging binaries in the Galactic Center: the eccentric Kozai-Lidov mechanism with stellar evolution. *MNRAS* **2016**, *460*, 3494–3504, [arXiv:astro-ph.SR/1603.02709]. doi:10.1093/mnras/stw1220. 1924
206. Lu, J.R.; Ghez, A.M.; Hornstein, S.D.; Morris, M.R.; Becklin, E.E.; Matthews, K. A Disk of Young Stars at the Galactic Center as Determined by Individual Stellar Orbits. *ApJ* **2009**, *690*, 1463–1487, [arXiv:astro-ph/0808.3818]. doi:10.1088/0004-637X/690/2/1463. 1925
207. Yelda, S.; Ghez, A.M.; Lu, J.R.; Do, T.; Meyer, L.; Morris, M.R.; Matthews, K. Properties of the Remnant Clockwise Disk of Young Stars in the Galactic Center. *ApJ* **2014**, *783*, 131, [arXiv:astro-ph.GA/1401.7354]. doi:10.1088/0004-637X/783/2/131. 1926
208. Naoz, S.; Ghez, A.M.; Hees, A.; Do, T.; Witzel, G.; Lu, J.R. Confusing Binaries: The Role of Stellar Binaries in Biasing Disk Properties in the Galactic Center. *ApJL* **2018**, *853*, L24, [arXiv:astro-ph.GA/1801.03934]. doi:10.3847/2041-8213/aaa6bf. 1927
209. Spitzer, L. *Dynamical evolution of globular clusters*; Princeton University Press: Princeton, NJ, 1987. 1928
210. Binney, J.; Tremaine, S. *Galactic Dynamics: Second Edition*; Princeton University Press: Princeton, NJ, 2008. 1929
211. Seth, A.C.; Dalcanton, J.J.; Hodge, P.W.; Debattista, V.P. Clues to Nuclear Star Cluster Formation from Edge-on Spirals. *AJ* **2006**, *132*, 2539–2555, [arXiv:astro-ph/astro-ph/0609302]. doi:10.1086/508994. 1930
212. Seth, A.C.; Blum, R.D.; Bastian, N.; Caldwell, N.; Debattista, V.P. The Rotating Nuclear Star Cluster in NGC 4244. *ApJ* **2008**, *687*, 997–1003, [arXiv:astro-ph/0807.3044]. doi:10.1086/591935. 1931
213. Spengler, C.; Côté, P.; Roediger, J.; Ferrarese, L.; Sánchez-Janssen, R.; Toloba, E.; Liu, Y.; Guhathakurta, P.; Cuillandre, J.C.; Gwyn, S.; et al. Virgo Redux: The Masses and Stellar Content of Nuclei in Early-type Galaxies from Multiband Photometry and Spectroscopy. *ApJ* **2017**, *849*, 55, [arXiv:astro-ph.GA/1709.00406]. doi:10.3847/1538-4357/aa8a78. 1932
214. Feldmeier, A.; Neumayer, N.; Seth, A.; Schödel, R.; Lützgendorf, N.; de Zeeuw, P.T.; Kissler-Patig, M.; Nishiyama, S.; Walcher, C.J. Large scale kinematics and dynamical modelling of the Milky Way nuclear star cluster. *A&A* **2014**, *570*, A2, [arXiv:astro-ph.GA/1406.2849]. doi:10.1051/0004-6361/201423777. 1933
215. Fahrion, K.; Lyubenova, M.; van de Ven, G.; Leaman, R.; Hilker, M.; Martín-Navarro, I.; Zhu, L.; Alfaro-Cuello, M.; Coccato, L.; Corsini, E.M.; et al. Constraining nuclear star cluster formation using MUSE-AO observations of the early-type galaxy FCC 47. *A&A* **2019**, *628*, A92, [arXiv:astro-ph.GA/1907.01007]. doi:10.1051/0004-6361/201935832. 1934
216. Rossa, J.; van der Marel, R.P.; Böker, T.; Gerssen, J.; Ho, L.C.; Rix, H.W.; Shields, J.C.; Walcher, C.J. Hubble Space Telescope STIS Spectra of Nuclear Star Clusters in Spiral Galaxies: Dependence of Age and Mass on Hubble Type. *AJ* **2006**, *132*, 1074–1099, [arXiv:astro-ph/astro-ph/0604140]. doi:10.1086/505968. 1935

217. Kacharov, N.; Neumayer, N.; Seth, A.C.; Cappellari, M.; McDermid, R.; Walcher, C.J.; Böker, T. Stellar populations and star formation histories of the nuclear star clusters in six nearby galaxies. *MNRAS* **2018**, *480*, 1973–1998, [arXiv:astro-ph.GA/1807.08765]. doi:10.1093/mnras/sty1985. 1963
1964
218. Filippenko, A.V.; Ho, L.C. A Low-Mass Central Black Hole in the Bulgeless Seyfert 1 Galaxy NGC 4395. *ApJL* **2003**, *588*, L13–L16, [arXiv:astro-ph/astro-ph/0303429]. doi:10.1086/375361. 1966
1967
219. Hilker, M.; Infante, L.; Vieira, G.; Kissler-Patig, M.; Richtler, T. The central region of the Fornax cluster. II. Spectroscopy and radial velocities of member and background galaxies. *A&AS* **1999**, *134*, 75–86, [arXiv:astro-ph/astro-ph/9807144]. doi:10.1051/aas:1999434. 1968
1969
220. Afanasiev, A.V.; Chilingarian, I.V.; Mieske, S.; Voggel, K.T.; Picotti, A.; Hilker, M.; Seth, A.; Neumayer, N.; Frank, M.; Romanowsky, A.J.; et al. A 3.5 million Solar masses black hole in the centre of the ultracompact dwarf galaxy fornax UCD3. *MNRAS* **2018**, *477*, 4856–4865, [arXiv:astro-ph.GA/1804.02938]. doi:10.1093/mnras/sty913. 1970
1971
1972
221. Bekki, K.; Couch, W.J.; Drinkwater, M.J. Galaxy Threshing and the Formation of Ultracompact Dwarf Galaxies. *ApJL* **2001**, *552*, L105–L108, [arXiv:astro-ph/astro-ph/0106402]. doi:10.1086/320339. 1973
1974
222. Bekki, K.; Couch, W.J.; Drinkwater, M.J.; Shioya, Y. Galaxy threshing and the origin of ultra-compact dwarf galaxies in the Fornax cluster. *MNRAS* **2003**, *344*, 399–411, [arXiv:astro-ph/astro-ph/0308243]. doi:10.1046/j.1365-8711.2003.06916.x. 1975
1976
223. Norris, M.A.; Kannappan, S.J.; Forbes, D.A.; Romanowsky, A.J.; Brodie, J.P.; Faifer, F.R.; Huxor, A.; Maraston, C.; Moffett, A.J.; Penny, S.J.; et al. The AIMSS Project - I. Bridging the star cluster-galaxy divide. *MNRAS* **2014**, *443*, 1151–1172, [arXiv:astro-ph.GA/1406.6065]. doi:10.1093/mnras/stu1186. 1977
1978
1979
224. Voggel, K.T.; Seth, A.C.; Sand, D.J.; Hughes, A.; Strader, J.; Crnojevic, D.; Caldwell, N. A Gaia-based Catalog of Candidate Stripped Nuclei and Luminous Globular Clusters in the Halo of Centaurus A. *ApJ* **2020**, *899*, 140, [arXiv:astro-ph.GA/2001.02243]. doi:10.3847/1538-4357/ab6f69. 1980
1981
1982
225. Ferrarese, L.; Côté, P.; Dalla Bontà, E.; Peng, E.W.; Merritt, D.; Jordán, A.; Blakeslee, J.P.; Hasegan, M.; Mei, S.; Piatek, S.; et al. A Fundamental Relation between Compact Stellar Nuclei, Supermassive Black Holes, and Their Host Galaxies. *ApJL* **2006**, *644*, L21–L24, [arXiv:astro-ph/astro-ph/0603840]. doi:10.1086/505388. 1983
1984
1985
226. Kormendy, J.; Ho, L.C. Coevolution (Or Not) of Supermassive Black Holes and Host Galaxies. *ARA&A* **2013**, *51*, 511–653, [arXiv:astro-ph.CO/1304.7762]. doi:10.1146/annurev-astro-082708-101811. 1986
1987
227. Loose, H.H.; Kruegel, E.; Tutukov, A. Bursts of star formation in the galactic centre. *A&A* **1982**, *105*, 342–350. 1988
228. Milosavljević, M.; Merritt, D. Formation of Galactic Nuclei. *ApJ* **2001**, *563*, 34–62, [arXiv:astro-ph/astro-ph/0103350]. doi:10.1086/323830. 1989
1990
229. Milosavljević, M. On the Origin of Nuclear Star Clusters in Late-Type Spiral Galaxies. *ApJL* **2004**, *605*, L13–L16, [arXiv:astro-ph/astro-ph/0310574]. doi:10.1086/420696. 1991
1992
230. Bekki, K.; Couch, W.J.; Shioya, Y. Dissipative Transformation of Nonnucleated Dwarf Galaxies into Nucleated Systems. *ApJL* **2006**, *642*, L133–L136, [arXiv:astro-ph/astro-ph/0604340]. doi:10.1086/504588. 1993
1994
231. Schinnerer, E.; Böker, T.; Emsellem, E.; Downes, D. Bar-driven mass build-up within the central 50 pc of NGC 6946. *A&A* **2007**, *462*, L27–L30, [arXiv:astro-ph/astro-ph/0701599]. doi:10.1051/0004-6361:20066711. 1995
1996
232. Bekki, K. The Formation of Stellar Galactic Nuclei through Dissipative Gas Dynamics. *PASA* **2007**, *24*, 77–94. doi:10.1071/AS07008. 1997
233. Nayakshin, S.; Wilkinson, M.I.; King, A. Competitive feedback in galaxy formation. *MNRAS* **2009**, *398*, L54–L57, [arXiv:astro-ph.CO/0907.1002]. doi:10.1111/j.1745-3933.2009.00709.x. 1998
1999
234. Emsellem, E.; Renaud, F.; Bournaud, F.; Elmegreen, B.; Combes, F.; Gabor, J.M. The interplay between a galactic bar and a supermassive black hole: nuclear fuelling in a subparsec resolution galaxy simulation. *MNRAS* **2015**, *446*, 2468–2482, [arXiv:astro-ph.GA/1410.6479]. doi:10.1093/mnras/stu2209. 2000
2001
2002
235. Antonini, F.; Barausse, E.; Silk, J. The Coevolution of Nuclear Star Clusters, Massive Black Holes, and Their Host Galaxies. *ApJ* **2015**, *812*, 72, [arXiv:astro-ph.GA/1506.02050]. doi:10.1088/0004-637X/812/1/72. 2003
2004
236. Brown, G.; Gnedin, O.Y.; Li, H. Nuclear Star Clusters in Cosmological Simulations. *ApJ* **2018**, *864*, 94, [arXiv:astro-ph.GA/1804.09819]. doi:10.3847/1538-4357/aad595. 2005
2006
237. Tremaine, S.D.; Ostriker, J.P.; Spitzer, L., J. The formation of the nuclei of galaxies. I. M31. *ApJ* **1975**, *196*, 407–411. doi:10.1086/153422. 2007
238. Capuzzo-Dolcetta, R. The Evolution of the Globular Cluster System in a Triaxial Galaxy: Can a Galactic Nucleus Form by Globular Cluster Capture? *ApJ* **1993**, *415*, 616, [arXiv:astro-ph/astro-ph/9301006]. doi:10.1086/173189. 2008
2009
239. Antonini, F.; Capuzzo-Dolcetta, R.; Mastrobuono-Battisti, A.; Merritt, D. Dissipationless Formation and Evolution of the Milky Way Nuclear Star Cluster. *ApJ* **2012**, *750*, 111, [arXiv:astro-ph.GA/1110.5937]. doi:10.1088/0004-637X/750/2/111. 2010
2011
240. Agarwal, M.; Milosavljević, M. Nuclear Star Clusters from Clustered Star Formation. *ApJ* **2011**, *729*, 35, [arXiv:astro-ph.CO/1008.2986]. doi:10.1088/0004-637X/729/1/35. 2012
2013
241. Antonini, F. Origin and Growth of Nuclear Star Clusters around Massive Black Holes. *ApJ* **2013**, *763*, 62, [arXiv:astro-ph.GA/1207.6589]. doi:10.1088/0004-637X/763/1/62. 2014
2015
242. Arca-Sedda, M.; Capuzzo-Dolcetta, R. The globular cluster migratory origin of nuclear star clusters. *MNRAS* **2014**, *444*, 3738–3755, [arXiv:astro-ph.GA/1405.7593]. doi:10.1093/mnras/stu1683. 2016
2017

243. Arca-Sedda, M.; Capuzzo-Dolcetta, R.; Antonini, F.; Seth, A. Henize 2-10: The Ongoing Formation of a Nuclear Star Cluster around a Massive Black Hole. *ApJ* **2015**, *806*, 220, [arXiv:astro-ph.GA/1501.04567]. doi:10.1088/0004-637X/806/2/220. 2018
2019
244. Tsatsi, A.; Mastrobuono-Battisti, A.; van de Ven, G.; Perets, H.B.; Bianchini, P.; Neumayer, N. On the rotation of nuclear star clusters formed by cluster inspirals. *MNRAS* **2017**, *464*, 3720–3727, [arXiv:astro-ph.GA/1610.01162]. doi:10.1093/mnras/stw2593. 2020
2021
245. Gnedin, O.Y.; Ostriker, J.P.; Tremaine, S. Co-evolution of Galactic Nuclei and Globular Cluster Systems. *ApJ* **2014**, *785*, 71, [arXiv:astro-ph.CO/1308.0021]. doi:10.1088/0004-637X/785/1/71. 2022
2023
246. Arca-Sedda, M.; Capuzzo-Dolcetta, R.; Spera, M. The dearth of nuclear star clusters in bright galaxies. *MNRAS* **2016**, *456*, 2457–2466, [arXiv:astro-ph.GA/1510.01137]. doi:10.1093/mnras/stv2835. 2024
2025
247. Fahrion, K.; Lyubenova, M.; van de Ven, G.; Hilker, M.; Leaman, R.; Falcón-Barroso, J.; Bittner, A.; Coccatto, L.; Corsini, E.M.; Gadotti, D.A.; et al. Diversity of nuclear star cluster formation mechanisms revealed by their star formation histories. *A&A* **2021**, *650*, A137, [arXiv:astro-ph.GA/2104.06412]. doi:10.1051/0004-6361/202140644. 2026
2027
2028
248. Fahrion, K.; Leaman, R.; Lyubenova, M.; van de Ven, G. Disentangling the formation mechanisms of nuclear star clusters. *A&A* **2022**, *658*, A172, [arXiv:astro-ph.GA/2112.05610]. doi:10.1051/0004-6361/202039778. 2029
2030
249. Fahrion, K.; Bulichi, T.E.; Hilker, M.; Leaman, R.; Lyubenova, M.; Müller, O.; Neumayer, N.; Pinna, F.; Rejkuba, M.; van de Ven, G. Nuclear star cluster formation in star-forming dwarf galaxies. *arXiv e-prints* **2022**, p. arXiv:2210.01556, [arXiv:astro-ph.GA/2210.01556]. 2031
2032
250. Bañados, E.; Venemans, B.P.; Mazzucchelli, C.; Farina, E.P.; Walter, F.; Wang, F.; Decarli, R.; Stern, D.; Fan, X.; Davies, F.B.; et al. An 800-million-solar-mass black hole in a significantly neutral Universe at a redshift of 7.5. *Nature* **2018**, *553*, 473–476, [arXiv:astro-ph.GA/1712.01860]. doi:10.1038/nature25180. 2033
2034
2035
251. Devecchi, B.; Volonteri, M.; Rossi, E.M.; Colpi, M.; Portegies Zwart, S. High-redshift formation and evolution of central massive objects - II. The census of BH seeds. *MNRAS* **2012**, *421*, 1465–1475, [arXiv:astro-ph.CO/1201.3761]. doi:10.1111/j.1365-2966.2012.20406.x. 2036
2037
252. Liu, B.; Bromm, V. Gravitational waves from the remnants of the first stars in nuclear star clusters. *MNRAS* **2021**, *506*, 5451–5467, [arXiv:astro-ph.GA/2106.02244]. doi:10.1093/mnras/stab2028. 2038
2039
253. Stone, N.C.; Küpper, A.H.W.; Ostriker, J.P. Formation of massive black holes in galactic nuclei: runaway tidal encounters. *MNRAS* **2017**, *467*, 4180–4199, [arXiv:astro-ph.GA/1606.01909]. doi:10.1093/mnras/stx097. 2040
2041
254. Kroupa, P. On the variation of the initial mass function. *MNRAS* **2001**, *322*, 231–246, [arXiv:astro-ph/astro-ph/0009005]. doi:10.1046/j.1365-8711.2001.04022.x. 2042
2043
255. Giacobbo, N.; Mapelli, M. Revising Natal Kick Prescriptions in Population Synthesis Simulations. *ApJ* **2020**, *891*, 141, [arXiv:astro-ph.HE/1909.06385]. doi:10.3847/1538-4357/ab7335. 2044
2045
256. Hobbs, G.; Lorimer, D.R.; Lyne, A.G.; Kramer, M. A statistical study of 233 pulsar proper motions. *MNRAS* **2005**, *360*, 974–992, [arXiv:astro-ph/astro-ph/0504584]. doi:10.1111/j.1365-2966.2005.09087.x. 2046
2047
257. Fryer, C.; Burrows, A.; Benz, W. Population Syntheses for Neutron Star Systems with Intrinsic Kicks. *ApJ* **1998**, *496*, 333–351, [arXiv:astro-ph/astro-ph/9710333]. doi:10.1086/305348. 2048
2049
258. Arzoumanian, Z.; Chernoff, D.F.; Cordes, J.M. The Velocity Distribution of Isolated Radio Pulsars. *ApJ* **2002**, *568*, 289–301, [arXiv:astro-ph/astro-ph/0106159]. doi:10.1086/338805. 2050
2051
259. Verbunt, F.; Igoshev, A.; Cator, E. The observed velocity distribution of young pulsars. *A&A* **2017**, *608*, A57, [arXiv:astro-ph.HE/1708.08281]. doi:10.1051/0004-6361/201731518. 2052
2053
260. Dessart, L.; Burrows, A.; Ott, C.D.; Livne, E.; Yoon, S.C.; Langer, N. Multidimensional Simulations of the Accretion-induced Collapse of White Dwarfs to Neutron Stars. *ApJ* **2006**, *644*, 1063–1084, [arXiv:astro-ph/astro-ph/0601603]. doi:10.1086/503626. 2054
2055
261. Giacobbo, N.; Mapelli, M. The impact of electron-capture supernovae on merging double neutron stars. *MNRAS* **2019**, *482*, 2234–2243, [arXiv:astro-ph.SR/1805.11100]. doi:10.1093/mnras/sty2848. 2056
2057
262. Ivanova, N.; Heinke, C.O.; Rasio, F.A.; Belczynski, K.; Fregeau, J.M. Formation and evolution of compact binaries in globular clusters - II. Binaries with neutron stars. *MNRAS* **2008**, *386*, 553–576, [arXiv:astro-ph/0706.4096]. doi:10.1111/j.1365-2966.2008.13064.x. 2058
2059
263. Arca-Sedda, M. On the formation of compact, massive subsystems in stellar clusters and its relation with intermediate-mass black holes. *MNRAS* **2016**, *455*, 35–50, [arXiv:astro-ph.GA/1502.01242]. doi:10.1093/mnras/stv2265. 2060
2061
264. Freitag, M.; Amaro-Seoane, P.; Kalogera, V. Stellar Remnants in Galactic Nuclei: Mass Segregation. *ApJ* **2006**, *649*, 91–117, [arXiv:astro-ph/astro-ph/0603280]. doi:10.1086/506193. 2062
2063
265. O’Leary, R.M.; Kocsis, B.; Loeb, A. Gravitational waves from scattering of stellar-mass black holes in galactic nuclei. *MNRAS* **2009**, *395*, 2127–2146, [arXiv:astro-ph/0807.2638]. doi:10.1111/j.1365-2966.2009.14653.x. 2064
2065
266. Keshet, U.; Hopman, C.; Alexander, T. Analytic Study of Mass Segregation Around a Massive Black Hole. *ApJL* **2009**, *698*, L64–L67, [arXiv:astro-ph.GA/0901.4343]. doi:10.1088/0004-637X/698/1/L64. 2066
2067
267. Faucher-Giguère, C.A.; Loeb, A. Pulsar-black hole binaries in the Galactic Centre. *MNRAS* **2011**, *415*, 3951–3961, [arXiv:astro-ph.HE/1012.0573]. doi:10.1111/j.1365-2966.2011.19019.x. 2068
2069
268. Arca-Sedda, M.; Capuzzo-Dolcetta, R. Dynamical Friction in Cuspy Galaxies. *ApJ* **2014**, *785*, 51, [arXiv:astro-ph.CO/1307.5717]. doi:10.1088/0004-637X/785/1/51. 2070
2071

269. Spitzer, Lyman, J.; Hart, M.H. Random Gravitational Encounters and the Evolution of Spherical Systems. II. Models. *ApJ* **1971**, *166*, 483. doi:10.1086/150977. 2072
2073
270. Chandrasekhar, S. Dynamical Friction. I. General Considerations: the Coefficient of Dynamical Friction. *ApJ* **1943**, *97*, 255. doi:10.1086/144517. 2074
2075
271. Breen, P.G.; Heggie, D.C. Dynamical evolution of black hole subsystems in idealized star clusters. *MNRAS* **2013**, *432*, 2779–2797, [arXiv:astro-ph.GA/1304.3401]. doi:10.1093/mnras/stt628. 2076
2077
272. Arca Sedda, M.; Askar, A.; Giersz, M. MOCCA-Survey Database - I. Unravelling black hole subsystems in globular clusters. *MNRAS* **2018**, *479*, 4652–4664, [arXiv:astro-ph.GA/1801.00795]. doi:10.1093/mnras/sty1859. 2078
2079
273. Portegies Zwart, S.F.; McMillan, S.L.W. The Runaway Growth of Intermediate-Mass Black Holes in Dense Star Clusters. *ApJ* **2002**, *576*, 899–907, [arXiv:astro-ph/astro-ph/0201055]. doi:10.1086/341798. 2080
2081
274. Giersz, M.; Leigh, N.; Hypki, A.; Lützgendorf, N.; Askar, A. MOCCA code for star cluster simulations - IV. A new scenario for intermediate mass black hole formation in globular clusters. *MNRAS* **2015**, *454*, 3150–3165, [arXiv:astro-ph.GA/1506.05234]. doi:10.1093/mnras/stv2162. 2082
2083
2084
275. Tagawa, H.; Haiman, Z.; Kocsis, B. Making a Supermassive Star by Stellar Bombardment. *ApJ* **2020**, *892*, 36, [arXiv:astro-ph.GA/1909.10517]. doi:10.3847/1538-4357/ab7922. 2085
2086
276. Marks, M.; Kroupa, P. Inverse dynamical population synthesis. Constraining the initial conditions of young stellar clusters by studying their binary populations. *A&A* **2012**, *543*, A8, [arXiv:astro-ph.GA/1205.1508]. doi:10.1051/0004-6361/201118231. 2087
2088
277. Arca Sedda, M. Birth, Life, and Death of Black Hole Binaries around Supermassive Black Holes: Dynamical Evolution of Gravitational Wave Sources. *ApJ* **2020**, *891*, 47, [arXiv:astro-ph.GA/2002.04037]. doi:10.3847/1538-4357/ab723b. 2089
2090
278. Janka, H.T. Explosion Mechanisms of Core-Collapse Supernovae. *Annual Review of Nuclear and Particle Science* **2012**, *62*, 407–451, [arXiv:astro-ph.SR/1206.2503]. doi:10.1146/annurev-nucl-102711-094901. 2091
2092
279. Giacobbo, N.; Mapelli, M.; Spera, M. Merging black hole binaries: the effects of progenitor’s metallicity, mass-loss rate and Eddington factor. *MNRAS* **2018**, *474*, 2959–2974, [arXiv:astro-ph.SR/1711.03556]. doi:10.1093/mnras/stx2933. 2093
2094
280. Baumgardt, H.; Amaro-Seoane, P.; Schödel, R. The distribution of stars around the Milky Way’s central black hole. III. Comparison with simulations. *A&A* **2018**, *609*, A28, [arXiv:astro-ph.GA/1701.03818]. doi:10.1051/0004-6361/201730462. 2095
2096
281. Panamarev, T.; Just, A.; Spurzem, R.; Berczik, P.; Wang, L.; Arca Sedda, M. Direct N-body simulation of the Galactic centre. *MNRAS* **2019**, *484*, 3279–3290, [arXiv:astro-ph.GA/1805.02153]. doi:10.1093/mnras/stz208. 2097
2098
282. Heggie, D.C. Binary evolution in stellar dynamics. *MNRAS* **1975**, *173*, 729–787. doi:10.1093/mnras/173.3.729. 2099
283. Hills, J.G. Encounters between binary and single stars and their effect on the dynamical evolution of stellar systems. *AJ* **1975**, *80*, 809–825. doi:10.1086/111815. 2100
2101
284. Heggie, D.C.; Hut, P. Binary–Single-Star Scattering. IV. Analytic Approximations and Fitting Formulae for Cross Sections and Reaction Rates. *ApJS* **1993**, *85*, 347. doi:10.1086/191768. 2102
2103
285. Rasio, F.A.; Heggie, D.C. The Orbital Eccentricities of Binary Millisecond Pulsars in Globular Clusters. *ApJL* **1995**, *445*, L133, [arXiv:astro-ph/astro-ph/9502105]. doi:10.1086/187907. 2104
2105
286. Heggie, D.C.; Rasio, F.A. The Effect of Encounters on the Eccentricity of Binaries in Clusters. *MNRAS* **1996**, *282*, 1064–1084, [arXiv:astro-ph/astro-ph/9506082]. doi:10.1093/mnras/282.3.1064. 2106
2107
287. Leigh, N.W.C.; Antonini, F.; Stone, N.C.; Shara, M.M.; Merritt, D. On the origins of enigmatic stellar populations in Local Group galactic nuclei. *MNRAS* **2016**, *463*, 1605–1623, [arXiv:astro-ph.GA/1608.02944]. doi:10.1093/mnras/stw2018. 2108
2109
288. Hamers, A.S.; Samsing, J. Analytic computation of the secular effects of encounters on a binary: features arising from second-order perturbation theory. *MNRAS* **2019**, *487*, 5630–5648, [arXiv:astro-ph.SR/1904.09624]. doi:10.1093/mnras/stz1646. 2110
2111
289. Alexander, T.; Pfuhl, O. Constraining the Dark Cusp in the Galactic Center by Long-period Binaries. *ApJ* **2014**, *780*, 148, [arXiv:astro-ph.GA/1308.6638]. doi:10.1088/0004-637X/780/2/148. 2112
2113
290. Fragione, G.; Loeb, A.; Kremer, K.; Rasio, F.A. Gravitational-wave Captures by Intermediate-mass Black Holes in Galactic Nuclei. *ApJ* **2020**, *897*, 46, [arXiv:astro-ph.GA/2002.02975]. doi:10.3847/1538-4357/ab94b2. 2114
2115
291. Hoang, B.M.; Naoz, S.; Kocsis, B.; Rasio, F.A.; Dosopoulou, F. Black Hole Mergers in Galactic Nuclei Induced by the Eccentric Kozai-Lidov Effect. *ApJ* **2018**, *856*, 140, [arXiv:astro-ph.HE/1706.09896]. doi:10.3847/1538-4357/aaafce. 2116
2117
292. Duquennoy, A.; Mayor, M. Multiplicity among Solar Type Stars in the Solar Neighbourhood - Part Two - Distribution of the Orbital Elements in an Unbiased Sample. *A&A* **1991**, *248*, 485. 2118
2119
293. Ghez, A.M.; Duchêne, G.; Matthews, K.; Hornstein, S.D.; Tanner, A.; Larkin, J.; Morris, M.; Becklin, E.E.; Salim, S.; Kremenek, T.; et al. The First Measurement of Spectral Lines in a Short-Period Star Bound to the Galaxy’s Central Black Hole: A Paradox of Youth. *ApJL* **2003**, *586*, L127–L131, [arXiv:astro-ph/astro-ph/0302299]. doi:10.1086/374804. 2120
2121
2122
294. Ghez, A.M.; Salim, S.; Hornstein, S.D.; Tanner, A.; Lu, J.R.; Morris, M.; Becklin, E.E.; Duchêne, G. Stellar Orbits around the Galactic Center Black Hole. *ApJ* **2005**, *620*, 744–757, [arXiv:astro-ph/astro-ph/0306130]. doi:10.1086/427175. 2123
2124

295. Do, T.; Lu, J.R.; Ghez, A.M.; Morris, M.R.; Yelda, S.; Martinez, G.D.; Wright, S.A.; Matthews, K. Stellar Populations in the Central 0.5 pc of the Galaxy. I. A New Method for Constructing Luminosity Functions and Surface-density Profiles. *ApJ* **2013**, *764*, 154, [arXiv:astro-ph.SR/1301.0539]. doi:10.1088/0004-637X/764/2/154. 2125
2126
296. Quinlan, G.D. The dynamical evolution of massive black hole binaries I. Hardening in a fixed stellar background. *New Astron.* **1996**, *1*, 35–56, [arXiv:astro-ph/astro-ph/9601092]. doi:10.1016/S1384-1076(96)00003-6. 2128
2129
297. Merritt, D. *Dynamics and Evolution of Galactic Nuclei*; Princeton University Press: Princeton, NJ, 2013. 2130
298. Alexander, T.; Hopman, C. Strong Mass Segregation Around a Massive Black Hole. *ApJ* **2009**, *697*, 1861–1869, [arXiv:astro-ph/0808.3150]. doi:10.1088/0004-637X/697/2/1861. 2131
2132
299. von Hoerner, S. Die numerische Integration des n-Körper-Problems für Sternhaufen. I. *Z. Astrophys.* **1960**, *50*, 184–214. 2133
300. van Albada, T.S. Numerical integrations of the N-body problem. *Bulletin of the Astronomical Institutes of the Netherlands* **1968**, *19*, 479. 2134
301. Aarseth, S.J.; Hills, J.G. The Dynamical Evolution of a Stellar Cluster with Initial Subclustering. *A&A* **1972**, *21*, 255. 2135
302. Retterer, J.M. The binding-energy distribution of the binaries in a star cluster. I - Time-independent, homogeneous cluster models. *AJ* **1980**, *85*, 249–264. doi:10.1086/112670. 2136
2137
303. Hut, P. The topology of three-body scattering. *AJ* **1983**, *88*, 1549–1559. doi:10.1086/113445. 2138
304. Goodman, J. Homologous evolution of stellar systems after core collapse. *ApJ* **1984**, *280*, 298–312. doi:10.1086/161996. 2139
305. Cohn, H.; Hut, P.; Wise, M. Gravothermal Oscillations after Core Collapse in Globular Cluster Evolution. *ApJ* **1989**, *342*, 814. doi:10.1086/167638. 2140
2141
306. Murphy, B.W.; Cohn, H.N.; Hut, P. Realistic models for evolving globular clusters - II. POST core collapse with a mass spectrum. *MNRAS* **1990**, *245*, 335. 2142
2143
307. Valtonen, M.; Mikkola, S. The few-body problem in astrophysics. *ARA&A* **1991**, *29*, 9–29. doi:10.1146/annurev.aa.29.090191.000301. 2144
308. Hut, P.; McMillan, S.; Goodman, J.; Mateo, M.; Phinney, E.S.; Pryor, C.; Richer, H.B.; Verbunt, F.; Weinberg, M. Binaries in Globular Clusters. *PASP* **1992**, *104*, 981. doi:10.1086/133085. 2145
2146
309. Lee, M.H. N-Body Evolution of Dense Clusters of Compact Stars. *ApJ* **1993**, *418*, 147. doi:10.1086/173378. 2147
310. Hoang, B.M.; Naoz, S.; Kremer, K. Neutron Star-Black Hole Mergers from Gravitational-wave Captures. *ApJ* **2020**, *903*, 8, [arXiv:astro-ph.HE/2007.08531]. doi:10.3847/1538-4357/abb66a. 2148
2149
311. Lee, H.M. Evolution of galactic nuclei with 10-M_⊙ black holes. *MNRAS* **1995**, *272*, 605–617, [arXiv:astro-ph/astro-ph/9409073]. doi:10.1093/mnras/272.3.605. 2150
2151
312. Quinlan, G.D.; Shapiro, S.L. The Collapse of Dense Star Clusters to Supermassive Black Holes: Binaries and Gravitational Radiation. *ApJ* **1987**, *321*, 199. doi:10.1086/165624. 2152
2153
313. Bahcall, J.N.; Wolf, R.A. Star distribution around a massive black hole in a globular cluster. *ApJ* **1976**, *209*, 214–232. doi:10.1086/154711. 2154
314. Lightman, A.P.; Shapiro, S.L. The distribution and consumption rate of stars around a massive, collapsed object. *ApJ* **1977**, *211*, 244–262. doi:10.1086/154925. 2155
2156
315. Cohn, H.; Kulsrud, R.M. The stellar distribution around a black hole: numerical integration of the Fokker-Planck equation. *ApJ* **1978**, *226*, 1087–1108. doi:10.1086/156685. 2157
2158
316. Duncan, M.J.; Shapiro, S.L. Monte Carlo simulations of the evolution of galactic nuclei containing massive, central black holes. *ApJ* **1983**, *268*, 565–581. doi:10.1086/160980. 2159
2160
317. Alexander, T. Stellar processes near the massive black hole in the Galactic center [review article]. *Phys. Rep.* **2005**, *419*, 65–142, [arXiv:astro-ph/astro-ph/0508106]. doi:10.1016/j.physrep.2005.08.002. 2161
2162
318. Preto, M.; Amaro-Seoane, P. On Strong Mass Segregation Around a Massive Black Hole: Implications for Lower-Frequency Gravitational-Wave Astrophysics. *ApJL* **2010**, *708*, L42–L46, [arXiv:astro-ph.GA/0910.3206]. doi:10.1088/2041-8205/708/1/L42. 2163
2164
319. Bahcall, J.N.; Wolf, R.A. The star distribution around a massive black hole in a globular cluster. II. Unequal star masses. *ApJ* **1977**, *216*, 883–907. doi:10.1086/155534. 2165
2166
320. Gürkan, M.A.; Freitag, M.; Rasio, F.A. Formation of Massive Black Holes in Dense Star Clusters. I. Mass Segregation and Core Collapse. *ApJ* **2004**, *604*, 632–652, [arXiv:astro-ph/astro-ph/0308449]. doi:10.1086/381968. 2167
2168
321. Trenti, M.; van der Marel, R. No energy equipartition in globular clusters. *MNRAS* **2013**, *435*, 3272–3282, [arXiv:astro-ph.GA/1302.2152]. doi:10.1093/mnras/stt1521. 2169
2170
322. Schödel, R.; Eckart, A.; Alexander, T.; Merritt, D.; Genzel, R.; Sternberg, A.; Meyer, L.; Kul, F.; Moulata, J.; Ott, T.; et al. The structure of the nuclear stellar cluster of the Milky Way. *A&A* **2007**, *469*, 125–146, [arXiv:astro-ph/astro-ph/0703178]. doi:10.1051/0004-6361:20065089. 2171
2172
2173
323. Dehnen, W. A Family of Potential-Density Pairs for Spherical Galaxies and Bulges. *MNRAS* **1993**, *265*, 250. doi:10.1093/mnras/265.1.250. 2174
324. Mikkola, S. Encounters of binaries. I - Equal energies. *MNRAS* **1983**, *203*, 1107–1121. doi:10.1093/mnras/203.4.1107. 2175
325. Trani, A.A.; Spera, M.; Leigh, N.W.C.; Fujii, M.S. The Keplerian Three-body Encounter. II. Comparisons with Isolated Encounters and Impact on Gravitational Wave Merger Timescales. *ApJ* **2019**, *885*, 135, [arXiv:astro-ph.GA/1904.07879]. doi:10.3847/1538-4357/ab480a. 2176
2177
326. Fragione, G.; Leigh, N.W.C.; Perna, R. Black hole and neutron star mergers in galactic nuclei: the role of triples. *MNRAS* **2019**, *488*, 2825–2835, [arXiv:astro-ph.GA/1903.09160]. doi:10.1093/mnras/stz180310.48550/arXiv.1903.09160. 2178
2179

327. Fishbach, M.; Holz, D.E. Where Are LIGO's Big Black Holes? *ApJL* **2017**, *851*, L25, [arXiv:astro-ph.HE/1709.08584]. doi:10.3847/2041-8213/aa9bf610.48550/arXiv.1709.08584. 2180
328. Sigurdsson, S.; Phinney, E.S. Binary–Single Star Interactions in Globular Clusters. *ApJ* **1993**, *415*, 631. doi:10.1086/173190. 2181
329. Hut, P.; Bahcall, J.N. Binary-single star scattering. I - Numerical experiments for equal masses. *ApJ* **1983**, *268*, 319–341. doi:10.1086/160956. 2182
330. Harrington, R.S. The Stellar Three-Body Problem. *Celestial Mechanics* **1969**, *1*, 200–209. doi:10.1007/BF01228839. 2183
331. Naoz, S.; Farr, W.M.; Lithwick, Y.; Rasio, F.A.; Teyssandier, J. Secular dynamics in hierarchical three-body systems. *MNRAS* **2013**, *431*, 2155–2171, [arXiv:astro-ph.EP/1107.2414]. doi:10.1093/mnras/stt302. 2184
332. Katz, B.; Dong, S.; Malhotra, R. Long-Term Cycling of Kozai-Lidov Cycles: Extreme Eccentricities and Inclinations Excited by a Distant Eccentric Perturber. *Phys. Rev. Lett.* **2011**, *107*, 181101, [arXiv:astro-ph.EP/1106.3340]. doi:10.1103/PhysRevLett.107.181101. 2185
333. Antognini, J.M.O. Timescales of Kozai-Lidov oscillations at quadrupole and octupole order in the test particle limit. *MNRAS* **2015**, *452*, 3610–3619, [arXiv:astro-ph.EP/1504.05957]. doi:10.1093/mnras/stv1552. 2186
334. Naoz, S.; Farr, W.M.; Lithwick, Y.; Rasio, F.A.; Teyssandier, J. Hot Jupiters from secular planet-planet interactions. *Nature* **2011**, *473*, 187–189, [arXiv:astro-ph.EP/1011.2501]. doi:10.1038/nature10076. 2187
335. Thompson, T.A. Accelerating Compact Object Mergers in Triple Systems with the Kozai Resonance: A Mechanism for “Prompt” Type Ia Supernovae, Gamma-Ray Bursts, and Other Exotica. *ApJ* **2011**, *741*, 82, [arXiv:astro-ph.HE/1011.4322]. doi:10.1088/0004-637X/741/2/82. 2188
336. Naoz, S.; Farr, W.M.; Rasio, F.A. On the Formation of Hot Jupiters in Stellar Binaries. *ApJL* **2012**, *754*, L36, [arXiv:astro-ph.EP/1206.3529]. doi:10.1088/2041-8205/754/2/L36. 2189
337. Shappee, B.J.; Thompson, T.A. The Mass-loss-induced Eccentric Kozai Mechanism: A New Channel for the Production of Close Compact Object-Stellar Binaries. *ApJ* **2013**, *766*, 64, [arXiv:astro-ph.SR/1204.1053]. doi:10.1088/0004-637X/766/1/64. 2190
338. Teyssandier, J.; Naoz, S.; Lizarraga, I.; Rasio, F.A. Extreme Orbital Evolution from Hierarchical Secular Coupling of Two Giant Planets. *ApJ* **2013**, *779*, 166, [arXiv:astro-ph.EP/1310.5048]. doi:10.1088/0004-637X/779/2/166. 2191
339. Prodan, S.; Antonini, F.; Perets, H.B. Secular Evolution of Binaries near Massive Black Holes: Formation of Compact Binaries, Merger/Collision Products and G2-like Objects. *ApJ* **2015**, *799*, 118, [arXiv:astro-ph.GA/1405.6029]. doi:10.1088/0004-637X/799/2/118. 2192
340. Naoz, S.; Fabrycky, D.C. Mergers and Obliquities in Stellar Triples. *ApJ* **2014**, *793*, 137, [arXiv:astro-ph.SR/1405.5223]. doi:10.1088/0004-637X/793/2/137. 2193
341. Li, G.; Naoz, S.; Kocsis, B.; Loeb, A. Implications of the eccentric Kozai-Lidov mechanism for stars surrounding supermassive black hole binaries. *MNRAS* **2015**, *451*, 1341–1349, [arXiv:astro-ph.GA/1502.03825]. doi:10.1093/mnras/stv1031. 2194
342. Stephan, A.P.; Naoz, S.; Gaudi, B.S. A-type Stars, the Destroyers of Worlds: The Lives and Deaths of Jupiters in Evolving Stellar Binaries. *AJ* **2018**, *156*, 128, [arXiv:astro-ph.SR/1806.04145]. doi:10.3847/1538-3881/aad6e5. 2195
343. Cheng, S.J.; Vinson, A.M.; Naoz, S. Interacting young M-dwarfs in triple system - Par 1802 binary system case study. *MNRAS* **2019**, *489*, 2298–2306, [arXiv:astro-ph.SR/1907.02542]. doi:10.1093/mnras/stz2360. 2196
344. Rose, S.C.; Naoz, S.; Geller, A.M. Companion-driven evolution of massive stellar binaries. *MNRAS* **2019**, *488*, 2480–2492, [arXiv:astro-ph.SR/1903.12185]. doi:10.1093/mnras/stz1846. 2197
345. Li, G.; Naoz, S.; Kocsis, B.; Loeb, A. Eccentricity Growth and Orbit Flip in Near-coplanar Hierarchical Three-body Systems. *ApJ* **2014**, *785*, 116, [arXiv:astro-ph.EP/1310.6044]. doi:10.1088/0004-637X/785/2/116. 2198
346. Li, G.; Naoz, S.; Holman, M.; Loeb, A. Chaos in the Test Particle Eccentric Kozai-Lidov Mechanism. *ApJ* **2014**, *791*, 86, [arXiv:astro-ph.EP/1405.0494]. doi:10.1088/0004-637X/791/2/86. 2199
347. Naoz, S.; Li, G.; Zanardi, M.; de Elía, G.C.; Di Sisto, R.P. The Eccentric Kozai-Lidov Mechanism for Outer Test Particle. *AJ* **2017**, *154*, 18, [arXiv:astro-ph.EP/1701.03795]. doi:10.3847/1538-3881/aa6fb0. 2200
348. Hansen, B.M.S.; Naoz, S. The stationary points of the hierarchical three-body problem. *MNRAS* **2020**, *499*, 1682–1700, [arXiv:astro-ph.EP/2011.07103]. doi:10.1093/mnras/staa2602. 2201
349. Fabrycky, D.; Tremaine, S. Shrinking Binary and Planetary Orbits by Kozai Cycles with Tidal Friction. *ApJ* **2007**, *669*, 1298–1315, [arXiv:astro-ph/0705.4285]. doi:10.1086/521702. 2202
350. Naoz, S.; Fabrycky, D.C. Mergers and Obliquities in Stellar Triples. *ArXiv e-prints* **2014**, [arXiv:astro-ph.SR/1405.5223]. 2203
351. Liu, B.; Muñoz, D.J.; Lai, D. Suppression of extreme orbital evolution in triple systems with short-range forces. *MNRAS* **2015**, *447*, 747–764, [arXiv:astro-ph.EP/1409.6717]. doi:10.1093/mnras/stu2396. 2204
352. Hut, P. Stability of tidal equilibrium. *A&A* **1980**, *92*, 167–170. 2205
353. Eggleton, P.P.; Kiseleva, L.G.; Hut, P. The Equilibrium Tide Model for Tidal Friction. *ApJ* **1998**, *499*, 853–+, [arXiv:astro-ph/9801246]. doi:10.1086/305670. 2206
354. Wu, Y. Diffusive Tidal Evolution for Migrating Hot Jupiters. *AJ* **2018**, *155*, 118, [arXiv:astro-ph.EP/1710.02542]. doi:10.3847/1538-3881/aaa970. 2207

355. Vick, M.; Lai, D.; Anderson, K.R. Chaotic tides in migrating gas giants: forming hot and transient warm Jupiters via Lidov-Kozai migration. *MNRAS* **2019**, *484*, 5645–5668, [arXiv:astro-ph.EP/1812.05618]. doi:10.1093/mnras/stz354. 2234
2235
356. Zahn, J.P. Tidal friction in close binary systems. *A&A* **1977**, *57*, 383–394. 2236
357. Claret, A.; Cunha, N.C.S. Circularization and synchronization times in Main-Sequence of detached eclipsing binaries II. Using the formalisms by Zahn. *A&A* **1997**, *318*, 187–197. 2237
2238
358. Wang, H.; Stephan, A.P.; Naoz, S.; Hoang, B.M.; Breivik, K. Gravitational-wave Signatures from Compact Object Binaries in the Galactic Center. *ApJ* **2021**, *917*, 76, [arXiv:astro-ph.HE/2010.15841]. doi:10.3847/1538-4357/ac088d. 2239
2240
359. Stegmann, J.; Antonini, F.; Moe, M. Evolution of massive stellar triples and implications for compact object binary formation. *arXiv e-prints* **2021**, p. arXiv:2112.10786, [arXiv:astro-ph.SR/2112.10786]. 2241
2242
360. Hopman, C. Binary Dynamics Near a Massive Black Hole. *ApJ* **2009**, *700*, 1933–1951, [arXiv:astro-ph.CO/0906.0374]. doi:10.1088/0004-637X/700/2/1933. 2243
2244
361. Antognini, J.M.; Shappee, B.J.; Thompson, T.A.; Amaro-Seoane, P. Rapid eccentricity oscillations and the mergers of compact objects in hierarchical triples. *MNRAS* **2014**, *439*, 1079–1091, [arXiv:astro-ph.HE/1308.5682]. doi:10.1093/mnras/stu039. 2245
2246
362. Ciurlo, A.; Campbell, R.D.; Morris, M.R.; Do, T.; Ghez, A.M.; Hees, A.; Sitarski, B.N.; Kosmo O’Neil, K.; Chu, D.S.; Martinez, G.D.; et al. A population of dust-enshrouded objects orbiting the Galactic black hole. *Nature* **2020**, *577*, 337–340, [arXiv:astro-ph.GA/2001.08325]. doi:10.1038/s41586-019-1883-y. 2247
2248
2249
363. Perets, H.B.; Kratter, K.M. The triple evolution dynamical instability: Stellar collisions in the field and the formation of exotic binaries. *ArXiv e-prints* **2012**, [arXiv:astro-ph.SR/1203.2914]. 2250
2251
364. Michaely, E.; Perets, H.B. Secular Dynamics in Hierarchical Three-body Systems with Mass Loss and Mass Transfer. *ApJ* **2014**, *794*, 122, [arXiv:astro-ph.SR/1406.3035]. doi:10.1088/0004-637X/794/2/122. 2252
2253
365. Toonen, S.; Hamers, A.; Portegies Zwart, S. The evolution of hierarchical triple star-systems. *Computational Astrophysics and Cosmology* **2016**, *3*, 6, [arXiv:astro-ph.SR/1612.06172]. doi:10.1186/s40668-016-0019-0. 2254
2255
366. Toonen, S.; Perets, H.B.; Hamers, A.S. Rate of WD-WD head-on collisions in isolated triples is too low to explain standard type Ia supernovae. *A&A* **2018**, *610*, A22, [arXiv:astro-ph.HE/1709.00422]. doi:10.1051/0004-6361/201731874. 2256
2257
367. Stephan, A.P.; Naoz, S.; Zuckerman, B. Throwing Icebergs at White Dwarfs. *ArXiv e-prints* **2017**, [arXiv:astro-ph.SR/1704.08701]. 2258
368. Paxton, B.; Bildsten, L.; Dotter, A.; Herwig, F.; Lesaffre, P.; Timmes, F. Modules for Experiments in Stellar Astrophysics (MESA). *ApJS* **2011**, *192*, 3, [arXiv:astro-ph.SR/1009.1622]. doi:10.1088/0067-0049/192/1/3. 2259
2260
369. Breivik, K.; Coughlin, S.; Zevin, M.; Rodriguez, C.L.; Kremer, K.; Ye, C.S.; Andrews, J.J.; Kurkowski, M.; Digman, M.C.; Larson, S.L.; et al. COSMIC Variance in Binary Population Synthesis. *ApJ* **2020**, *898*, 71, [arXiv:astro-ph.HE/1911.00903]. doi:10.3847/1538-4357/ab9d85. 2261
2262
2263
370. Hansen, B.M.S.; Phinney, E.S. The pulsar kick velocity distribution. *MNRAS* **1997**, *291*, 569, [astro-ph/9708071]. doi:10.1093/mnras/291.3.569. 2264
371. Hobbs, G.; Lyne, A.G.; Kramer, M.; Martin, C.E.; Jordan, C. Long-term timing observations of 374 pulsars. *MNRAS* **2004**, *353*, 1311–1344. doi:10.1111/j.1365-2966.2004.08157.x. 2265
2266
372. Kalogera, V. Spin-Orbit Misalignment in Close Binaries with Two Compact Objects. *ApJ* **2000**, *541*, 319–328, [arXiv:astro-ph/9911417]. doi:10.1086/309400. 2267
2268
373. Pijloo, J.T.; Caputo, D.P.; Portegies Zwart, S.F. Asymmetric supernova in hierarchical multiple star systems and application to J1903+0327. *MNRAS* **2012**, *424*, 2914–2925, [1207.0009]. doi:10.1111/j.1365-2966.2012.21431.x. 2269
2270
374. Lu, C.X.; Naoz, S. Supernovae kicks in hierarchical triple systems. *MNRAS* **2019**, *484*, 1506–1525, [arXiv:astro-ph.SR/1805.06897]. doi:10.1093/mnras/stz036. 2271
2272
375. Hamers, A.S. Secular dynamics of hierarchical multiple systems composed of nested binaries, with an arbitrary number of bodies and arbitrary hierarchical structure - II. External perturbations: flybys and supernovae. *MNRAS* **2018**, *476*, 4139–4161, [arXiv:astro-ph.SR/1802.05716]. doi:10.1093/mnras/sty428. 2273
2274
2275
376. Bortolas, E.; Mapelli, M.; Spera, M. Supernova kicks and dynamics of compact remnants in the Galactic Centre. *MNRAS* **2017**, *469*, 1510–1520, [1704.05850]. doi:10.1093/mnras/stx930. 2276
2277
377. Hoang, B.M.; Naoz, S.; Sloneker, M. Binary Natal Kicks in the Galactic Center: X-Ray Binaries, Hypervelocity Stars, and Gravitational Waves. *ApJ* **2022**, *934*, 54, [arXiv:astro-ph.HE/2204.03661]. doi:10.3847/1538-4357/ac7787. 2278
2279
378. Antonini, F.; Perets, H.B. Secular Evolution of Compact Binaries near Massive Black Holes: Gravitational Wave Sources and Other Exotica. *ApJ* **2012**, *757*, 27, [arXiv:astro-ph.GA/1203.2938]. doi:10.1088/0004-637X/757/1/27. 2280
2281
379. Will, C.M. Post-Newtonian effects in N-body dynamics: conserved quantities in hierarchical triple systems. *Classical and Quantum Gravity* **2014**, *31*, 244001, [arXiv:astro-ph.GA/1404.7724]. doi:10.1088/0264-9381/31/24/244001. 2282
2283
380. Lim, H.; Rodriguez, C.L. Relativistic three-body effects in hierarchical triples. *Phys. Rev. D* **2020**, *102*, 064033, [arXiv:astro-ph.HE/2001.03654]. doi:10.1103/PhysRevD.102.064033. 2284
2285
381. Will, C.M. Orbital flips in hierarchical triple systems: Relativistic effects and third-body effects to hexadecapole order. *Phys. Rev. D* **2017**, *96*, 023017, [arXiv:astro-ph.EP/1705.03962]. doi:10.1103/PhysRevD.96.023017. 2286
2287

382. Barker, B.M.; O'Connell, R.F. Gravitational two-body problem with arbitrary masses, spins, and quadrupole moments. *Phys. Rev. D* **1975**, *12*, 329–335. doi:10.1103/PhysRevD.12.329. 2288
2289
383. Storch, N.I.; Anderson, K.R.; Lai, D. Chaotic dynamics of stellar spin in binaries and the production of misaligned hot Jupiters. *Science* **2014**, *345*, 1317–1321, [arXiv:astro-ph.EP/1409.3247]. doi:10.1126/science.1254358. 2290
2291
384. Storch, N.I.; Lai, D. Chaotic dynamics of stellar spin driven by planets undergoing Lidov-Kozai oscillations: resonances and origin of chaos. *MNRAS* **2015**, *448*, 1821–1834, [arXiv:astro-ph.EP/1411.0739]. doi:10.1093/mnras/stv119. 2292
2293
385. Liu, B.; Lai, D.; Wang, Y.H. Binary Mergers near a Supermassive Black Hole: Relativistic Effects in Triples. *ApJL* **2019**, *883*, L7, [arXiv:astro-ph.HE/1906.07726]. doi:10.3847/2041-8213/ab40c0. 2294
2295
386. Peters, P.C. Gravitational Radiation and the Motion of Two Point Masses. *Physical Review* **1964**, *136*, 1224–1232. doi:10.1103/PhysRev.136.1224. 2296
387. Gould, A. Gravitational Pulse Astronomy. *ApJL* **2011**, *729*, L23, [arXiv:astro-ph.SR/1011.4518]. doi:10.1088/2041-8205/729/2/L23. 2297
388. Seto, N. Highly Eccentric Kozai Mechanism and Gravitational-Wave Observation for Neutron-Star Binaries. *Physical Review Letters* **2013**, *111*, 061106, [arXiv:astro-ph.CO/1304.5151]. doi:10.1103/PhysRevLett.111.061106. 2298
2299
389. Rauch, K.P.; Tremaine, S. Resonant relaxation in stellar systems. *New Astron.* **1996**, *1*, 149–170, [arXiv:astro-ph/astro-ph/9603018]. doi:10.1016/S1384-1076(96)00012-7. 2300
2301
390. Madigan, A.M.; Levin, Y.; Hopman, C. A New Secular Instability of Eccentric Stellar Disks around Supermassive Black Holes, with Application to the Galactic Center. *ApJL* **2009**, *697*, L44–L48, [arXiv:astro-ph/0812.3395]. doi:10.1088/0004-637X/697/1/L44. 2302
2303
391. Kocsis, B.; Tremaine, S. A numerical study of vector resonant relaxation. *MNRAS* **2015**, *448*, 3265–3296, [arXiv:astro-ph.GA/1406.1178]. doi:10.1093/mnras/stv057. 2304
2305
392. Petrovich, C.; Antonini, F. Greatly Enhanced Merger Rates of Compact-object Binaries in Non-spherical Nuclear Star Clusters. *ApJ* **2017**, *846*, 146, [arXiv:astro-ph.HE/1705.05848]. doi:10.3847/1538-4357/aa8628. 2306
2307
393. Hopman, C.; Alexander, T. Resonant Relaxation near a Massive Black Hole: The Stellar Distribution and Gravitational Wave Sources. *ApJ* **2006**, *645*, 1152–1163, [arXiv:astro-ph/astro-ph/0601161]. doi:10.1086/504400. 2308
2309
394. Kocsis, B.; Tremaine, S. Resonant relaxation and the warp of the stellar disc in the Galactic Centre. *MNRAS* **2011**, *412*, 187–207, [arXiv:astro-ph.GA/1006.0001]. doi:10.1111/j.1365-2966.2010.17897.x. 2310
2311
395. Bar-Or, B.; Alexander, T. The statistical mechanics of relativistic orbits around a massive black hole. *Classical and Quantum Gravity* **2014**, *31*, 244003, [arXiv:astro-ph.GA/1404.0351]. doi:10.1088/0264-9381/31/24/244003. 2312
2313
396. Sridhar, S.; Touma, J.R. Stellar dynamics around a massive black hole - II. Resonant relaxation. *MNRAS* **2016**, *458*, 4143–4161, [arXiv:astro-ph.GA/1509.02401]. doi:10.1093/mnras/stw543. 2314
2315
397. Fouvry, J.B.; Pichon, C.; Magorrian, J. The secular evolution of discrete quasi-Keplerian systems. I. Kinetic theory of stellar clusters near black holes. *A&A* **2017**, *598*, A71, [arXiv:astro-ph.GA/1606.05501]. doi:10.1051/0004-6361/201629138. 2316
2317
398. Bar-Or, B.; Fouvry, J.B. Scalar Resonant Relaxation of Stars around a Massive Black Hole. *ApJL* **2018**, *860*, L23, [arXiv:astro-ph.GA/1802.08890]. doi:10.3847/2041-8213/aac88e. 2318
2319
399. Fragione, G.; Grishin, E.; Leigh, N.W.C.; Perets, H.B.; Perna, R. Black hole and neutron star mergers in galactic nuclei. *MNRAS* **2019**, *488*, 47–63, [arXiv:astro-ph.GA/1811.10627]. doi:10.1093/mnras/stz1651. 2320
2321
400. Hamers, A.S.; Bar-Or, B.; Petrovich, C.; Antonini, F. The Impact of Vector Resonant Relaxation on the Evolution of Binaries near a Massive Black Hole: Implications for Gravitational-wave Sources. *ApJ* **2018**, *865*, 2, [arXiv:astro-ph.HE/1805.10313]. doi:10.3847/1538-4357/aadae2. 2322
2323
2324
401. Genzel, R.; Schödel, R.; Ott, T.; Eisenhauer, F.; Hofmann, R.; Lehnert, M.; Eckart, A.; Alexander, T.; Sternberg, A.; Lenzen, R.; et al. The Stellar Cusp around the Supermassive Black Hole in the Galactic Center. *ApJ* **2003**, *594*, 812–832, [arXiv:astro-ph/astro-ph/0305423]. doi:10.1086/377127. 2325
2326
2327
402. Schödel, R.; Ott, T.; Genzel, R.; Eckart, A.; Mouawad, N.; Alexander, T. Stellar Dynamics in the Central Arcsecond of Our Galaxy. *ApJ* **2003**, *596*, 1015–1034, [arXiv:astro-ph/astro-ph/0306214]. doi:10.1086/378122. 2328
2329
403. Löckmann, U.; Baumgardt, H.; Kroupa, P. Constraining the initial mass function of stars in the Galactic Centre. *MNRAS* **2010**, *402*, 519–525, [arXiv:astro-ph.GA/0910.4960]. doi:10.1111/j.1365-2966.2009.15906.x. 2330
2331
404. Shakura, N.I.; Sunyaev, R.A. Black holes in binary systems. Observational appearance. *A&A* **1973**, *24*, 337–355. 2332
405. Novikov, I.D.; Thorne, K.S. Astrophysics of black holes. *Black Holes (Les Astres Occlus)*, 1973, pp. 343–450. 2333
406. Artymowicz, P.; Lin, D.N.C.; Wampller, E.J. Star Trapping and Metallicity Enrichment in Quasars and Active Galactic Nuclei. *ApJ* **1993**, *409*, 592. doi:10.1086/172690. 2334
2335
407. Rauch, K.P. Dynamical evolution of star clusters around a rotating black hole with an accretion disc. *MNRAS* **1995**, *275*, 628–640. doi:10.1093/mnras/275.3.628. 2336
2337
408. Rauch, K.P. Collisional Stellar Dynamics around Massive Black Holes in Active Galactic Nuclei. *ApJ* **1999**, *514*, 725–745. doi:10.1086/306953. 2338
2339
409. Šubr, L.; Karas, V.; Huré, J.M. Star-disc interactions in a galactic centre and oblateness of the inner stellar cluster. *MNRAS* **2004**, *354*, 1177–1188, [arXiv:astro-ph/astro-ph/0408053]. doi:10.1111/j.1365-2966.2004.08276.x. 2340
2341

410. Vilkoviskij, E.Y.; Czerny, B. The role of the central stellar cluster in active galactic nuclei. I. Semi-analytical model. *A&A* **2002**, *387*, 804–817, [arXiv:astro-ph/astro-ph/0203226]. doi:10.1051/0004-6361:20020255. 2342
411. Just, A.; Yurin, D.; Makukov, M.; Berczik, P.; Omarov, C.; Spurzem, R.; Vilkoviskij, E.Y. Enhanced Accretion Rates of Stars on Supermassive Black Holes by Star-Disk Interactions in Galactic Nuclei. *ApJ* **2012**, *758*, 51, [arXiv:astro-ph.CO/1208.4954]. doi:10.1088/0004-637X/758/1/51. 2344
412. Tagawa, H.; Kimura, S.S.; Haiman, Z.; Perna, R.; Tanaka, H.; Bartos, I. Can Stellar-mass Black Hole Growth Disrupt Disks of Active Galactic Nuclei? The Role of Mechanical Feedback. *ApJ* **2022**, *927*, 41, [arXiv:astro-ph.HE/2112.01544]. doi:10.3847/1538-4357/ac45f8. 2346
413. Papaloizou, J.C.B.; Larwood, J.D. On the orbital evolution and growth of protoplanets embedded in a gaseous disc. *MNRAS* **2000**, *315*, 823–833, [arXiv:astro-ph/astro-ph/9911431]. doi:10.1046/j.1365-8711.2000.03466.x. 2348
414. Goldreich, P.; Tremaine, S. Disk-satellite interactions. *ApJ* **1980**, *241*, 425–441. doi:10.1086/158356. 2349
415. Ward, W.R. Protoplanet Migration by Nebula Tides. *Icarus* **1997**, *126*, 261–281. doi:10.1006/icar.1996.5647. 2350
416. Tanaka, H.; Takeuchi, T.; Ward, W.R. Three-Dimensional Interaction between a Planet and an Isothermal Gaseous Disk. I. Corotation and Lindblad Torques and Planet Migration. *ApJ* **2002**, *565*, 1257–1274. doi:10.1086/324713. 2351
417. Lin, D.N.C.; Papaloizou, J. On the Tidal Interaction between Protoplanets and the Protoplanetary Disk. III. Orbital Migration of Protoplanets. *ApJ* **1986**, *309*, 846. doi:10.1086/164653. 2352
418. Haiman, Z.; Kocsis, B.; Menou, K. The Population of Viscosity- and Gravitational Wave-driven Supermassive Black Hole Binaries Among Luminous Active Galactic Nuclei. *ApJ* **2009**, *700*, 1952–1969, [arXiv:astro-ph.CO/0904.1383]. doi:10.1088/0004-637X/700/2/1952. 2353
419. Duffell, P.C.; Haiman, Z.; MacFadyen, A.I.; D’Orazio, D.J.; Farris, B.D. The Migration of Gap-opening Planets is Not Locked to Viscous Disk Evolution. *ApJL* **2014**, *792*, L10, [arXiv:astro-ph.EP/1405.3711]. doi:10.1088/2041-8205/792/1/L10. 2354
420. Kanagawa, K.D.; Tanaka, H.; Szuszkiewicz, E. Radial Migration of Gap-opening Planets in Protoplanetary Disks. I. The Case of a Single Planet. *ApJ* **2018**, *861*, 140, [arXiv:astro-ph.EP/1805.11101]. doi:10.3847/1538-4357/aac8d9. 2355
421. Paardekooper, S.J.; Mellema, G. Halting type I planet migration in non-isothermal disks. *A&A* **2006**, *459*, L17–L20, [arXiv:astro-ph/astro-ph/0608658]. doi:10.1051/0004-6361:20066304. 2356
422. Pepliński, A.; Artymowicz, P.; Mellema, G. Numerical simulations of type III planetary migration - I. Disc model and convergence tests. *MNRAS* **2008**, *386*, 164–178, [arXiv:astro-ph/0709.3622]. doi:10.1111/j.1365-2966.2008.13045.x. 2357
423. Lyra, W.; Paardekooper, S.J.; Mac Low, M.M. Orbital Migration of Low-mass Planets in Evolutionary Radiative Models: Avoiding Catastrophic Infall. *ApJL* **2010**, *715*, L68–L73, [arXiv:astro-ph.EP/1003.0925]. doi:10.1088/2041-8205/715/2/L68. 2358
424. Horn, B.; Lyra, W.; Mac Low, M.M.; Sándor, Z. Orbital Migration of Interacting Low-mass Planets in Evolutionary Radiative Turbulent Models. *ApJ* **2012**, *750*, 34, [arXiv:astro-ph.EP/1202.1868]. doi:10.1088/0004-637X/750/1/34. 2359
425. Paardekooper, S.J.; Baruteau, C.; Kley, W. A torque formula for non-isothermal Type I planetary migration - II. Effects of diffusion. *MNRAS* **2011**, *410*, 293–303, [arXiv:astro-ph.EP/1007.4964]. doi:10.1111/j.1365-2966.2010.17442.x. 2360
426. Hellary, P.; Nelson, R.P. Global models of planetary system formation in radiatively-inefficient protoplanetary discs. *MNRAS* **2012**, *419*, 2737–2757, [arXiv:astro-ph.EP/1112.2997]. doi:10.1111/j.1365-2966.2011.19815.x. 2361
427. Coleman, G.A.L.; Nelson, R.P. On the formation of planetary systems via oligarchic growth in thermally evolving viscous discs. *MNRAS* **2014**, *445*, 479–499, [arXiv:astro-ph.EP/1408.6993]. doi:10.1093/mnras/stu1715. 2362
428. Dittkrist, K.M.; Mordasini, C.; Klahr, H.; Alibert, Y.; Henning, T. Impacts of planet migration models on planetary populations. Effects of saturation, cooling and stellar irradiation. *A&A* **2014**, *567*, A121, [arXiv:astro-ph.EP/1402.5969]. doi:10.1051/0004-6361/201322506. 2363
429. Paardekooper, S.J. Dynamical corotation torques on low-mass planets. *MNRAS* **2014**, *444*, 2031–2042, [arXiv:astro-ph.EP/1409.0372]. doi:10.1093/mnras/stu1542. 2364
430. Pierens, A. Fast migration of low-mass planets in radiative discs. *MNRAS* **2015**, *454*, 2003–2014, [arXiv:astro-ph.EP/1508.07817]. doi:10.1093/mnras/stv2024. 2365
431. Benítez-Llambay, P.; Masset, F.; Koenigsberger, G.; Szulágyi, J. Planet heating prevents inward migration of planetary cores. *Nature* **2015**, *520*, 63–65, [arXiv:astro-ph.EP/1510.01778]. doi:10.1038/nature14277. 2366
432. Masset, F.S. Coorbital thermal torques on low-mass protoplanets. *MNRAS* **2017**, *472*, 4204–4219, [arXiv:astro-ph.EP/1708.09807]. doi:10.1093/mnras/stx2271. 2367
433. Eklund, H.; Masset, F.S. Evolution of eccentricity and inclination of hot protoplanets embedded in radiative discs. *MNRAS* **2017**, *469*, 206–217, [arXiv:astro-ph.EP/1704.01931]. doi:10.1093/mnras/stx856. 2368
434. Secunda, A.; Bellovary, J.; Mac Low, M.M.; Ford, K.E.S.; McKernan, B.; Leigh, N.W.C.; Lyra, W.; Sándor, Z. Orbital Migration of Interacting Stellar Mass Black Holes in Disks around Supermassive Black Holes. *ApJ* **2019**, *878*, 85, [arXiv:astro-ph.HE/1807.02859]. doi:10.3847/1538-4357/ab20ca. 2369
435. Pan, Z.; Yang, H. Formation rate of extreme mass ratio inspirals in active galactic nuclei. *Phys. Rev. D* **2021**, *103*, 103018, [arXiv:astro-ph.HE/2101.09146]. doi:10.1103/PhysRevD.103.103018. 2370
436. Goldreich, P.; Lithwick, Y.; Sari, R. Formation of Kuiper-belt binaries by dynamical friction and three-body encounters. *Nature* **2002**, *420*, 643–646, [arXiv:astro-ph/astro-ph/0208490]. doi:10.1038/nature01227. 2371

437. McKernan, B.; Ford, K.E.S.; Kocsis, B.; Lyra, W.; Winter, L.M. Intermediate-mass black holes in AGN discs - II. Model predictions and observational constraints. *MNRAS* **2014**, *441*, 900–909, [arXiv:astro-ph.GA/1403.6433]. doi:10.1093/mnras/stu553. 2397
2398
438. Tagawa, H.; Kocsis, B.; Haiman, Z.; Bartos, I.; Omukai, K.; Samsing, J. Eccentric Black Hole Mergers in Active Galactic Nuclei. *ApJL* **2021**, *907*, L20, [arXiv:astro-ph.HE/2010.10526]. doi:10.3847/2041-8213/abd4d3. 2399
2400
439. Tiede, C.; Zrake, J.; MacFadyen, A.; Haiman, Z. Gas-driven Inspiral of Binaries in Thin Accretion Disks. *ApJ* **2020**, *900*, 43, [arXiv:astro-ph.GA/2005.09555]. doi:10.3847/1538-4357/aba432. 2401
2402
440. Stone, N.C.; Metzger, B.D.; Haiman, Z. Assisted inspirals of stellar mass black holes embedded in AGN discs: solving the ‘final au problem’. *MNRAS* **2017**, *464*, 946–954, [arXiv:astro-ph.GA/1602.04226]. doi:10.1093/mnras/stw2260. 2403
2404
441. Duffell, P.C.; D’Orazio, D.; Derdzinski, A.; Haiman, Z.; MacFadyen, A.; Rosen, A.L.; Zrake, J. Circumbinary Disks: Accretion and Torque as a Function of Mass Ratio and Disk Viscosity. *ApJ* **2020**, *901*, 25, [arXiv:astro-ph.SR/1911.05506]. doi:10.3847/1538-4357/abab95. 2405
2406
2407
442. Wen, L. On the Eccentricity Distribution of Coalescing Black Hole Binaries Driven by the Kozai Mechanism in Globular Clusters. *ApJ* **2003**, *598*, 419–430, [arXiv:astro-ph/astro-ph/0211492]. doi:10.1086/378794. 2408
2409
443. Sesana, A. Prospects for Multiband Gravitational-Wave Astronomy after GW150914. *Phys. Rev. Lett.* **2016**, *116*, 231102, [arXiv:gr-qc/1602.06951]. doi:10.1103/PhysRevLett.116.231102. 2410
2411
444. Amaro-Seoane, P.; Aoudia, S.; Babak, S.; Binétruy, P.; Berti, E.; Bohé, A.; Caprini, C.; Colpi, M.; Cornish, N.J.; Danzmann, K.; et al. eLISA: Astrophysics and cosmology in the millihertz regime. *GW Notes* **2013**, *6*, 4–110, [arXiv:astro-ph.CO/1201.3621]. 2412
2413
445. Amaro-Seoane, P.; Audley, H.; Babak, S.; Baker, J.; Barausse, E.; Bender, P.; Berti, E.; Binétruy, P.; Born, M.; Bortoluzzi, D.; et al. Laser Interferometer Space Antenna. *arXiv e-prints* **2017**, p. arXiv:1702.00786, [arXiv:astro-ph.IM/1702.00786]. 2414
2415
446. Amaro-Seoane, P.; Andrews, J.; Arca Sedda, M.; Askar, A.; Balasov, R.; Bartos, I.; Bavera, S.S.; Bellovary, J.; Berry, C.P.L.; Berti, E.; et al. Astrophysics with the Laser Interferometer Space Antenna. *arXiv e-prints* **2022**, p. arXiv:2203.06016, [arXiv:gr-qc/2203.06016]. 2416
2417
447. Luo, J.; Chen, L.S.; Duan, H.Z.; Gong, Y.G.; Hu, S.; Ji, J.; Liu, Q.; Mei, J.; Milyukov, V.; Sazhin, M.; et al. TianQin: a space-borne gravitational wave detector. *Classical and Quantum Gravity* **2016**, *33*, 035010, [arXiv:astro-ph.IM/1512.02076]. doi:10.1088/0264-9381/33/3/035010. 2418
2419
2420
448. Luo, Z.; Wang, Y.; Wu, Y.; Hu, W.; Jin, G. The Taiji program: A concise overview. *Progress of Theoretical and Experimental Physics* **2021**, *2021*, 05A108. doi:10.1093/ptep/ptaa083. 2421
2422
449. Gong, Y.; Luo, J.; Wang, B. Concepts and status of Chinese space gravitational wave detection projects. *Nature Astronomy* **2021**, *5*, 881–889, [arXiv:astro-ph.IM/2109.07442]. doi:10.1038/s41550-021-01480-3. 2423
2424
450. Bender, P.L.; Begelman, M.C.; Gair, J.R. Possible LISA follow-on mission scientific objectives. *Classical and Quantum Gravity* **2013**, *30*, 165017. doi:10.1088/0264-9381/30/16/165017. 2425
2426
451. Kawamura, S.; Ando, M.; Seto, N.; Sato, S.; Nakamura, T.; Tsubono, K.; Kanda, N.; Tanaka, T.; Yokoyama, J.; Funaki, I.; et al. The Japanese space gravitational wave antenna: DECIGO. *Classical and Quantum Gravity* **2011**, *28*, 094011. doi:10.1088/0264-9381/28/9/094011. 2427
2428
2429
452. Kawamura, S.; Ando, M.; Seto, N.; Sato, S.; Musha, M.; Kawano, I.; Yokoyama, J.; Tanaka, T.; Ioka, K.; Akutsu, T.; et al. Current status of space gravitational wave antenna DECIGO and B-DECIGO. *Progress of Theoretical and Experimental Physics* **2021**, *2021*, 05A105, [arXiv:gr-qc/2006.13545]. doi:10.1093/ptep/ptab019. 2430
2431
2432
453. Arca Sedda, M.; Berry, C.P.L.; Jani, K.; Amaro-Seoane, P.; Auclair, P.; Baird, J.; Baker, T.; Berti, E.; Breivik, K.; Burrows, A.; et al. The missing link in gravitational-wave astronomy: discoveries waiting in the decihertz range. *Classical and Quantum Gravity* **2020**, *37*, 215011, [arXiv:gr-qc/1908.11375]. doi:10.1088/1361-6382/abb5c1. 2433
2434
2435
454. Jani, K.; Loeb, A. Gravitational-Wave Lunar Observatory for Cosmology. *arXiv e-prints* **2020**, p. arXiv:2007.08550, [arXiv:gr-qc/2007.08550]. 2436
2437
455. Harms, J.; Ambrosino, F.; Angelini, L.; Braitto, V.; Branchesi, M.; Brocato, E.; Cappellaro, E.; Coccia, E.; Coughlin, M.; Della Ceca, R.; et al. Lunar Gravitational-wave Antenna. *ApJ* **2021**, *910*, 1, [arXiv:gr-qc/2010.13726]. doi:10.3847/1538-4357/abe5a7. 2438
2439
456. Acernese, F.; Agathos, M.; Agatsuma, K.; Aisa, D.; Allemandou, N.; Allocca, A.; Amarni, J.; Astone, P.; Balestri, G.; Ballardin, G.; et al. Advanced Virgo: a second-generation interferometric gravitational wave detector. *Classical and Quantum Gravity* **2015**, *32*, 024001, [arXiv:gr-qc/1408.3978]. doi:10.1088/0264-9381/32/2/024001. 2440
2441
2442
457. Abbott, B.P.; Abbott, R.; Abbott, T.D.; Abernathy, M.R.; Acernese, F.; Ackley, K.; Adams, C.; Adams, T.; Addesso, P.; Adhikari, R.X.; et al. Prospects for observing and localizing gravitational-wave transients with Advanced LIGO, Advanced Virgo and KAGRA. *Living Reviews in Relativity* **2018**, *21*, 3, [arXiv:gr-qc/1304.0670]. doi:10.1007/s41114-018-0012-9. 2443
2444
2445
458. Punturo, M.; Abernathy, M.; Acernese, F.; Allen, B.; Andersson, N.; Arun, K.; Barone, F.; Barr, B.; Barsuglia, M.; Beker, M.; et al. The Einstein Telescope: a third-generation gravitational wave observatory. *Classical and Quantum Gravity* **2010**, *27*, 194002. doi:10.1088/0264-9381/27/19/194002. 2446
2447
2448
459. Sathyaprakash, B.; Abernathy, M.; Acernese, F.; Ajith, P.; Allen, B.; Amaro-Seoane, P.; Andersson, N.; Aoudia, S.; Arun, K.; Astone, P.; et al. Corrigendum: Scientific objectives of Einstein telescope. *Classical and Quantum Gravity* **2013**, *30*, 079501. doi:10.1088/0264-9381/30/7/079501. 2449
2450
2451

460. Abbott, B.P.; Abbott, R.; Abbott, T.D.; Abernathy, M.R.; Ackley, K.; Adams, C.; Addesso, P.; Adhikari, R.X.; Adya, V.B.; Affeldt, C.; et al. Exploring the sensitivity of next generation gravitational wave detectors. *Classical and Quantum Gravity* **2017**, *34*, 044001, [arXiv:astro-ph.IM/1607.08697]. doi:10.1088/1361-6382/aa51f4. 2452-2453-2454
461. Reitze, D.; Adhikari, R.X.; Ballmer, S.; Barish, B.; Barsotti, L.; Billingsley, G.; Brown, D.A.; Chen, Y.; Coyne, D.; Eisenstein, R.; et al. Cosmic Explorer: The U.S. Contribution to Gravitational-Wave Astronomy beyond LIGO. *Bulletin of the American Astronomical Society*, 2019, Vol. 51, p. 35, [arXiv:astro-ph.IM/1907.04833]. 2455-2456-2457
462. Cutler, C.; Flanagan, É.E. Gravitational waves from merging compact binaries: How accurately can one extract the binary's parameters from the inspiral waveform? *Phys. Rev. D* **1994**, *49*, 2658–2697, [arXiv:gr-qc/9402014]. doi:10.1103/PhysRevD.49.2658. 2458-2459
463. Toubiana, A.; Marsat, S.; Babak, S.; Baker, J.; Dal Canton, T. Parameter estimation of stellar-mass black hole binaries with LISA. *Phys. Rev. D* **2020**, *102*, 124037, [arXiv:gr-qc/2007.08544]. doi:10.1103/PhysRevD.102.124037. 2460-2461
464. Buscicchio, R.; Klein, A.; Roebber, E.; Moore, C.J.; Gerosa, D.; Finch, E.; Vecchio, A. Bayesian parameter estimation of stellar-mass black-hole binaries with LISA. *Phys. Rev. D* **2021**, *104*, 044065, [arXiv:astro-ph.HE/2106.05259]. doi:10.1103/PhysRevD.104.044065. 2462-2463
465. Pürrer, M.; Hannam, M.; Ajith, P.; Husa, S. Testing the validity of the single-spin approximation in inspiral-merger-ringdown waveforms. *Phys. Rev. D* **2013**, *88*, 064007, [arXiv:gr-qc/1306.2320]. doi:10.1103/PhysRevD.88.064007. 2464-2465
466. Pürrer, M.; Hannam, M.; Ohme, F. Can we measure individual black-hole spins from gravitational-wave observations? *Phys. Rev. D* **2016**, *93*, 084042, [arXiv:gr-qc/1512.04955]. doi:10.1103/PhysRevD.93.084042. 2466-2467
467. Racine, E. Analysis of spin precession in binary black hole systems including quadrupole-monopole interaction. *Phys. Rev. D* **2008**, *78*, 044021. doi:10.1103/PhysRevD.78.044021. 2468-2469
468. Ajith, P.; Hannam, M.; Husa, S.; Chen, Y.; Brüggmann, B.; Dorband, N.; Müller, D.; Ohme, F.; Pollney, D.; Reisswig, C.; et al. Inspiral-Merger-Ringdown Waveforms for Black-Hole Binaries with Nonprecessing Spins. *Phys. Rev. Lett.* **2011**, *106*, 241101. doi:10.1103/PhysRevLett.106.241101. 2470-2471-2472
469. Santamaría, L.; Ohme, F.; Ajith, P.; Brüggmann, B.; Dorband, N.; Hannam, M.; Husa, S.; Mösta, P.; Pollney, D.; Reisswig, C.; et al. Matching post-Newtonian and numerical relativity waveforms: Systematic errors and a new phenomenological model for nonprecessing black hole binaries. *Phys. Rev. D* **2010**, *82*, 064016. doi:10.1103/PhysRevD.82.064016. 2473-2474-2475
470. Damour, T. Coalescence of two spinning black holes: An effective one-body approach. *Phys. Rev. D* **2001**, *64*, 124013, [arXiv:gr-qc/gr-qc/0103018]. doi:10.1103/PhysRevD.64.124013. 2476-2477
471. Ajith, P. Addressing the spin question in gravitational-wave searches: Waveform templates for inspiralling compact binaries with nonprecessing spins. *Phys. Rev. D* **2011**, *84*, 084037, [arXiv:gr-qc/1107.1267]. doi:10.1103/PhysRevD.84.084037. 2478-2479
472. Miller, S.; Callister, T.A.; Farr, W.M. The Low Effective Spin of Binary Black Holes and Implications for Individual Gravitational-wave Events. *ApJ* **2020**, *895*, 128, [arXiv:astro-ph.HE/2001.06051]. doi:10.3847/1538-4357/ab80c0. 2480-2481
473. Biscoveanu, S.; Isi, M.; Varma, V.; Vitale, S. Measuring the spins of heavy binary black holes. *Phys. Rev. D* **2021**, *104*, 103018, [arXiv:gr-qc/2106.06492]. doi:10.1103/PhysRevD.104.103018. 2482-2483
474. Biscoveanu, S.; Callister, T.A.; Haster, C.J.; Ng, K.K.Y.; Vitale, S.; Farr, W.M. The Binary Black Hole Spin Distribution Likely Broadens with Redshift. *ApJL* **2022**, *932*, L19, [arXiv:astro-ph.HE/2204.01578]. doi:10.3847/2041-8213/ac71a8. 2484-2485
475. Fishbach, M.; Kalogera, V. Apples and Oranges: Comparing Black Holes in X-Ray Binaries and Gravitational-wave Sources. *ApJL* **2022**, *929*, L26, [arXiv:astro-ph.HE/2111.02935]. doi:10.3847/2041-8213/ac64a5. 2486-2487
476. Fishbach, M.; Kimball, C.; Kalogera, V. Limits on Hierarchical Black Hole Mergers from the Most Negative χ_{eff} Systems. *ApJL* **2022**, *935*, L26, [arXiv:astro-ph.HE/2207.02924]. doi:10.3847/2041-8213/ac86c4. 2488-2489
477. Schmidt, P.; Ohme, F.; Hannam, M. Towards models of gravitational waveforms from generic binaries: II. Modelling precession effects with a single effective precession parameter. *Phys. Rev. D* **2015**, *91*, 024043. doi:10.1103/PhysRevD.91.024043. 2490-2491
478. Wysocki, D.; Lange, J.; O'Shaughnessy, R. Reconstructing phenomenological distributions of compact binaries via gravitational wave observations. *Phys. Rev. D* **2019**, *100*, 043012, [arXiv:gr-qc/1805.06442]. doi:10.1103/PhysRevD.100.043012. 2492-2493
479. Hinder, I.; Kidder, L.E.; Pfeiffer, H.P. Eccentric binary black hole inspiral-merger-ringdown gravitational waveform model from numerical relativity and post-Newtonian theory. *Phys. Rev. D* **2018**, *98*, 044015, [arXiv:gr-qc/1709.02007]. doi:10.1103/PhysRevD.98.044015. 2494-2495
480. Gayathri, V.; Healy, J.; Lange, J.; O'Brien, B.; Szczepańczyk, M.; Bartos, I.; Campanelli, M.; Klimentenko, S.; Lousto, C.O.; O'Shaughnessy, R. Eccentricity estimate for black hole mergers with numerical relativity simulations. *Nature Astronomy* **2022**, *6*, 344–349. doi:10.1038/s41550-021-01568-w. 2496-2497-2498
481. Payne, E.; Talbot, C.; Thrane, E. Higher order gravitational-wave modes with likelihood reweighting. *Phys. Rev. D* **2019**, *100*, 123017, [arXiv:astro-ph.IM/1905.05477]. doi:10.1103/PhysRevD.100.123017. 2499-2500
482. Romero-Shaw, I.M.; Lasky, P.D.; Thrane, E. Searching for eccentricity: signatures of dynamical formation in the first gravitational-wave transient catalogue of LIGO and Virgo. *MNRAS* **2019**, *490*, 5210–5216, [arXiv:astro-ph.HE/1909.05466]. doi:10.1093/mnras/stz2996. 2501-2502
483. Abbott, B.P.; Abbott, R.; Abbott, T.D.; Abernathy, M.R.; Acernese, F.; Ackley, K.; Adams, C.; Adams, T.; Addesso, P.; Adhikari, R.X.; et al. Binary Black Hole Mergers in the First Advanced LIGO Observing Run. *Physical Review X* **2016**, *6*, 041015, [arXiv:gr-qc/1606.04856]. doi:10.1103/PhysRevX.6.041015. 2503-2504-2505

484. Gerosa, D.; Berti, E. Escape speed of stellar clusters from multiple-generation black-hole mergers in the upper mass gap. *Phys. Rev. D* **2019**, *100*, 041301, [arXiv:astro-ph.HE/1906.05295]. doi:10.1103/PhysRevD.100.041301. 2506
485. Fragione, G.; Silk, J. Repeated mergers and ejection of black holes within nuclear star clusters. *MNRAS* **2020**, *498*, 4591–4604, [arXiv:astro-ph.GA/2006.01867]. doi:10.1093/mnras/staa2629. 2508
486. Zhang, F.; Shao, L.; Zhu, W. Gravitational-wave Merging Events from the Dynamics of Stellar-mass Binary Black Holes around the Massive Black Hole in a Galactic Nucleus. *ApJ* **2019**, *877*, 87, [arXiv:astro-ph.GA/1903.02685]. doi:10.3847/1538-4357/ab1b28. 2510
487. Rasskazov, A.; Kocsis, B. The Rate of Stellar Mass Black Hole Scattering in Galactic Nuclei. *ApJ* **2019**, *881*, 20, [arXiv:astro-ph.HE/1902.03242]. doi:10.3847/1538-4357/ab2c74. 2512
488. Moore, C.J.; Gerosa, D.; Klein, A. Are stellar-mass black-hole binaries too quiet for LISA? *MNRAS* **2019**, *488*, L94–L98, [arXiv:astro-ph.HE/1905.11998]. doi:10.1093/mnrasl/slz104. 2514
489. Hoang, B.M.; Naoz, S.; Kocsis, B.; Farr, W.M.; McIver, J. Detecting Supermassive Black Hole-induced Binary Eccentricity Oscillations with LISA. *ApJL* **2019**, *875*, L31, [arXiv:astro-ph.HE/1903.00134]. doi:10.3847/2041-8213/ab14f7. 2516
490. Liu, B.; Lai, D. Spin-Orbit Misalignment of Merging Black Hole Binaries with Tertiary Companions. *ApJL* **2017**, *846*, L11, [arXiv:astro-ph.HE/1706.02309]. doi:10.3847/2041-8213/aa8727. 2518
491. Liu, B.; Lai, D. Black Hole and Neutron Star Binary Mergers in Triple Systems: Merger Fraction and Spin-Orbit Misalignment. *ApJ* **2018**, *863*, 68, [arXiv:astro-ph.HE/1805.03202]. doi:10.3847/1538-4357/aad09f. 2520
492. Reynolds, C.S. The spin of supermassive black holes. *Classical and Quantum Gravity* **2013**, *30*, 244004, [arXiv:astro-ph.HE/1307.3246]. doi:10.1088/0264-9381/30/24/244004. 2522
493. Reynolds, C.S. Observational Constraints on Black Hole Spin. *ARA&A* **2021**, *59*, 117–154, [arXiv:astro-ph.HE/2011.08948]. doi:10.1146/annurev-astro-112420-035022. 2524
494. Liu, B.; Lai, D. Merging compact binaries near a rotating supermassive black hole: Eccentricity excitation due to apsidal precession resonance. *Phys. Rev. D* **2020**, *102*, 023020, [arXiv:astro-ph.HE/2004.10205]. doi:10.1103/PhysRevD.102.023020. 2526
495. Fang, Y.; Chen, X.; Huang, Q.G. Impact of a Spinning Supermassive Black Hole on the Orbit and Gravitational Waves of a Nearby Compact Binary. *ApJ* **2019**, *887*, 210, [arXiv:astro-ph.HE/1908.01443]. doi:10.3847/1538-4357/ab510e. 2528
496. Fang, Y.; Huang, Q.G. Secular evolution of compact binaries revolving around a spinning massive black hole. *Phys. Rev. D* **2019**, *99*, 103005, [arXiv:gr-qc/1901.05591]. doi:10.1103/PhysRevD.99.103005. 2530
497. Fang, Y.; Huang, Q.G. Three body first post-Newtonian effects on the secular dynamics of a compact binary near a spinning supermassive black hole. *Phys. Rev. D* **2020**, *102*, 104002, [arXiv:gr-qc/2004.09390]. doi:10.1103/PhysRevD.102.104002. 2532
498. Yu, H.; Chen, Y. Direct Determination of Supermassive Black Hole Properties with Gravitational-Wave Radiation from Surrounding Stellar-Mass Black Hole Binaries. *Phys. Rev. Lett.* **2021**, *126*, 021101, [arXiv:gr-qc/2009.02579]. doi:10.1103/PhysRevLett.126.021101. 2534
499. Liu, B.; Lai, D. Probing the Spins of Supermassive Black Holes with Gravitational Waves from Surrounding Compact Binaries. *ApJ* **2022**, *924*, 127, [arXiv:astro-ph.HE/2105.02230]. doi:10.3847/1538-4357/ac3aef. 2536
500. Antonini, F.; Rodriguez, C.L.; Petrovich, C.; Fischer, C.L. Precessional dynamics of black hole triples: binary mergers with near-zero effective spin. *MNRAS* **2018**, *480*, L58–L62, [arXiv:astro-ph.HE/1711.07142]. doi:10.1093/mnrasl/sly126. 2538
501. Su, Y.; Lai, D.; Liu, B. Spin-orbit misalignments in tertiary-induced binary black-hole mergers: Theoretical analysis. *Phys. Rev. D* **2021**, *103*, 063040, [arXiv:gr-qc/2010.11951]. doi:10.1103/PhysRevD.103.063040. 2540
502. McKernan, B.; Ford, K.E.S.; O’Shaughnessy, R.; Wysocki, D. Monte Carlo simulations of black hole mergers in AGN discs: Low χ_{eff} mergers and predictions for LIGO. *MNRAS* **2020**, *494*, 1203–1216, [arXiv:astro-ph.HE/1907.04356]. doi:10.1093/mnras/staa740. 2542
503. Bogdanović, T.; Reynolds, C.S.; Miller, M.C. Alignment of the Spins of Supermassive Black Holes Prior to Coalescence. *ApJL* **2007**, *661*, L147–L150, [arXiv:astro-ph/astro-ph/0703054]. doi:10.1086/518769. 2544
504. Tagawa, H.; Haiman, Z.; Bartos, I.; Kocsis, B. Spin Evolution of Stellar-mass Black Hole Binaries in Active Galactic Nuclei. *ApJ* **2020**, *899*, 26, [arXiv:astro-ph.HE/2004.11914]. doi:10.3847/1538-4357/aba2cc. 2546
505. Tagawa, H.; Haiman, Z.; Bartos, I.; Kocsis, B.; Omukai, K. Signatures of hierarchical mergers in black hole spin and mass distribution. *MNRAS* **2021**, *507*, 3362–3380, [arXiv:astro-ph.HE/2104.09510]. doi:10.1093/mnras/stab2315. 2548
506. Graham, M.J.; Ford, K.E.S.; McKernan, B.; Ross, N.P.; Stern, D.; Burdge, K.; Coughlin, M.; Djorgovski, S.G.; Drake, A.J.; Duev, D.; et al. Candidate Electromagnetic Counterpart to the Binary Black Hole Merger Gravitational-Wave Event S190521g*. *Phys. Rev. Lett.* **2020**, *124*, 251102, [arXiv:astro-ph.HE/2006.14122]. doi:10.1103/PhysRevLett.124.251102. 2550
507. Ashton, G.; Ackley, K.; Hernandez, I.M.; Piotrkowski, B. Current observations are insufficient to confidently associate the binary black hole merger GW190521 with AGN J124942.3 + 344929. *Classical and Quantum Gravity* **2021**, *38*, 235004, [arXiv:astro-ph.HE/2009.12346]. doi:10.1088/1361-6382/ac33bb. 2552
508. Estellés, H.; Husa, S.; Colleoni, M.; Mateu-Lucena, M.; Planas, M.d.L.; García-Quirós, C.; Keitel, D.; Ramos-Buades, A.; Mehta, A.K.; Buonanno, A.; et al. A Detailed Analysis of GW190521 with Phenomenological Waveform Models. *ApJ* **2022**, *924*, 79, [arXiv:gr-qc/2105.06360]. doi:10.3847/1538-4357/ac33a0. 2554

509. Palmese, A.; Fishbach, M.; Burke, C.J.; Annis, J.; Liu, X. Do LIGO/Virgo Black Hole Mergers Produce AGN Flares? The Case of GW190521 and Prospects for Reaching a Confident Association. *ApJL* **2021**, *914*, L34, [arXiv:astro-ph.HE/2103.16069]. doi:10.3847/2041-8213/ac0883. 2559
2560
510. Bartos, I.; Haiman, Z.; Marka, Z.; Metzger, B.D.; Stone, N.C.; Marka, S. Gravitational-wave localization alone can probe origin of stellar-mass black hole mergers. *Nature Communications* **2017**, *8*, 831, [arXiv:astro-ph.HE/1701.02328]. doi:10.1038/s41467-017-00851-7. 2562
2563
511. Kopparapu, R.K.; Hanna, C.; Kalogera, V.; O’Shaughnessy, R.; González, G.; Brady, P.R.; Fairhurst, S. Host Galaxies Catalog Used in LIGO Searches for Compact Binary Coalescence Events. *ApJ* **2008**, *675*, 1459–1467, [arXiv:astro-ph/0706.1283]. doi:10.1086/527348. 2564
2565
512. Abadie, J.; Abbott, B.P.; Abbott, R.; Abernathy, M.; Accadia, T.; Acernese, F.; Adams, C.; Adhikari, R.; Ajith, P.; Allen, B.; et al. TOPICAL REVIEW: Predictions for the rates of compact binary coalescences observable by ground-based gravitational-wave detectors. *Classical and Quantum Gravity* **2010**, *27*, 173001, [arXiv:astro-ph.HE/1003.2480]. doi:10.1088/0264-9381/27/17/173001. 2566
2567
2568
513. McKernan, B.; Ford, K.E.S.; Bellovary, J.; Leigh, N.W.C.; Haiman, Z.; Kocsis, B.; Lyra, W.; Mac Low, M.M.; Metzger, B.; O’Dowd, M.; et al. Constraining Stellar-mass Black Hole Mergers in AGN Disks Detectable with LIGO. *ApJ* **2018**, *866*, 66, [arXiv:astro-ph.HE/1702.07818]. doi:10.3847/1538-4357/aadae5. 2569
2570
2571
514. Baldry, I.K.; Driver, S.P.; Loveday, J.; Taylor, E.N.; Kelvin, L.S.; Liske, J.; Norberg, P.; Robotham, A.S.G.; Brough, S.; Hopkins, A.M.; et al. Galaxy And Mass Assembly (GAMA): the galaxy stellar mass function at $z < 0.06$. *MNRAS* **2012**, *421*, 621–634, [arXiv:astro-ph.CO/1111.5707]. doi:10.1111/j.1365-2966.2012.20340.x. 2572
2573
2574
515. Ho, L.C. Nuclear activity in nearby galaxies. *ARA&A* **2008**, *46*, 475–539, [arXiv:astro-ph/0803.2268]. doi:10.1146/annurev.astro.45.051806.2575
2576
516. Miller, M.C.; Davies, M.B. An Upper Limit to the Velocity Dispersion of Relaxed Stellar Systems without Massive Black Holes. *ApJ* **2012**, *755*, 81, [arXiv:astro-ph.GA/1206.6167]. doi:10.1088/0004-637X/755/1/81. 2576
2577
517. Haehnelt, M.G.; Rees, M.J. The formation of nuclei in newly formed galaxies and the evolution of the quasar population. *MNRAS* **1993**, *263*, 168–178. doi:10.1093/mnras/263.1.168. 2578
2579
518. King, A.; Nixon, C. AGN flickering and chaotic accretion. *MNRAS* **2015**, *453*, L46–L47, [arXiv:astro-ph.HE/1507.05960]. doi:10.1093/mnrasl/slv098. 2580
2581
519. Schwinski, K.; Koss, M.; Berney, S.; Sartori, L.F. Active galactic nuclei flicker: an observational estimate of the duration of black hole growth phases of $\sim 10^5$ yr. *MNRAS* **2015**, *451*, 2517–2523, [arXiv:astro-ph.GA/1505.06733]. doi:10.1093/mnras/stv1136. 2582
2583
520. McKernan, B.; Ford, K.E.S.; O’Shaughnessy, R. Black hole, neutron star, and white dwarf merger rates in AGN discs. *MNRAS* **2020**, *498*, 4088–4094, [arXiv:astro-ph.HE/2002.00046]. doi:10.1093/mnras/staa2681. 2584
2585
521. VanLandingham, J.H.; Miller, M.C.; Hamilton, D.P.; Richardson, D.C. The Role of the Kozai–Lidov Mechanism in Black Hole Binary Mergers in Galactic Centers. *ApJ* **2016**, *828*, 77, [arXiv:astro-ph.HE/1604.04948]. doi:10.3847/0004-637X/828/2/77. 2586
2587
522. Li, G.P. Time-dependent stellar-mass binary black hole mergers in AGN disks: Mass distribution of hierarchical mergers. *Phys. Rev. D* **2022**, *105*, 063006, [arXiv:astro-ph.HE/2202.09961]. doi:10.1103/PhysRevD.105.063006. 2588
2589
523. Ford, K.E.S.; McKernan, B. Binary Black Hole Merger Rates in AGN Disks versus Nuclear Star Clusters: Loud beats Quiet. *arXiv e-prints* **2021**, p. arXiv:2109.03212, [arXiv:astro-ph.HE/2109.03212]. 2590
2591
524. Secunda, A.; Bellovary, J.; Mac Low, M.M.; Ford, K.E.S.; McKernan, B.; Leigh, N.W.C.; Lyra, W.; Sándor, Z.; Adorno, J.I. Orbital Migration of Interacting Stellar Mass Black Holes in Disks around Supermassive Black Holes. II. Spins and Incoming Objects. *ApJ* **2020**, *903*, 133, [arXiv:astro-ph.HE/2004.11936]. doi:10.3847/1538-4357/abbc1d. 2592
2593
2594
525. Gröbner, M.; Ishibashi, W.; Tiwari, S.; Haney, M.; Jetzer, P. Binary black hole mergers in AGN accretion discs: gravitational wave rate density estimates. *A&A* **2020**, *638*, A119, [arXiv:astro-ph.GA/2005.03571]. doi:10.1051/0004-6361/202037681. 2595
2596
526. Mandel, I.; Broekgaarden, F.S. Rates of compact object coalescences. *Living Reviews in Relativity* **2022**, *25*, 1, [arXiv:astro-ph.HE/2107.14239]. doi:10.1007/s41114-021-00034-3. 2597
2598
527. Gerosa, D.; Ma, S.; Wong, K.W.K.; Berti, E.; O’Shaughnessy, R.; Chen, Y.; Belczynski, K. Multiband gravitational-wave event rates and stellar physics. *Phys. Rev. D* **2019**, *99*, 103004, [arXiv:astro-ph.HE/1902.00021]. doi:10.1103/PhysRevD.99.103004. 2599
2600
528. Amaro Seoane, P.; Arca Sedda, M.; Babak, S.; Berry, C.P.L.; Berti, E.; Bertone, G.; Blas, D.; Bogdanović, T.; Bonetti, M.; Breivik, K.; et al. The effect of mission duration on LISA science objectives. *General Relativity and Gravitation* **2022**, *54*, 3, [arXiv:astro-ph.IM/2107.09665]. doi:10.1007/s10714-021-02889-x. 2601
2602
2603
529. Randall, L.; Xianyu, Z.Z. Observing Eccentricity Oscillations of Binary Black Holes in LISA. *arXiv e-prints* **2019**, p. arXiv:1902.08604, [arXiv:astro-ph.HE/1902.08604]. 2604
2605
530. Gupta, P.; Suzuki, H.; Okawa, H.; Maeda, K.i. Gravitational waves from hierarchical triple systems with Kozai-Lidov oscillation. *Phys. Rev. D* **2020**, *101*, 104053, [arXiv:gr-qc/1911.11318]. doi:10.1103/PhysRevD.101.104053. 2606
2607
531. Emami, R.; Loeb, A. Probing intermediate-mass black holes in M87 through multiwavelength gravitational wave observations. *MNRAS* **2020**, *495*, 536–543, [arXiv:astro-ph.GA/1910.04828]. doi:10.1093/mnras/staa1200. 2608
2609
532. Deme, B.; Hoang, B.M.; Naoz, S.; Kocsis, B. Detecting Kozai-Lidov Imprints on the Gravitational Waves of Intermediate-mass Black Holes in Galactic Nuclei. *ApJ* **2020**, *901*, 125, [arXiv:astro-ph.HE/2005.03677]. doi:10.3847/1538-4357/abafa3. 2610
2611
533. Damour, T.; Deruelle, N. Radiation reaction and angular momentum loss in small angle gravitational scattering. *Physics Letters A* **1981**, *87*, 81–84. doi:10.1016/0375-9601(81)90567-3. 2612
2613

534. Inayoshi, K.; Tamanini, N.; Caprini, C.; Haiman, Z. Probing stellar binary black hole formation in galactic nuclei via the imprint of their center of mass acceleration on their gravitational wave signal. *Phys. Rev. D* **2017**, *96*, 063014, [arXiv:astro-ph.HE/1702.06529]. doi:10.1103/PhysRevD.96.063014. 2614
2615
535. Wong, K.W.K.; Baibhav, V.; Berti, E. Binary radial velocity measurements with space-based gravitational-wave detectors. *MNRAS* **2019**, *488*, 5665–5670, [arXiv:astro-ph.HE/1902.01402]. doi:10.1093/mnras/stz2077. 2617
2618
536. Tamanini, N.; Klein, A.; Bonvin, C.; Barausse, E.; Caprini, C. Peculiar acceleration of stellar-origin black hole binaries: Measurement and biases with LISA. *Phys. Rev. D* **2020**, *101*, 063002, [arXiv:astro-ph.IM/1907.02018]. doi:10.1103/PhysRevD.101.063002. 2619
2620
537. Zhang, F.; Chen, X.; Shao, L.; Inayoshi, K. The Eccentric and Accelerating Stellar Binary Black Hole Mergers in Galactic Nuclei: Observing in Ground and Space Gravitational-wave Observatories. *ApJ* **2021**, *923*, 139, [arXiv:astro-ph.HE/2109.14842]. doi:10.3847/1538-4357/ac2c07. 2621
2622
2623
538. Yu, H.; Wang, Y.; Seymour, B.; Chen, Y. Detecting gravitational lensing in hierarchical triples in galactic nuclei with space-borne gravitational-wave observatories. *Phys. Rev. D* **2021**, *104*, 103011, [arXiv:gr-qc/2107.14318]. doi:10.1103/PhysRevD.104.103011. 2624
2625
539. Sberna, L.; Babak, S.; Marsat, S.; Caputo, A.; Cusin, G.; Toubiana, A.; Barausse, E.; Caprini, C.; Dal Canton, T.; Sesana, A.; et al. Observing GW190521-like binary black holes and their environment with LISA. *arXiv e-prints* **2022**, p. arXiv:2205.08550, [arXiv:gr-qc/2205.08550]. 2626
2627
2628
540. Meiron, Y.; Kocsis, B.; Loeb, A. Detecting Triple Systems with Gravitational Wave Observations. *ApJ* **2017**, *834*, 200, [arXiv:astro-ph.HE/1604.02148]. doi:10.3847/1538-4357/834/2/200. 2629
2630
541. Chen, X.; Li, S.; Cao, Z. Mass-redshift degeneracy for the gravitational-wave sources in the vicinity of supermassive black holes. *MNRAS* **2019**, *485*, L141–L145, [arXiv:astro-ph.HE/1703.10543]. doi:10.1093/mnrasl/slz046. 2631
2632
542. D’Orazio, D.J.; Loeb, A. Repeated gravitational lensing of gravitational waves in hierarchical black hole triples. *Phys. Rev. D* **2020**, *101*, 083031, [arXiv:astro-ph.HE/1910.02966]. doi:10.1103/PhysRevD.101.083031. 2633
2634
543. Torres-Orjuela, A.; Chen, X.; Amaro-Seoane, P. Phase shift of gravitational waves induced by aberration. *Phys. Rev. D* **2020**, *101*, 083028, [arXiv:astro-ph.HE/2001.00721]. doi:10.1103/PhysRevD.101.083028. 2635
2636
544. Takahashi, R.; Nakamura, T. Wave Effects in the Gravitational Lensing of Gravitational Waves from Chirping Binaries. *ApJ* **2003**, *595*, 1039–1051, [arXiv:astro-ph/astro-ph/0305055]. doi:10.1086/377430. 2637
2638
545. Gondán, L.; Kocsis, B. Astrophysical gravitational-wave echoes from galactic nuclei. *MNRAS* **2022**, *515*, 3299–3318, [arXiv:astro-ph.HE/2110.09540]. doi:10.1093/mnras/stac1985. 2639
2640
546. Will, C.M. Incorporating post-Newtonian effects in N-body dynamics. *Phys. Rev. D* **2014**, *89*, 044043, [arXiv:astro-ph.GA/1312.1289]. doi:10.1103/PhysRevD.89.044043. 2641
2642
547. Pechetti, R.; Seth, A.; Kamann, S.; Caldwell, N.; Strader, J.; den Brok, M.; Luetzgendorf, N.; Neumayer, N.; Voggel, K. Detection of a 100,000 M_{\odot} black hole in M31’s Most Massive Globular Cluster: A Tidally Stripped Nucleus. *ApJ* **2022**, *924*, 48, [arXiv:astro-ph.GA/2111.08720]. doi:10.3847/1538-4357/ac339f. 2643
2644
2645
548. Chen, X.; Xuan, Z.Y.; Peng, P. Fake Massive Black Holes in the Milli-Hertz Gravitational-wave Band. *ApJ* **2020**, *896*, 171, [arXiv:astro-ph.HE/2003.08639]. doi:10.3847/1538-4357/ab919f. 2646
2647